

Expression and Purification of Aquaporin-6 in Different Systems

**Comparison of cell-free, *Semliki Forest virus*, and
Pichia pastoris expression systems**

Inauguraldissertation

zur

Erlangung der Würde eines Doktors der Philosophie

vorgelegt der

Philosophisch-Naturwissenschaftlichen Fakultät

der

Universität Basel

von

André Krüger

aus

Hattingen, Deutschland

Basel, 2012

Genehmigt von der Philosophisch-Naturwissenschaftlichen Fakultät
auf Antrag von

Prof. Dr. Andreas Engel und Prof. Dr. Henning Stahlberg

Basel, den 26.06.2012

Prof. Dr. Martin Spiess
Dekan

Table of Contents

1. Introduction	1
1.1 Biological membranes: composition and function	1
1.2 ‘Transport’ of water across biological membranes	1
1.1.1 Types and functions of human AQPs	2
1.1.2 Aquaporin-6	9
1.2 Heterologous expression of Aquaporins	18
1.2.1 Cell-free membrane protein expression	21
1.2.2 The <i>Semliki</i> Forest Virus expression system	26
1.2.3 The <i>Pichia pastoris</i> expression system	30
1.3 Aim of this work	32
2 Methods	35
2.1 Cell-free protein expression	35
2.1.1 DNA template design	35
2.1.2 Transcription and translation	35
2.1.2.1 Preparation of T7 RNA polymerase for cell-free expression	35
2.1.2.2 Preparation of <i>E. coli</i> S30 extract	36
2.1.2.3 Analytical and preparative scale cell-free expression	37
2.1.2.4 Liposome preparation	39
2.1.3 Purification	40
2.2 Protein expression with the <i>Semliki</i> Forest virus system	41
2.2.1 DNA template design	41
2.2.2 Transcription and translation	41
2.2.2.1 <i>In vitro</i> transcription	41
2.2.2.2 Transfection of mammalian cells	42
2.2.2.3 Harvesting and activation of recombinant virus	42
2.2.2.4 Titer determination	43
2.2.2.5 Infection of mammalian cells and protein expression	43
2.2.3 Purification	43
2.2.3.1 Membrane preparation and solubilization	43
2.2.3.2 Ni-NTA purification (IMAC)	44
2.2.3.3 Reconstitution	45
2.2.4 General cell culture methods	45
2.3 Protein expression with <i>Pichia pastoris</i>	47
2.3.1 DNA template design	47
2.3.2 Transcription and translation	48
2.3.3 Purification	48
2.4 Protein analysis	50
2.4.1 Determination of protein concentration	50
2.4.2 SDS-PAGE	50
2.4.3 Western blot analysis	50
2.4.4 Size exclusion chromatography	50

2.4.5	Single particle negative stain transmission electron microscopy	51
2.5	Protein reconstitution into liposomes	52
2.6	Freeze fracture electron microscopy	54
2.6.1	Sample preparation.....	54
2.6.2	Sample analysis.....	54
2.7	Water conductance measurements of proteoliposomes.....	55
3	Results & Discussion.....	57
3.1	Cell-free expression of AQP6	57
3.1.1	Template design	57
3.1.2	Transcription and translation	58
3.1.2.1	Basic protocol	58
3.1.2.2	Buffer conditions.....	59
3.1.2.3	Optimizing parameters for expression.....	59
3.1.2.4	Altering N-terminal tags to optimize transcription and translation.....	61
3.1.2.5	Evaluation of detergents for expression and solubilization.....	62
3.1.3	Purification	65
3.1.4	Single particle analysis	69
3.1.5	Reconstitution into liposomes.....	69
3.1.5	Co-translational reconstitution.....	73
3.1.6	Water conductance of cell-free expressed AQP6	77
3.2	<i>Semliki</i> Forest virus expression of AQP6	80
3.2.1	Template design	80
3.2.2	Transcription.....	80
3.2.2.1	<i>In vitro</i> transcription	80
3.2.2.2	Virus production.....	82
3.2.2	Translation.....	82
3.2.3	Solubilization	84
3.2.4	Purification	85
3.2.5	Single particle analysis	89
3.2.6	Reconstitution into liposomes.....	90
3.2.7	Water conductance of heterogously expressed AQP6	93
3.3	<i>Pichia pastoris</i> expression of AQP6	97
3.3.1	Template design	97
3.3.2	Transcription and translation	97
3.3.3	Solubilization	99
3.3.4	Purification	100
3.3.5	Single particle analysis	103
4	Conclusion.....	105
Appendix A - Materials.....		109
A.1	Bacterial Strains	109
A.2	Oligonucleotides.....	109
A.3	Vectors	110

A.4 Chemicals, reagents and buffers	110
A.4.1 Chemicals and reagent solutions.....	110
A.4.2 Buffers & media	112
A.4.3 Antibodies	114
A.4.4 Detergents.....	114
A.4.5 Lipids.....	114
A.4.6 Equipment.....	115
Appendix B - Sequences	116
Abbreviations	119
References	121
<i>Curriculum vitae</i>	129

1. Introduction

1.1 Biological membranes: composition and function

Cells are the basic modules of life and surrounded by a membrane. Biological membranes separate cells from their environment and create separated spaces within cells by forming barriers. Consequently, biological membranes are of vital importance for the separation of biological compartments. Biological membranes are composed of a lipid bilayer containing proteins. The major classes of membrane lipids are phospholipids, glycolipids and cholesterol. Phospholipids and glycolipids consist of two long hydrophobic alkyl chains linked to a hydrophilic head group, while cholesterol is a steroid and required to regulate membrane fluidity [1] (*review on membrane lipids in* [2]). Membrane proteins are integrated or attached to the lipid bilayer and control the transport of nutrients and metabolites, enable the formation of ion gradients and permit signal transduction across biological membrane [3]. The importance of membrane proteins becomes clear from a genetical and pharmacological point of view: nearly one third of all known genes encode for membrane proteins. More than 50 % of the human membrane proteins are potential drug targets. For this reason the knowledge of structure-function relationships of membrane proteins is of vital importance for medicine and pharmacology [4].

1.2 'Transport' of water across biological membranes

In all tissues water is the major component of cells. Because water is such a major part of cells, the movement of fluids across biological membranes is important. One possibility for water to cross the plasma membrane or other biological membranes is the simple diffusion through the lipid bilayer. However, the water permeability of the plasma membrane must be caused by an additional phenomenon for several reasons: there are variations in the permeability for water with regard to different cell types. The highest water transport rates can be found in tissues like the renal tube and secretory glands. The high transport rates can not be explained by diffusion through the plasma membrane alone, because large amounts of energy are needed in relation to the water transported. An activation energy of >10 kcal/mol is required for water to cross the hydrophobic part of the membrane [5]. In the 1970s this fact led to the prediction of a selective water channel with a high transport capacity [6]. The discovery of the predicted aquaporins (AQPs) in the early 1990s [7] and the first structure of aquaporin-1 (AQP1) with atomic resolution in 2000 led to a profound understanding about selective water transport mechanisms across biological

membranes [8-10]. The water transport is mainly mediated by AQPs: diffusion through the lipid bilayer occurs only to some small extent. Most AQPs have high water selectivity, while protons and hydronium ions do not pass. In AQPs water diffuses bidirectional. The net water movement is driven by the osmotic gradient, which also drives the water diffusion through the bilayer.

1.1.1 Types and functions of human AQPs

AQPs are conserved throughout lower organisms, the animal and plant kingdoms. The family of AQPs can be divided into two branches: The classical AQPs that exclusively transport channels and the aquaglycoporins that in addition permit passage of glycerol and other small solutes (Figure 1.1).

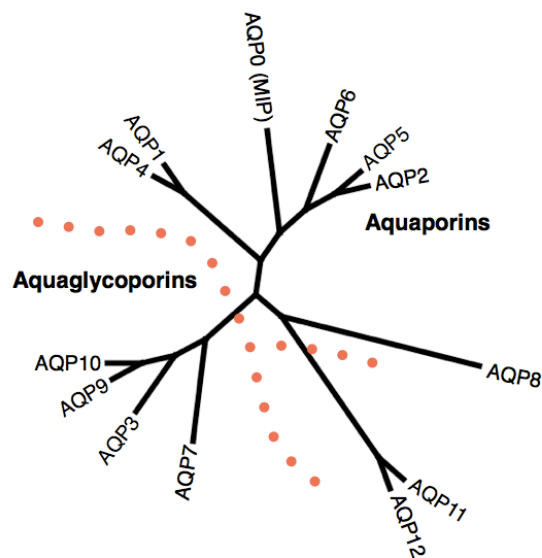


Figure 1.1: Phylogenetic tree of human AQPs, clustering into two families: The classical AQP water channels and the aquaglycoporins. Pore properties of AQP11 and AQP12 remain unclear.

The 13 mammalian AQPs are widely distributed in specific cell types in many organs and tissues. In particular AQPs are strongly expressed and functionally important in kidney, eye, skin, exocrine glands and the central nervous system [11]. Their primary function is to facilitate water across the cell membrane; some AQPs also transport small solutes such as glycerol [12]. Water-selective AQPs are involved in epithelial fluid transport, brain swelling, cell migration and neuroexcitation. AQPs are expressed in lung, gastrointestinal organs and muscles, but their functional importance in these tissues is not fully understood yet [11]. Because of the importance of AQPs in a wide range of physiological processes their dysfunction is the reason for several human diseases. Table 1.1 provides an overview over the 13 mammalian AQPs, the tissues of expression, the function and their relation with diseases.

Table 1.1: Human AQPs. Blue: function primarily as water-selective transporter. Grey: Aquaglyceroporins: transport of water and glycerol. White: function obscure.

Name	Tissue	Permeability Low / High	Function	Related disease	Ref.
AQP0 (MIP)	Eye lens fiber	Water	Membrane junctions, water channel and adhesions protein	Congenital cataract	[13]
AQP1	Kidney (renal proximal tubulus) & red blood cells	Water	Water reabsorption	Defective urinary concentrating	[14, 15]
AQP2	Kidney	Water	Water reabsorption Vasopressin regulated	Nephrogenic diabetes insipidus Congestive heart failure Cirrhosis	[16-18]
AQP3	Kidney, basolateral collecting duct cells, sweat glands (Epithelial cells)	Water & glycerol	Water reabsorption Not vasopressin regulated	Cutaneous wound healing	[19, 20]
AQP4	Brain	Water	Cell adhesion, water level regulation in brain	Upregulation in brain infection and trauma	[21, 22]
AQP5		Water	Fluid secretion by salivary	Dry eyes and mouths in an autoimmune disease due to decreased expression	[23]
AQP6	Intracellular vesicles	Water & Anions	Acid secretion		[24]
AQP7	Fat tissue	Water, glycerol & urea	Glycerol release, Fat metabolism	Obesity	[25]
AQP8	Intracellular vesicles	Water & ammonia			[26]
AQP9	Liver	Water & glycerol	Glycerol uptake, gluconeogenesis	Obesity	[25, 27]
AQP10	Small intestine	Water & glycerol, urea			[28, 29]
AQP11		None			[30]
AQP12	Pancreas, acinar cells	None			[31]

AQP0 is expressed in eye lens fiber membrane junctions. It is functional as water channel and cell adhesions protein. AQP0 is involved in diseases like congenital cataract [13]. **AQP1** is expressed in the kidney in proximal tubules in the thin descending limb of *Henle* epithelia and in descending *vasa recta* endothelia. It is the key player in reabsorption of water filtered by the kidney. About 90% of the daily 180 l filtered water is reabsorbed by AQP1. It is also present in the plasma membrane of red blood cells [32]. Remaining water in the collecting duct is reabsorbed by **AQP2** that is localized in the apical membrane of the collecting-duct. This additional water reabsorption is vasopressin-regulated by translocation of intra-cellular vesicles, containing AQP2 to the apical membrane upon ligand binding to the vasopressin receptor. Mutations in the AQP2 encoding gene can result in diabetes insipidus [16]. **AQP4** is expressed in basolateral membranes of epithelial cells of the collecting duct and in the brain, where it is functional as water channel and as cell adhesion protein like AQP0 [21] and has high water permeability. AQP4 facilitates brain water accumulation in cytotoxic edema and clearance of excess brain water in vasogenic and interstitial edema. **AQP5** also is highly permeable for water and is expressed in salivary, lacrimal and sweat glands, apical plasma membranes as well as in lung and cornea. The deletion of AQP5 in mice harms fluid secretion by salivary and airway submucosal glands, resulting in a reduced secretion of a hyperosmolar fluid [33]. **AQP6** is an intracellular water channel that is localized in intracellular vesicles of acid-secreting intercalated cells of the collecting duct. In these vesicles AQP6 is co-localized with vascular-type H⁺-ATPase (vH⁺-ATPase). In contrast to other AQPs, AQP6 was shown to be permeable for anions and water. The ion channel function of AQP6 is activated by a pH lower than 5.5 [34]. A detailed view on AQP6 is provided in the following chapter. **AQP8** shows an intracellular localization like AQP6, but it functions as an ammonia channel [26].

Aquaglycoporins are permeable for water as well as for glycerol. **AQP3** is expressed in several epithelial cells like the basolateral membranes of kidney collecting duct cells, airway epithelia and sweat glands [19]. It facilitates the glycerol transport in skin and has a functional role in epidermal and *stratum corneum* hydration [20]. **AQP7** is expressed in the plasma membrane of adipocytes and is responsible for glycerol release during starvation. It might have a central role in fat metabolism [35]. In the liver **AQP9** facilitates glycerol uptake for gluconeogenesis [27]. **AQP7** and **AQP9** are potential metabolic regulators in diabetes and obesity, because adipocyte glycerol permeability might regulate the adipocyte metabolism and whole-body fat-mass [25]. **AQP10** is expressed in the intestine and is present in two splice variations. One is

highly permeable for water, urea and glycerol. The other isoform shows lower water permeability and is not permeable for glycerol and urea. The specific expression of AQP10 suggests a role in contribution to water transport in the upper portion of the small intestine [28, 29]. **AQP11** and **AQP12** are neither members of the classic AQP nor of the aquaglycoporin subfamilies. **AQP11** is present in tissues as diverse as kidney, liver testis, and brain. Located in the plasma membrane, it neither functions as a water, glycerol nor ion channel [30] and hence is functionally distinct from other AQPs. The function of **AQP12**, expressed intracellularly in pancreatic acinar cells [31], is still not known, although a role in digestive enzyme secretion was suggested.

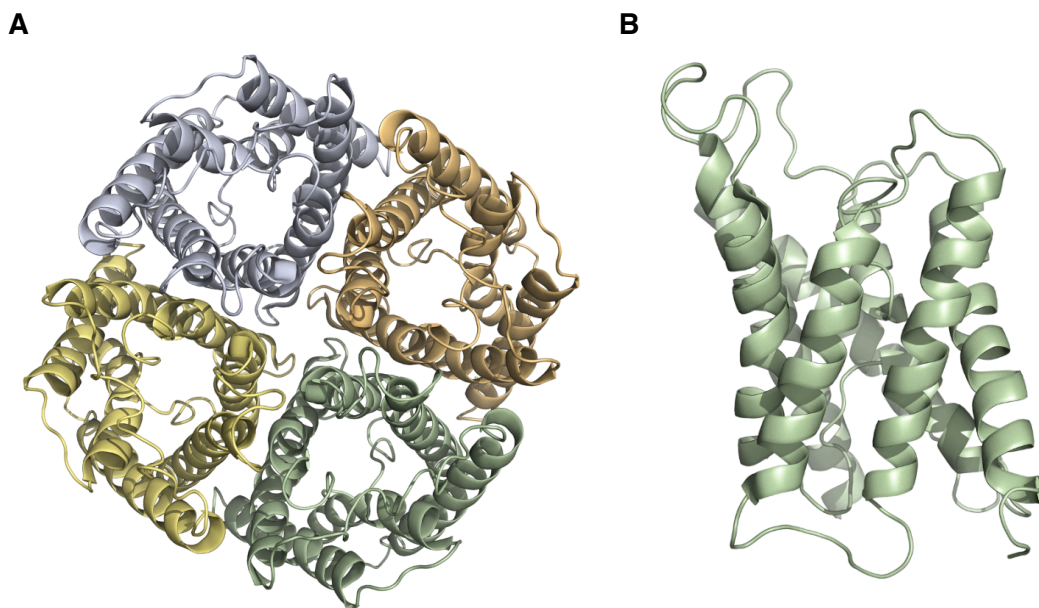


Figure 1.2: AQP homotetramer (A) and monomer (B), high-resolution structural model of AQP1 (PDB entry: 1FQY).

Structure

Structurally, mammalian AQPs have been investigated close to atomic level and at atomic level. There are high-resolution 3D structure models derived from 2D crystals by electron crystallography and 3D crystals by X-ray diffraction techniques (summary in Table 1.2).

Table 1.2: Structural investigation of mammalian AQPs at atomic-level.

Aquaporin	Resolution 3D (Å)	Method	Year	PDB entry	Reference
AQP0	1.9	Electron crystallography	2004	1SOR	[13]
AQP1	3.8	Electron crystallography	2000	1FQY	[36]
AQP1	3.7	Electron crystallography	2001	1IH5	[37]
AQP1	3.5	Electron crystallography, refined	2001	1H6I	[38]
AQP1	2.2	X-ray diffraction	2001	1J4N	[10]
AQP2	4.5	Electron crystallography	2005	Not atomic	[39]
AQP4	1.8	X-ray diffraction	2009	3GD8	[40]
AQP4M23	3.2	Electron crystallography	2006	2D57	[21]
AQP4	2.8	Electron crystallography	2009	2ZZ9	[41]
AQP5	2.0	X-ray diffraction	2008	3D9S	[42]
AQP8	8 (projection map)	Electron crystallography	2012	Not atomic	[43]
AQP9	7 (projection map)	Electron crystallography	2007	Not atomic	[44]

The first high-resolution structure model of an AQP was obtained by electron crystallography of human AQP1 in the year 2000 [36] (Figure 1.2). At the same time the structure of GlpF, a bacterial glycerol channel, was solved by X-ray crystallography [45]. The structural studies of AQP1 provided the first insight into the molecular mechanism of water permeation through AQPs. Strikingly, despite their homotetrameric architecture, the functional unit is a monomer. Each monomer

contains six membrane-spanning α -helices connected by loops of variable lengths, with the N- and C- termini located in the cytosol. Because of the high sequence homology between the first half and the second half of AQPs it is assumed that these two have evolved from an ancient gene duplication event [46]. Additional features that all AQPs have in common are the loops between transmembrane α -helices TM2 and TM3 (loop B), and the loop between TM5 and TM6 (loop E). The highly selective pore is structured by these loops, folding back from both sides of the membrane and facing each other in the middle of the membrane, which is called hourglass model. In the middle of the membrane the polar amino acid asparagine and the non-polar amino acids proline and alanine that are highly conserved on loop B and E meet and form the narrowest part of the pore (NPA motif).

Function

Molecular dynamics (MD) simulations, mainly performed on AQP1 explained the the highly efficient and specific mechanism of water permeation in AQPs [47]. The driving force of the non-active transport of water through the AQP channel is an osmotic gradient. In this study water permeates at a rate of 3×10^9 s⁻¹ water molecules per single AQP1 channel, whereas the transport of protons is prevented at the same time [48]. The pore is a constricted pathway formed by the six transmembrane α -helices and the conserved loops (Figure 1.3). It is approximately 25 Å long and bears two sites strongly interacting with water; the constriction and the NPA motif. Permeating molecules are coordinated to the channel through a combination of backbone carbonyl and amino acid side-chain interactions. At the extracellular side, the pore is relatively wide and water molecules interact mainly with the A and C loops through Lys36 and Ser123, respectively [49]. Into the narrowest constriction of AQP1, the aromatic residue / arginine constriction (ar/R), with a diameter of approximately 2.8 Å, a single water molecule fits in, which has the same diameter. It is formed by four residues: Phe56, His180, Cys189, and Arg159. A histidine is typical for water-specific AQPs, which together with the highly conserved arginine provides a hydrophilic edge in arrangement to an aromatic residue. The fixed positive charge on the adjacent arginine is involved in proton exclusion [49]. Within this region, between loop E and TM5, the hydrophobic side chain of Phe56 orientates the water molecules such as to enforce strong hydrogen bonds to Arg195 and His180. Further down the channel, the carbonyl groups of residues Ile191, Gly190 and Cys189 interact with the water molecules in the pore [49]. The sulfhydryl group of Cys189 extends into the pore and is the binding site for the inhibitor of AQP1, HgCl₂. A second constriction site that is less narrow is located in the center of the pore in the NPA region. The water molecules interact with both

asparagines on the one side and the hydrophobic side chains of Phe23, Val17, and Ile191 on the other. The two asparagines are the capping amino acids at the positive ends of helices TM2 and TM5. They act as hydrogen donors to the oxygen atoms of passing water. In addition, the dipoles of the half helices TM2 and TM5 reorient by an 180° turn the water molecules that enter this region, such that hydrogen bonds between neighboring water molecules in the chain are disrupted. Molecular dynamics simulations combined with quantum mechanical calculations of proton hopping probabilities demonstrated that protons are excluded from the central region of the channel by a strong free energy barrier, resulting from the dipole moments of TM2 and TM5 [49-51]. Hydrophobic residues line the remaining part of the AQP pore surface. These oxygens that are distributed as a ladder along one side of the pore and serve as hydrogen acceptor sites to efficiently funnel water molecules through the AQP channel. Formation of hydrogen bonds between AQP and water compensates for the solvation energy, when a molecule enters from the bulk solution into the pore [49]. Since the channel is rather symmetric in its nature, water permeation occurs in both directions, with the net water flux following the osmotic gradient [49].

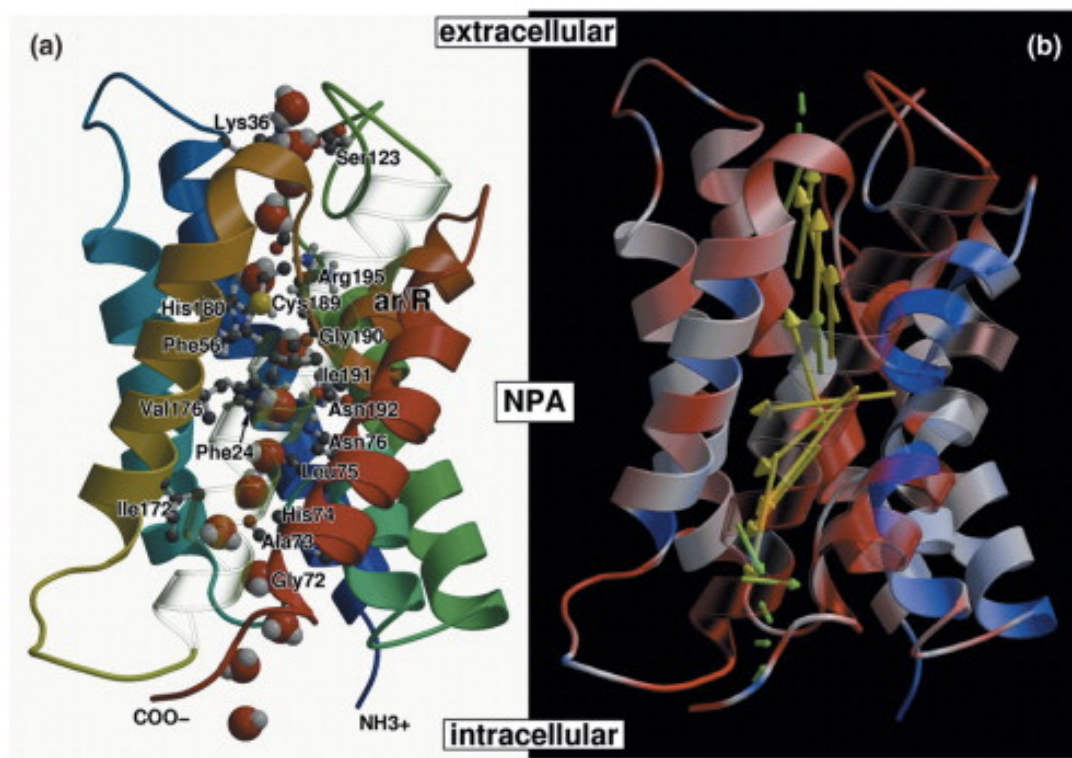


Figure 1.3: (a) Pathway of water molecules through the AQP1 pore, pore lining residues are labeled; (b) Orientational distribution of water dipoles within the pore, due to the electrostatic field in the channel, water molecules show a bipolar orientation within the pore, with the symmetry center located in the NPA region, structural model, taken from [51].

1.1.2 Aquaporin-6

It was not possible to obtain sufficient amounts of pure protein, as heterologous overexpression turned out to be difficult, due to low expression rates and cytotoxicity issues [52]. Therefore, AQP6 has not been available for structural studies until today. Compared to other AQPs, AQP6 has a unique distribution and a distinct function. It is an intracellular channel that is gated and permeated by water and anions.

Expression in kidney and intracellular localization

Isolating a rat cDNA clone encoding AQP6 by PCR-based homologous cloning from a rat kidney cDNA library proved existence of AQP6 on cDNA level. AQP6 has high sequence homology to AQP0, AQP2 and AQP5. The genes encoding AQP2, AQP5, and AQP6 are localized at chromosome band 12q13 as a family gene cluster at this locus. The function and localization of AQP6 is different from AQP0, AQP2 and AQP5 [24].

AQP6 is localized in intracellular vesicles, mainly in the kidney, but also in other tissues. The co-localization of AQP6 with vH^+ -ATPase in intracellular vesicles of acid secreting cells in collecting ducts of kidney was shown by immunolabeling and immunoelectron microscopy (immuno-EM) [53]. The distribution of AQP6 in rat kidney was examined with rabbit polyclonal antibodies against the C-terminus of rat AQP6. The anti-AQP6 antibody showed a major 30 kDa band and a 28 kDa band on immunoblots of rat renal cortex, outer medulla, and inner medulla. The 30 kDa band was completely digested by peptide/N-glycosidase F or by endoglycosidase Hf, suggesting that AQP6 is a N-glycosylated protein. Immunohistochemistry revealed that AQP6 is abundant in intercalated cells of connecting tubules, cortical collecting ducts, the outer and inner medullary collecting ducts. The labeling pattern implied labeling of type A intercalated cells, which was confirmed by immunocytochemistry using anti-AQP2 to label adjacent principal cells in parallel semi thin cryosections and by immuno-EM. Immuno-EM of type-A intercalated cells revealed that AQP6 is localized in intracellular vesicles and cisternal profiles, both in the subapical and in basolateral domains. Double labeling indicated that AQP6 is co-localized alongside vH^+ -ATPase in intracellular vesicles, but not at all in the plasma membrane where vH^+ -ATPase is translocated at stimulation of acid secretion. The pore opening for anions is regulated by low pH (pH 5.5). These observations strongly suggest that AQP6 is an intracellular vesicle water channel. Therefore, AQP6 may play a role in acid-base regulation, but not in water reabsorption [24].

Extra renal expression

Although AQP6 was initially cloned from the kidney and is most abundant in the kidney the evidence shows extra renal distribution of AQP6 (Table 1.3), for example in synaptic vesicles or the inner ear [54, 55].

Physiology

The cellular function of AQP6 is not clear yet and still subject of discussions. The localization of AQP6 in intracellular vesicles might be an indication of its role in the cellular context, suggesting that a role in acid-base homeostasis is likely.

The physiological relevance of AQP6 was examined using *in vivo* rat models. AQP6 abundance and mRNA expression were significantly regulated in response to chronically altered acid/alkali loads, as well as in response to changes in water balance. A marked increase in AQP6 abundance was observed in water loading of rats with lithium induced nephrogenic diabetes insipidus, where AQP2 abundance in the kidney is significantly reduced. This indicated that AQP6 is not important for urinary concentration. AQP6 expression was also significantly upregulated in chronic alkali-loaded (NaHCO₃-loaded) rats. In contrast, NH₄Cl loading in rats did not show changes in AQP6 expression. In addition there was no evidence of trafficking of AQP6 from intracellular vesicles to plasma membrane. Chloride-depleted metabolic alkalosis was associated with a withdrawal of vH⁺-ATPase from apical plasma membrane to subapical cytoplasmic tubulovesicles in type-A intercalated cells, where AQP6 is localized, and resulted in an increased number of numerous subapical tubulovesicles. The upregulation of AQP6 expression in response to alkali loading may be important for endocytic processes [24].

Table 1.3: Studies and reviews on AQP6 during the last twelve years. Localization, co-expression with other AQPs and role in diseases. Blue: evidence for localization in intracellular vesicles, red: outer membrane, white: not commented.

Localization	Evidence	(Proposed) Function	Date	Ref.
Rat retina	AQP6 RT-PCR	Glia-mediated osmo and ion regulation	2011	[56]
Secretory vesicle	G-protein mediated water channel (AQP6)	Synaptic vesicle swelling	2011	[54]
Secretory vesicle	AQP6, vH ⁺ -ATPase	Vesicle acidification for AQP6 mediated gating of water into synaptic vesicles	2010	[57]
Rat inner ear	AQP6 RT-PCR, immunohistochemistry	Outer hair cell motility, modulating OHCs' responses (because water and anion) permeable	2010	[58]
Rat Kidney	Rat kidney cDNA library	Distinct from AQP0, AQP2 and AQP5	2009	[24]
Kidney collecting duct	Pull-down by calmodulin	Calmodulin binding Putative N-terminal binding site	2009	[59]
Gastrointestinal tract	RT-PCR and immunoblotting	55 kDa band – AQP6 dimer Movement of water and anions	2009	[60]
Salivary gland acinar cells	RT-PCR, western blotting	Secretion of anions Hg ²⁺ enhanced	2009	[61]
Intracellular vesicles of the stria vascularis, endolymphatic sac, vestibule, rat inner ear	RT-PCR, immunolocalization	No expression in plasma membrane	2008	[62]
Rat parotid acinar cells	RT-PCR western-blotting	Secretory granules, water and anion transport in plasma membranes near tight junctions	2008	[63]
Rat kidney type-A intercalated cells of the collecting duct	A: like rat AQP6 B: no function as water or anion channel	Two splice variants in mouse, regulated age and tissue specific	2007	[64]
Human inner ear	Immunoblotting	AQP6: apical portion of interdental cells in the spiral limbus, Inner ear water homeostasis	2007	[55]
Renal collecting ducts	N-terminus is critical for trafficking	Exclusively localized intercellular vesicles in acid secreting type-A intercalated cells	2006	[53]
Synaptic vesicles	Immunoblotting	Vesicle swelling AQP1 and AQP 6	2005	[65]
Genetics	AQP6 mutation	Causes <i>Diabetes insipidus</i> ?	2005	[66]
AQP6 water and anion channel?	<i>Review</i>	Water channel function of AQP6 cannot determined with confidence	2004	[67]
Renal AQP	<i>Review</i>	From molecule to disease	2003	[68]
Heterologous expression in transfected HEK cells	GFP-AQP6 in plasma membranes	pH induced anion currents High nitrate permeability, then Cl ⁻	2002	[69]
Heterologous expression on oocytes	Patch clamp	Hg ²⁺ & low pH activates Cl ⁻ and Na ⁺ channel, Cys155 and Cys190 activation sites	2002	[70]
Expression in rat kidney	Immunohistochemistry	Inner and outer medullar collecting ducts: intercalated cells, cells also express vH ⁺ ATPase; no glomerular expression	2001	[71]
Collecting duct intercalated cells	Immunohistochemistry Immunoblotting	Exclusively intracellular vesicles expression is regulated by altered acid/alkali load or water balance, AQP6 may contribute to maintenance of acid-base homeostasis and water balance	2000	[72]

Sequence analysis / Secondary structure

AQP6 has high sequence homology to AQP0, AQP5 and the genetically closest sequence to AQP2 (Figure 1.6). The amino acid sequence of AQP6 reveals that AQP6 potentially meets the mechanisms for permeation of water and for repulsing ions, based on the atomic structure model of AQP1. Like other AQPs AQP6 has a molecular weight around 30 kDa (28,860 kDa). The secondary structure of the functional monomer is comprised of two tandem repeats with three transmembrane domains each, and cytoplasmic N- and C- termini. The functional monomer forms homo-tetramers as conserved throughout AQPs. The transmembrane topology of AQP6 is depicted in Figure 1.5.

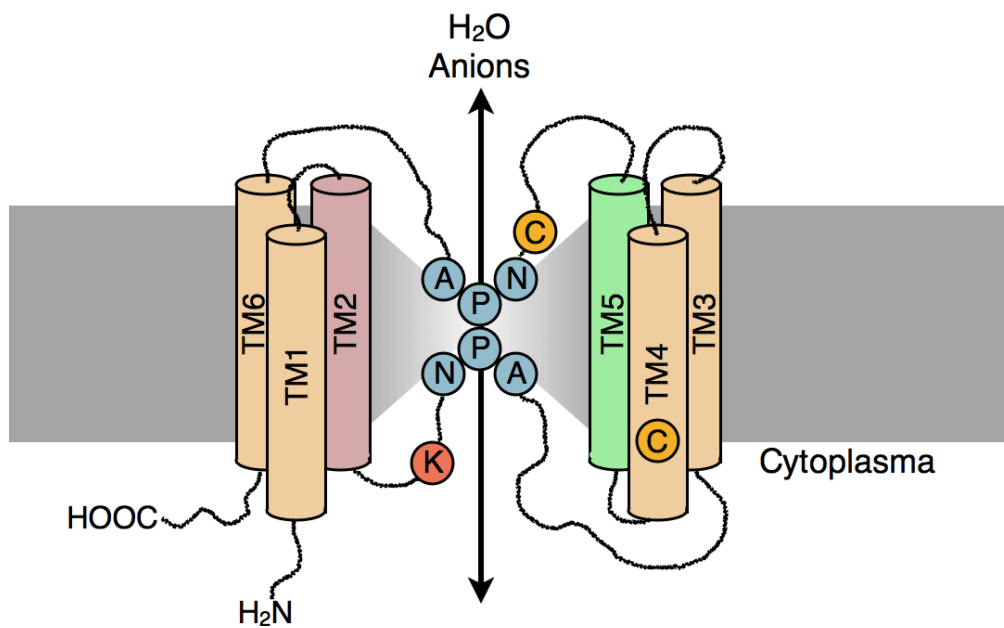


Figure 1.5: Schematic view of AQP6 transmembrane topology. Blue: highly conserved N, P and A residues forming the aqueous pore, Red: pore lining charged residue Lys-72, Yellow: Hg^{2+} activation sites Cys-155 and Cys-190, derived from [34].

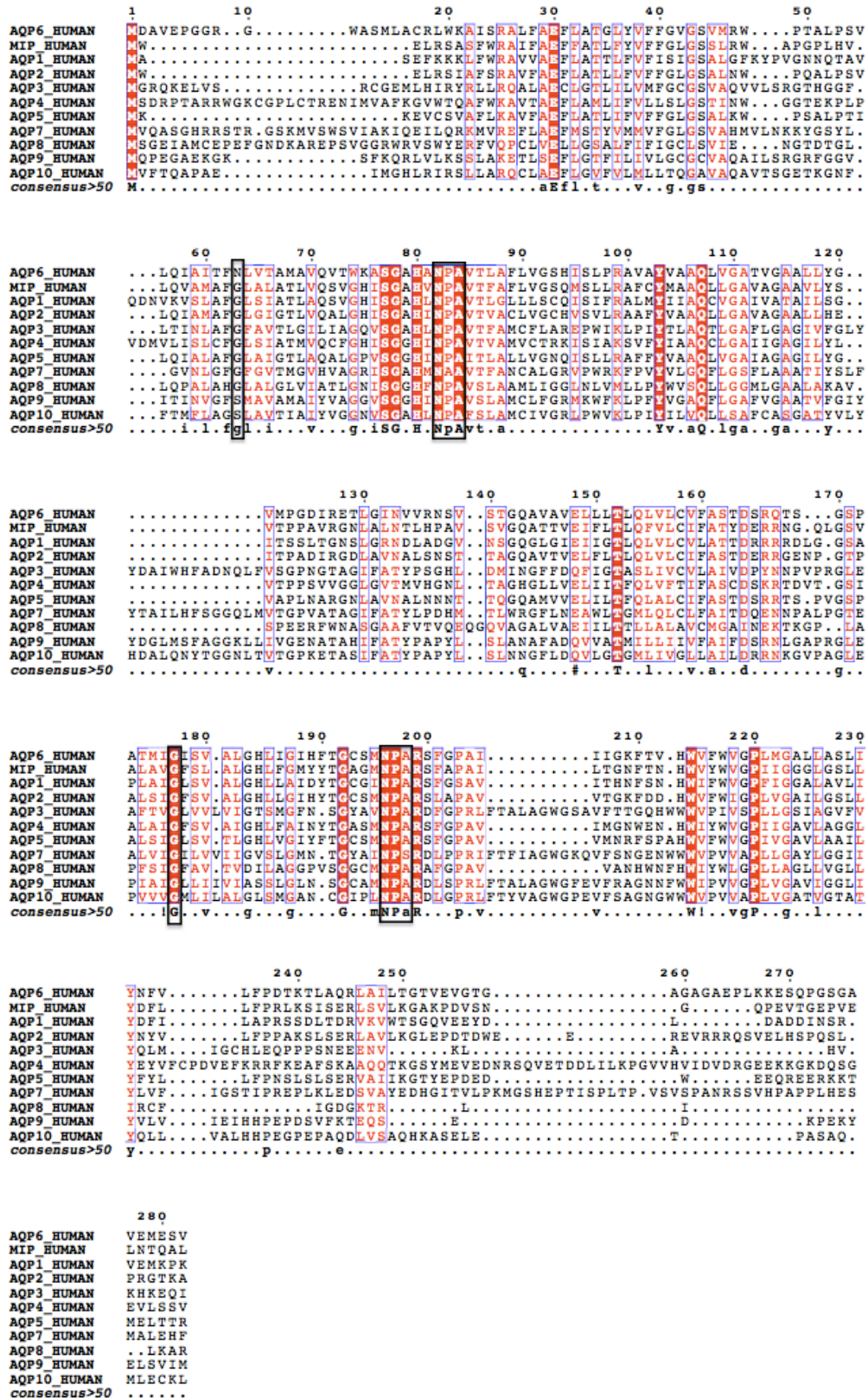


Figure 1.6: Sequence alignment of human AQPs. Black frames depict NPA regions, AQP6 Asn63 and Gly177. Sequence alignment was visualized using ESPrIt [73].

AQP6 is permeated by anions, suggesting that minor differences in the sequence of AQP6 may lead to major differences in biophysical function. Critical amino acid residues for anion permeability of AQP6 were identified by analysis of the sequence (Figure 1.6). A series of site-directed mutagenesis revealed that Asn60 in rat AQP6 is critical for ion permeation. Asn60 in rat AQP6 corresponds to Asn63 in human AQP6 and Gly57 in human AQP1. The glycine residue at this position is conserved among all mammalian AQPs. The atomic model of AQP1 revealed that Gly57 is located in the middle of TM2 and interacts with Gly174 (corresponding to Gly177 in human AQP6), which is also conserved among all mammalian AQPs in the middle of TM5. TM2 and TM5 are closely packed as result of the Gly-x-x-Gly-x-x-x-Gly motif packing, where alanine or serine often replaces glycine [74]. The fitting of ridges into grooves in TM2 and TM5 locks the two AQP1 helical bundles together near the fourfold axis of the tetramer. This implies that the structure of AQP1 is relatively rigid. The presence of an asparagine residue at this position allows AQP6 channel gating of anion permeability. A single amino acid substitution at Asn60 for Gly60 (N60G) totally eliminates the anion permeability of AQP6 when expressed in *Xenopus laevis* oocytes [75]. The AQP6 N60G mutant expressed in oocytes, shows significantly increased water permeability, which is not inhibited by HgCl₂. Taken together, a single amino acid substitution (Asn60 for Gly60) switches the function of AQP6 from that of an anion channel to that of a water-selective channel. N60G/G174N double mutations and reciprocal glycine to asparagine mutations in AQP0, AQP1 and AQP2 all failed to traffic to the plasma membrane, suggesting that the interaction of TM2 and TM5 is precisely defined and that slight differences at this position lead to significant conformational changes [75].

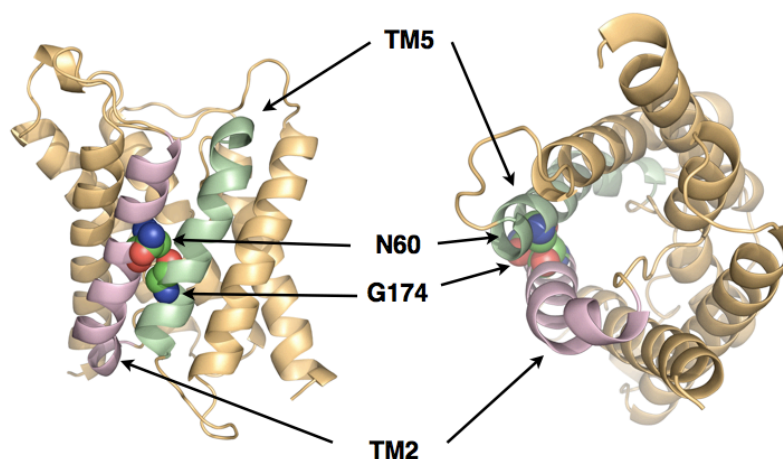


Figure 1.7: Homology model of AQP6. Left: side view, right: top view. Interacting transmembrane helices TM2 and TM5 are highlighted. The asparagine residue in middle of TM2 is in close contact to glycine 174 in TM5 and critical for anion permeability of AQP6. Homology modeling was performed on the basis of AQP5 (PDB code: 3D9S) using MODELLER 8.2 [76]. AQP5 was chosen as starting model, because of close genetically relation.

Functions / Regulation

In terms of function, AQP6 can be characterized as an aquaglycoporin, like AQP3, AQP7 and AQP9. It allows glycerol and urea to pass through its pore. But in terms of its amino acid sequence and genetic localization AQP6 is closer related to the AQP water channels [77].

Table 1.4: Functional studies on AQP6.

System	Finding	Year	Ref.
Oocytes	N60G in rat AQP6 eliminates the anion permeability, Higher water permeability	2005	[75]
Oocytes	Activated by Hg ²⁺ Water, glycerol and urea uptake?	2004	[78]
HEK cells GFP-AQP6 in plasma membrane	pH induced anion currents high nitrate permeability, then Cl ⁻	2002	[69]
Patch clamp	Hg ²⁺ or low pH activates Cl ⁻ and Na ⁺ channel Cys155 and Cys190 activation sites	2002	[70]
Oocytes	Function as anion channel	1999	[34]
Mouse parotid acinar cells	Function as anion channel	2009	[61]

Channel properties of AQP6 were mainly studied with AQP6 heterologously expressed in *Xenopus laevis* oocytes. Expressed in this system, AQP6 is not localized in intracellular compartments, but in the plasma membrane of the oocytes in contrast to native expression for example in kidney tissue. The localization in the plasma membrane enabled the investigation of AQP6 by electrophysiological assessments using the two-electrode voltage clamp technique. The osmotic water permeability of AQP6 was limited under basal conditions and significantly increased in the presence of HgCl₂ in concentrations around 0.1 mM [34, 70]. This is an unanticipated result, because HgCl₂ is known to inhibit the water permeability of most AQPs. AQP6 is the only AQP that is activated by HgCl₂, which also induces the urea and glycerol permeability [78]. Cell-attached patch recordings of AQP6 expressed in oocytes indicated that AQP6 is a gated channel with intermediate conductance induced by 10 μM HgCl₂. The Hg²⁺-induced AQP6 conductance is voltage-independent [67, 70]. Further experiments revealed that the rapid activation of AQP6 by HgCl₂ is restricted

by β -mercaptoethanol. Both, water and ion permeability of AQP6 is probably activated by Hg^{2+} binding to Cys-155 or Cys-190 in each monomer. Site-directed mutagenesis revealed that changes in water permeability resulted in equivalent changes in ion conductance. These findings suggest that each monomer forms a pore region for water and ions, rather than ionic permeation through the center of homotetramer [24]. The colocalization of AQP6 with vH^+ -ATPase in intracellular vesicles of acid-secreting intercalated cells in renal collecting ducts implies that AQP6 might be regulated by low pH. In fact, a membrane current rapidly appeared in AQP6 oocytes at pH 4.0, slightly outward rectifying, which was immediately reversed after return to pH 7.5 [34]. The current induced by low pH is much more selective to Cl^- ions than to Na^+ ions. The anion selectivity was changed in K72E mutant AQP6 [34, 69]. The position of Lys-72 at the cytoplasmic vestibule of the aqueous pore indicates that the membrane currents in AQP6 oocytes are inherent channel permeation properties of AQP6 [24].

Anion and nitrate transport

Ion permeation by AQP6 was evaluated not only in oocytes, where low pH activates AQP6 as an anion channel, with high permeation rates by nitrate [34], but also in mammalian cells. AQP6 is not expressed at the plasma membranes in transiently transfected mammalian cell lines like *in vivo* rat kidney tissues. The addition of a green fluorescence protein (GFP) tag to the N-terminus of rat AQP6 (GFP-AQP6) redirects the protein to the plasma membrane of transfected HEK (human embryo kidney) 293 cells [69]. At pH 4.0, currents are rapidly and reversibly activated in HEK 293 cells expressing GFP-AQP6. The features of acid-induced currents in cells expressing GFP-AQP6 are similar to measurements of AQP6 overexpressed in oocytes. A series of ion replacement experiments gave the following halide permeability sequence: $\text{NO}_3^- > \text{I}^- \gg \text{Br}^- > \text{Cl}^- \gg \text{F}^-$. Altogether, AQP6 is a pH-regulated anion channel with high permeability for nitrate. Site-directed mutagenesis revealed that the pore lining threonine residue (Thr-63) at the midpoint of the channel is important for $\text{NO}_3^-/\text{Cl}^-$ selectivity, supporting the theory that nitrate ions permeate through the aqueous pore of AQP6 [24, 69].

RT-PCR, western blotting and immunohistochemical analyses demonstrated AQP6 expression in the apical membrane of mouse salivary gland acinar cells. Electrophysiological experiments showed an anion permeability sequence: thiocyanate (SCN^-) $> \text{NO}_3^- > \text{I}^- > \text{Br}^- > \text{Cl}^-$. NO_3^- currents were enhanced by application of extracellular Hg^{2+} [61].

Involvement in synaptic vesicle swelling

There were indications that AQP6 is involved in synaptic vesicle swelling, a mechanism that is partially unsolved. AQP6 is, besides vH⁺-ATPase and the heterotrimeric G_o protein, associated with synaptic vesicles and participates in their swelling [65]. An AQP6 mediated water transport into synaptic vesicles as a consequence of vH⁺-ATPase-induced intracellular acidification was proposed [57].

Summary

AQP6 is a genetic member of the water channel family, but its physiological function is most likely not (only) water transport. The exact physiological function of AQP6 is still obscure. It has been detected in several distinct tissues, in intracellular vesicles and the outer membrane, but the intracellular localization and the involvement in acid base homeostasis are most likely. The molecular mechanism of the functional switch from a water to an anion channel is still not understood.

1.2 Heterologous expression of Aquaporins

Many eukaryotic AQPs are not expressed in high amounts *in vivo* (exceptions, AQP0, AQP1). For this reason heterologous expression is required for structural studies. In our lab AQP2, AQP8 and SoPIP have been heterologously expressed in *Spodoptera frugiperda* (Sf9) insect cells (AQP2) and *Pichia pastoris* so far. Several AQPs were heterologously expressed, characterized functionally and structurally. Table 1.5 gives a partial insight into different expression systems applied for heterologous AQP expression.

Table 1.5: Examples of heterologous expressed AQPs for structural studies in different systems. Many AQPs were purified by affinity chromatography using a hexa-histidine (6xHis) tag.

Aquaporin	Expression system	Purification	Application	Result	Ref.
Human AQP2	Baculo virus/ Sf9 insect cells	N-terminal 6xHis	Electron crystallography	4.5 Å 3D structure	[39]
AQP8	<i>P. pastoris</i>	C-terminal 6xHis	Electron crystallography	2D crystals	[43]
SoPIP2;1 (spinach)	<i>P. pastoris</i>	Ion exchange	Electron crystallography	5 Å 3D structure	[79]
Rat AQP4	Baculo virus / Sf9 insect cells	Poly-His	Electron crystallography	2.8 Å 3D structure	[41]
Human AQP4	<i>P. pastoris</i> X-33 cells	N-terminal 8xHis + flag + 3C cleavage site	3D crystallization	1.8 Å 3D structure	[40]
Mouse AQP4	Cell free expression	6xHis	Reconstitution into liposomes	Activity measurements	[80]
Human AQP5	<i>P. pastoris</i> X- 33 cells	Cation exchange	3D crystallization	2.0 Å 3D structure	[42]
Bacterial AQPZ	Cell free expression	6xHis	Expression into liposomes	Activity measurements	[81]
Bacterial AQPZ	<i>E. coli</i>	N-terminal 6xHis	3D crystallization	2.5 Å 3D structure	[82]

	Cell-free	<i>E. coli</i>	Yeast	Insect cells	Mammalian cells	<i>C. elegans</i>	<i>Xenopus</i> oocytes
Setup and costs	Red	Green					
(Cell growth) time	Red						
Preparative scale	Red	Red					
Native environment	Green						

Figure 1.8: Properties of expression systems based on different organisms for the expression of mammalian membrane proteins. Green: advantage, red: disadvantage. Besides the systems introduced here in more detail, insect cell (*e.g. Sf9*), *C. elegans* [83] and *Xenopus* oocytes [84] have been used for mammalian membrane protein expression.

Bacterial expression systems are easy to set up and relatively time saving. They are well established for soluble proteins. However, expression of eukaryotic membrane proteins might lead to misfolded protein and formation of inclusion bodies [85].

Eukaryotic *yeast* has several advantages for the heterologous expression of membrane proteins. It is easy to grow and handle, large-scale production in fermenters is possible and yeast is capable to introduce posttranslational modifications like glycosylation and disulfide bridges. A widely used system is *Saccharomyces cerevisiae*. Recently the methyl tropic yeast *Pichia pastoris* is of growing importance for membrane protein production [40, 42, 79].

Heterologous overexpression in *mammalian cells* has the advantage that the configuration for folding, posttranslational modifications, membrane insertion and translocation of membrane proteins is present. Nevertheless, the major disadvantages are that mammalian cells grow slowly, consume expensive media and are not easy to handle, especially when cells are not suitable for suspension culture [52]. It might be very time-consuming to establish stable membrane protein-expressing cell lines. Another approach is the use of alpha viral expression systems like *Semliki Forest virus* or *Sindbis virus* expression systems.

Cell-free protein expression is an attractive option for proteins that are difficult to express or fail to express in cell based conventional expression systems like bacterial, yeast or mammalian cells. The main difference to protein production in conventional expression systems is that expression takes places in an entirely open system, e.g. protein expression takes not place behind cell walls like in *in vivo* systems. It is possible to add compounds that stabilize produced proteins like ligands, co-factors, inhibitors,

as well as the addition of cytotoxic compounds or the expression of proteins with cytotoxic effects. Cell-free systems are an attractive alternative for the expression of membrane proteins. Because of its open character the addition of detergents, lipids, liposomes, bicelles and nanodiscs is feasible. Furthermore, membrane protein production in cell-free systems is independent of transport and translocation pathways, and inclusion body formation. However, especially for the expression of eukaryotic proteins in prokaryotic systems, molecular chaperones which are essential for correct folding of membrane proteins are not present [86]. For cell-free expressed bacterial AQPZ [81] and mouse AQP4 [80] it was demonstrated that both proteins show similar activity to protein from cell-based expression systems.

AQP6 has low expression rates in native tissue. For this reason a purification of AQP6 from native tissue is not practicable. Furthermore, expression of AQP6 in transiently transfected mammalian cell lines was not successful [52]. Heterologous expression is the method of choice to obtain greater amounts of AQP6. For heterologous overexpression, many systems are available, based on bacteria, yeast, insect cells or mammalian cells. An alternative to explore is the cell-free expression technology. When choosing the best expression system some factors should be considered: total yield, time, manageability, upscaling ability, safety, membrane insertion, translocation, folding, and posttranslational modifications.

As most mammalian membrane proteins, AQP6 is glycosylated. It has one potential glycosylation site, N134 in the region of loop B. This N-linked glycosylation might be essential for translocation and function. Therefore heterologous expression of AQP6 should be carried out in a system, which has the ability for posttranslational modifications or where translocation is not necessary (cell-free).

1.2.1 Cell-free membrane protein expression

Principle

Living cells are not essential for biological protein synthesis. Cell-free protein expression is the combination of recombinantly produced transcription proteins and translation systems from cell extracts with amino acids and energy regenerating systems.

In the 1950s, the first single compartment cell-free systems were introduced. Productivity of recombinant proteins was in the nanogram or microgram scale, because of a limited protein synthesis time. The lifetime was restricted by fast the consumption of precursors and inhibition of the translation process through accumulation of breakdown products [87-89].

Higher production rates were achieved by the separation of the reaction chamber into two compartments. In recent cell-free expression systems, the reaction mixture (RM) and the feeding mixture (FM) are separated by a semi permeable membrane [90, 91]. The protein synthesis takes places in the RM, which contains the transcription and translation machinery. The FM provides a reservoir of low molecular mass precursors in a fixed volume. The membrane ensures the removal of undesired breakdown products from the RM and the permanent supply of fresh precursors and energy substrates from the FM by diffusion, while the transcription and translation machinery and synthesized protein are not able to pass the membrane. With this continuous exchange setup (continuous exchange cell-free (CECF)), an extended protein synthesis is achievable for several hours. This enables the production of recombinant protein in milligram scales overnight (Figure 1.8) [92, 93].

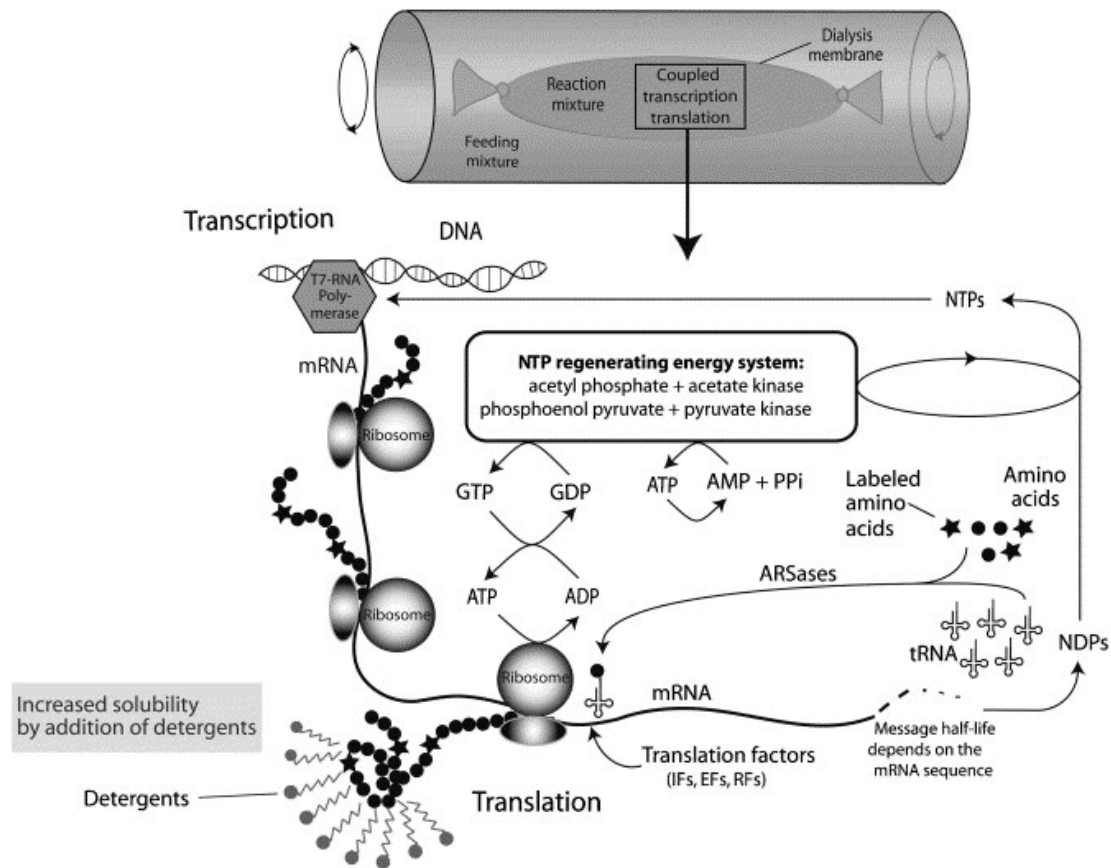


Figure 1.9: Schematic configuration of a coupled transcription/translation reaction in a CEFC system. Taken from [94].

For the production of membrane protein reactions with or without addition of detergent to the FM and RM are options. During cell-free expression without detergent (P-CF), the freshly synthesized membrane protein precipitates. In contrast in the presence of detergent (D-CF), in concentrations above the critical micelle concentration (cmc), the membrane protein is typically solubilized in detergent micelles. In addition, cell-free expression in presence of pre-formed liposomes (L-CF) is possible, where membrane protein might insert during translation. To enhance protein insertion, an addition of detergent to liposomes in order to destabilize them might be useful. All modes P-CF, D-CF and L-CF were used for successful membrane protein expression (Figure 1.10) [81, 94, 95].

In order to produce functionally active protein, subsequent solubilization and reconstitution parameters should be screened for different detergents, lipids and concentrations. An optimal strategy should be analyzed for each new membrane protein target. While yields are generally higher in the P-CF configuration, D-CF might result instantly in the functionally folded membrane protein [93].

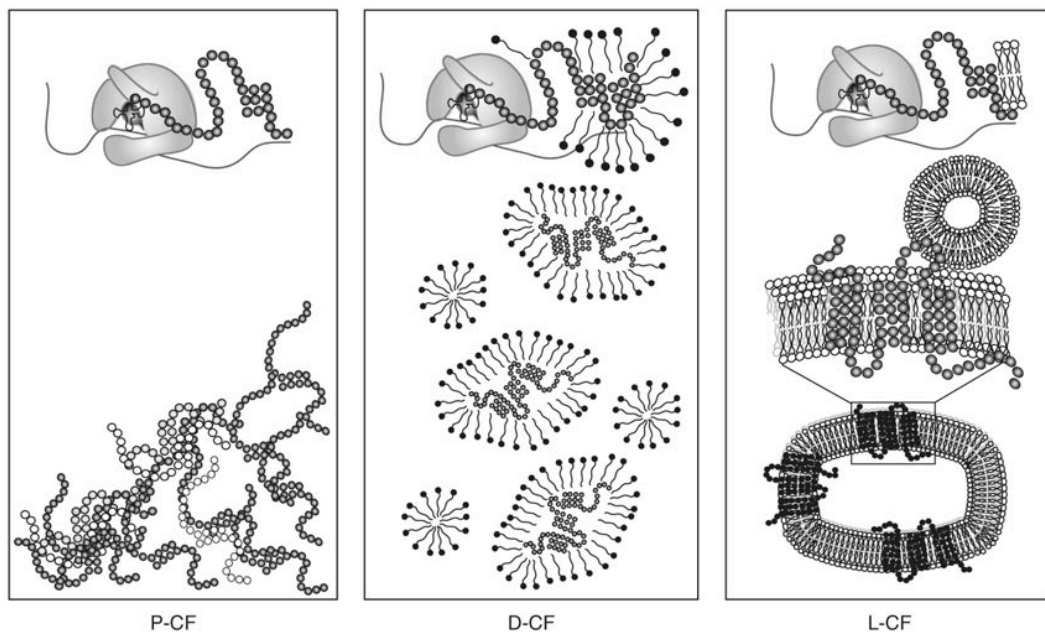


Figure 1.10: Schematic view of CF approaches for the production of membrane proteins. P-CF: proteins are synthesized in the absence of detergents and precipitate after translation. D-CF: proteins are kept in a soluble form by insertion into detergent micelles provided. L-CF: proteins can insert into liposomes. Taken from [96].

Equipment & Reagents

In general, individual systems or systems which are commercially available like the Rapid Translation System (RTS, 5-Prime) [97-99] or the Expressway milligram system (Invitrogen) [100] can be used. Using a self-developed, individual system reduces costs per reaction to 1/50 compared to a commercial system. For continuous exchange cell-free reactions, the reaction container should be extensible for housing a dialyses membrane or a complete dialyses cassette.

A major and important part of cell-free expression systems is the extract containing the transcription and translation machineries. Cell-free expression systems are classified by the source of their extract, because they are premised on different extracts: for example extracts from wheat germ, insect cells or *E. coli*. The most common systems are based on extracts made from *E. coli* or wheat germ lysates [91, 95, 101, 102]. A feature of cell-free expression systems based on wheat germ extracts is its high stability. Extended reaction times up to several days are achievable. Because of the low endogenous RNase activity the translation with purified mRNA as a template is possible. In contrast, *E. coli* extracts are used in coupled transcription/translation systems with double stranded DNA as a template. The expression yields of both systems are comparable [103]. Protocols for individual systems are based on crude cell lysates, optimized buffer and salt conditions, all additional components required for

transcription and translation. Since T7 RNA polymerase is needed in high amounts and concentrations for mRNA synthesis, the most efficient way to obtain it, is the heterologous overexpression in *E. coli*, followed by purification [104]. The energy regenerating system is based on high energy phosphate donors: phosphoenol pyruvate, acetyl phosphate, creatine phosphate and their corresponding kinases that ensure the recycling of hydrolyzed nucleotide triphosphates [105].

DNA template design

Templates for cell-free reactions can be plasmid DNA or PCR amplification products [106]. Since the *in vitro* transcription to generate mRNA is the first step of cell-free expression, target gene should be under control of a strong promoter like T7 or SP6. Expression vectors that are employed for expression in *E. coli* and offer a T7 promoter like pET or pIVEX are used. The introduction of 18 bp to 24 bp large N-terminal tags can significantly improve the efficiency of cell free expression reaction and the yield of synthesized protein [107].

Transcription & translation

In *E. coli* based cell-free systems, transcription and translation reactions are coupled. Plasmid DNA is directly introduced to the reaction mixture. The concentrations of polymerase and plasmid DNA need to be optimized. Further target specific optimizations to enhance the reaction efficiency are detergent, lipids, co-factors, inhibitors and substrates addition. The first optimizations steps of expressing a new target were carried out in the P-CF mode in order to optimize for highest yields. In a second step the D-CF or L-CF mode was carried out, optimizing for protein quality.

Purification

The choice of purification protocols for cell-free expressed protein depends on the expression mode. First purification steps of P-CF expressed protein are pelleting and solubilization. Then, an affinity tag purification step could be carried out like for protein produced in the D-CF mode. L-CF produced proteins which are inserted into liposomes might be purified by sucrose gradient centrifugation or solubilization and affinity chromatography.

Table 1.9: Consideration of advantages and disadvantages of cell-free expression systems.

Advantage	Disadvantage
Open system, individual reaction conditions for each individual target protein like addition of detergents, lipids etc.	Intensive optimization of reaction conditions required
Direct translation of PCR products possible, high throughput screening	High quality control of reaction components essential
Production of toxic proteins, circumvention of cytotoxic effects	Relatively high costs
Miniaturization (e.g. 50 μ l reaction), screening for ideal conditions	Preparation of extracts necessary
Eukaryotic systems available	Complexity of system requires experience

Application

An extensive number of membrane proteins from different organisms was expressed using cell-free systems until today. *E. coli* based systems are considered as a promising tool for preparative expression of mammalian membrane proteins [95, 98, 99]. Functionality of expressed proteins was mostly proven by ligand binding, disregarding that only a minor amount of protein might contribute to ligand binding. Until today there is no high-resolution crystal structure of a cell-free expressed membrane protein. The assembly of a large complex consisting of cell-free expressed soluble and membrane protein subunits was shown with the F_1F_0 ATP-Synthase complex from *Caldalkalibacillus thermarum* using negative stain single particle electron microscopy [108].

1.2.2 The *Semliki Forest Virus* expression system

Principle

The *Semliki Forest virus* (SFV) is an alpha virus that belongs to the family of *Togaviridae*. The virus has a broad host range and the capability to infect mammals, birds, insects and reptiles through inhalation and gastrointestinal exposure. It causes encephalitis. The SFV is a RNA virus whose genome is encoded on single stranded RNA of positive polarity and a total size of 11,5 kB. The genomic 42 S RNA is packed into 240 capsid proteins that form the envelope and are covered by a lipid bilayer membrane. The membrane is spanned by the viral spike glycoproteins E1, E2, E3 [109]. The spike proteins concede endocytosis with target cells, because the glycoproteins are recognized by cell receptors of the host cell. The fusion of virus membrane and lysosomal membrane of the target cell follows subsequently to this recognition. After endocytosis, the viral RNA is released into the cytosol [110].

The genomic 42S RNA serves as mRNA and is translated into the viral non-structure polyprotein. After auto cleaving, the originated four proteins are setting up the replicase complex, a RNA polymerase and the transcription of (+)-strand RNA into (-)-strand RNA is initiated. The (-)-strand RNA serves as template for additional (+)-strand RNA. In addition, the (-)-strand RNA functions as template for subgenomic 26S RNA, coding for the viral structure proteins the capsid protein and E1, E2, E3. The capsid protein binds to genomic RNA and forms a nucleocapsid. The structure proteins are translated as one precursor of E2 and E3, p61 and p62 the precursor of E1. p61 and p62 form a dimer in the ER membrane. While transported to the plasma membrane the structure proteins are processed to glycoproteins. The virus is released by budding. It is a nucleocapsid surrounded by spike-protein containing cell membrane. (*Virus replication and protein expression are reviewed in [109]*).

For the usage of heterologous membrane protein expression the viral genome was distributed to two plasmid vectors as cDNA copies. The expression vector (pSFV) contains the nonstructural genes, the strong subgenomic 26S promotor, a multi-cloning site for the introduction of foreign genes and a packing signal sequence [111]. The helper vector (pHelper) encodes for the structure proteins and the capsid and is not packed into particles, due to a lack of the packing signal. For this reason, virus particles contain the recombinant RNA from the expression vector, but not the helper RNA. As a result, the virus can infect cells but not build new virus particles in host cells after infection. Besides the wild type Helper vector, pHelper1, the pHelper2 vector is widely used. It carries three point mutations in the p62 structure protein. Three Arg were

introduced at the E2-E3 interface instead of Ser, Gln and Leu. These mutations prevent the cleavage of p62 into E2 and E3, which is crucial for mediating the virus intake [112]. This means that a virus with this mutation is not infectious for eukaryotic cells. Only after activation of the virus by chymotrypsin treatment that causes the cleavage of p62 into E2 and E3 it can be used to infect cells. These mutations and the lacking packing signal for the structural proteins prevent the release of virus, which is infectious and has the ability to replicate itself. As a result, for the work with pHelper2 safety level one is sufficient.

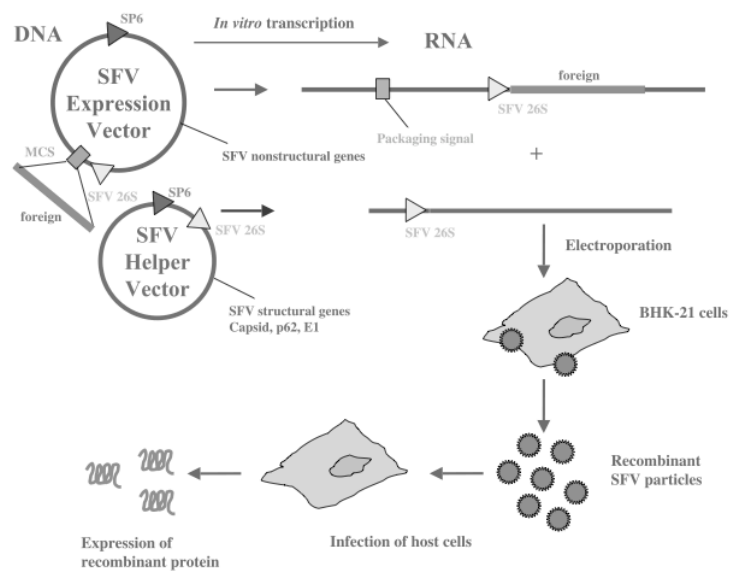


Figure 1.11: Schematic illustration of the production of SFV particles. Recombinant and helper RNAs are *in vitro* transcribed from linearized DNA plasmid. BHK cells are co-electroporated and recombinant SFV particles are harvested. Generated particles can be used for infection of cells after activation with α -chymotrypsin. Taken from [111].

Equipment & Reagents

The application of the SFV expression system is relatively expensive, because cell culture equipment is needed. Safety level 2 facilities are not obligatory. Due to the mutation of the pHelper vector, untreated virus is not infectious.

DNA template design

In the SFV expression system, the virus genome is distributed over two plasmids: the helper vector (pHelper) and the expression vector (pSFV). The gene of interest is cloned into the pSFV vector, which has a multiple cloning site. Both vectors carry a SP6-RNA polymerase promoter that is used for RNA production by *in vitro* transcription. In addition, pSFV and pHelper vectors have a restriction site at the 3'-ends of the coding regions to allow linearization.

Transcription & translation

For every expression experiment new RNA for virus production is produced by *in vitro* translation, after linearization of both vectors. Mammalian cells are co-transfected with the resulting RNA to produce virus particles that carry the coding sequence of the gene of interest. After activation of the virus with α -chymotrypsin mammalian cells are treated with the infectious virus. After virus entry by endocytosis the target genes which are under control of the strong 26S promoter are translated after generating multiple transcripts within the cells.

Purification

Lysis of mammalian cells is easy, because cells are more sensitive to rupture than yeast or bacteria. Due to lower culture volumes, only small amounts of cell material are the starting point for solubilization and purification of membranes and proteins. Besides this, there are no differences in purification compared to other systems. Affinity tag purification is possible, since proteins can be manipulated at DNA levels to introduce affinity tags.

Pros & Cons

An immense advantage of the SFV expression system is the native environment for the production of mammalian membrane proteins. A disadvantage is that large-scale membrane protein production is relatively time consuming and expensive. Large amounts of virus are needed for the infection of cells.

Application

Mammalian membrane protein expression using the SFV systems has been carried out for different types of protein before. Table 1.10 provides an overview of approaches.

Table 1.10: Overview of mammalian membrane proteins that can be heterologously expressed using the SFV system.

Protein	Species	Type	Experiment	Ref.
5-HT ₃	Mouse	Ligand gated ion channel	Large-scale expression	[113]
P2X ₁ , P2X ₂	Human	Ligand gated ion channel	Binding	[114]
P2X ₂	Rat/Human	Ligand gated ion channel	Binding, electrophysiology	[113]
Ste2p	Yeast	GPCR	Binding	[52]
P2X ₂	Rat	Ligand gated ion channel	Electrophysiology	
P2Y ₂	Human	GPCR	Binding	
V2R	Human	GPCR	Binding	
HCN2	Mouse	Voltage gated cation channel	Electrophysiology	

1.2.3 The *Pichia pastoris* expression system

Principle

Just as yeast, *Pichia pastoris* is an eukaryotic system that is easy to manipulate and culture, comparable to bacteria. This makes it attractive for protein expression. In comparison to expression systems derived from higher eukaryotes, it is faster and easier to handle and less expensive [115].

P. pastoris is methylotroph, which means that it is able to use methanol as single carbon source. The metabolism of methanol starts with the oxidation of methanol to formaldehyde with molecular oxygen. This reaction is catalyzed by alcohol oxidase (AOX1) in specialized cell organelles, the peroxisomes. Peroxisomes protect the cell for toxic hydrogen peroxide, which is generated as product of methanol metabolism. The affinity of AOX1 to oxygen is very poor. To compensate for that, *P. pastoris* synthesizes large amounts of AOX1 that can make up to 30 % of total soluble protein when methanol is the growth-limiting factor [116]. This phenotype is called Mut⁺ (methanol utilization wild type). In *P. pastoris*, there is an additional alcoholoxidase, AOX2, which is expressed at lower levels. When AOX2 is the only functional alcoholoxidase it leads to the slowly growing phenotype Mut^s (methanol utilization slow). AOX1 expression is efficiently suppressed by glucose and induced by methanol to high levels, when no alternative carbon source is present. For this reason the AOX1 promotor, which controls the AOX1 expression at the level of transcription, is a good choice to control the heterologous expression of proteins. (*The P. pastoris expression system is reviewed in [117] and [118]*).

Equipment & Reagents

A shaking incubator at a temperature of 30 °C is needed for expression using the *P. pastoris* system. Suitable sizes of expression culture are in the range of 10 – 100 ml in analytical scale and 2 – 9 l in preparative scale. The use of baffled shaker flask is recommended, because baffled flasks ensure a better aeration.

DNA template design

The target gene for overexpression has to be present in a vector that carries the AOX recombination sites and resistance against Zeocin. Zeocin is a bleomycine, that is effective against both, pro- and eukaryotes. The Zeocin resistance is another important feature to increase the manageability of the expression system. The resistance gene from *Streptoalloteichus hindustanus* is part of the expression vector pPICZ α and makes

cloning and selection more efficient. The integration of the target gene into the *P. pastoris* genome, generating stable transformants, is taking place by homologous recombination between AOX1 genes, shared by the vector and the genome. The recombination is initiated after transformation with linear vector DNA. Small amounts of the transformants are integrating a multiple number of copies of the target gene into their genome. Due to the gen-dose-effect, they exhibit a high expression rate of recombinant protein. It is possible to identify the multi copy clones by selection with increasing Zeocin concentrations, because the Zeocin resistance gene is part of the recombinated genes.

Transcription & translation

The target gene for heterologous over expression is incorporated into the *P. pastoris* genome. After identification of a highly expressing clone, it can be used multiple times for expression. With adjusted pre-culture volume an upscaling is straightforward; transcription and translation are taking place within *P. pastoris*. Methanol addition for induction has to be adjusted to the final volume. A limitation is the available shaker space. In addition, fermentation cultures are possible and widely used.

Purification

P. pastoris membranes should be urea washed to remove additional membrane associated proteins. Yeast membranes are more resistant to solubilization with detergents. Thus, detergent concentrations and solubilization time have to be increased.

Pros & Cons

Advantages of the *P. pastoris* expression system are that it is easy to handle and upscaleable with relatively low media costs and the option of cultivation in fermenters. As eukaryotic expression system it has the ability for protein folding and posttranslational modifications (*e.g.* disulfide bond formation or glycosylation).

Application

A wide range of mammalian membrane proteins has been produced so far with the *P. pastoris* expression system [115] and used for structural studies including a human ABC transporter [119], a tetraspanin [120] and AQPs (Table 1.5).

1.3 Aim of this work

In contrast to many (mammalian) AQPs, AQP6 has not been characterized in a purified form, because protocols for heterologous overexpression, solubilization and purification have not yet been established. The initial aim of this work was to determine parameters for the expression and purification of AQP6 using an expression system, which is able to produce AQP6 in adequate amounts and quality for functional and crystallographic studies. For 2D and 3D crystallization as well as for functional studies, a large-scale protein expression system is required, that provides up to 10 mg of purified protein in a functional form. Neither wild type AQP6, nor N60G mutant crystal structures have been determined so far. The structural comparison of these isoforms will give a better understanding of how AQP6 is permeated by anions and why other AQPs are not permeated by any ions, including protonated water.

In the first step, an appropriate expression system has to be chosen. In order to identify the best system in terms of sample quantity and quality, overexpression in several systems should be investigated. Initial expression trials in *E. coli* have not shown expression of AQP6. It is known that the ion channel functionality of AQP6 is cytotoxic [52]. Therefore, a cell-free expression system was initially considered, which additionally offers several approaches for membrane proteins. As an open system, cell-free expression allows different detergents, lipids and liposomes to be explored for enhancing protein quality and quantity. Moreover, the toxic effects of an open anion channel can be ignored in a cell-free environment. Due to these considerations, the expression of AQP6 should be carried out using a cell-free system, despite the fact that there is no high-resolution structure of a mammalian protein expressed in a cell-free system available, yet. Another approach is the expression in mammalian cells using the SFV expression system, which was used for expression of GPCRs in the past. It offers the most native environment, since expression is performed in mammalian cells. With a stringent control of the pH in the expression media, cytotoxic effects should be circumvented. Expression in *Pichia pastoris* is another interesting option, because AQPs expressed in *P. pastoris* have been successfully crystallized. The expression of a non-functional AQP6 mutant is a way to evaluate the implications of the opened ion channel in terms of expression, when comparing it to the wild type AQP6.

In order to successfully crystallize a protein, the quantity of the protein is an important factor. Furthermore, it is crucial to determine its quality during purification. To screen for protein quality, several methods were applied. Homogeneity and integrity of the

AQP6 sample can be assessed by single particle electron microscopy of negatively stained samples. Determining protein classes and calculating averages would provide a more detailed picture of sample quality. Successful reconstitution into liposomes would be possible criterion for correct folding. This could be monitored by freeze fracture electron microscopy. Finally, investigating the channel properties, for example water flow of AQP6 reconstituted into liposomes is a way to demonstrate protein functionality.

The initial plan to purify sufficient amounts of protein for 2D crystallization had to be revised; it turned out that the protein quality from cell-free expression and protein quantity from cell-based expression were not sufficient. The modified goal of this work is therefore to establish solubilization and purification protocols for AQP6 expressed in different systems.

2 Methods

2.1 Cell-free protein expression

2.1.1 DNA template design

For DNA template construction, standard molecular cloning techniques were applied. A DNA fragment containing the AQP6 gene followed by a 6xHis-tag was cloned into pET21 vector using *EcoRI* and *XhoI* restriction sites. The pET21 vector was chosen because it contains a T7 promoter site and offers the possibility to use T7 RNA polymerase for transcription of DNA templates. All plasmids DNAs exploited for protein expression were sequenced. For pET21 vectors T7 promoter (forward) and T7 terminator (reverse) sites were used for sequencing primer binding.

2.1.2 Transcription and translation

The most important components of the cell-free expression system are T7 RNA polymerase (T7RNAP) for transcription of the DNA template and mRNA generation and the *E. coli* based cell-free extract, which contains the translation machinery. Since these two components are needed in high amounts and high concentrations for efficient transcription, they have to be prepared manually before starting the cell-free expression reactions.

2.1.2.1 Preparation of T7 RNA polymerase for cell-free expression

T7RNAP, which has a molecular weight of 98 kDa and a pI of 6.77, is the most expensive component of a cell free reaction and has to be supplied in high amounts to provide a sufficient transcription. In addition to the high costs of commercial available T7RNAP, it is often too low in concentration. For overexpression and purification of T7RNAP a previously described and modified protocol [104, 121] was applied.

Overexpression was carried out in a 1 l culture of *E. coli* BL21 Star in LB medium, which was inoculated 1:100 with an overnight culture. The expression culture was incubated at 37 °C under rigorous shaking until an OD₆₀₀ of 0.6 - 0.8 was reached. Expression of T7RNAP was induced with IPTG at 1 mM final concentration and incubated for 5 h with shaking at 37 °C. After incubation, cells were harvested by centrifugation at 4,500 g for 20 min at 4 °C. Pelleted cells with a wet weight of ca. 50 g were resuspended in 100 ml T7 buffer (A.4.2) and stored at -80°C. Since the activity of T7RNAP is sensitive to oxidation, all further steps were carried out under reducing conditions. Resuspended cells were disrupted using a Fluidizer (5 cycles, 1,000 bar) followed by a centrifugation at 20,000 g and 4 °C for 30 min to pellet cell debris and membranes. The supernatant

was adjusted to 2 % streptomycin sulfate by drop wise addition of a 10 % streptomycin stock solution under gentle stirring. Precipitated DNA was removed from the turbid solution by pelleting at 25,000 g for 45 min at 4 °C. T7RNAP was purified from the supernatant by anion exchange chromatography using an FPLC system (AEKTA purifier). To this end a Q-Sepharose column was equilibrated with T7 buffer before the supernatant was loaded with a flow rate of 1 ml/min. T7RNAP was eluted with a gradient from 50 - 500 mM NaCl in 15 column volumes at a flow rate of 2 ml/min. Elution of T7RNAP started approximately at a concentration of 150 mM NaCl, which was visible as a single peak in the chromatogram. Collected peak fractions that contain T7RNAP were pooled and the buffer was exchanged to 10 mM Tris (pH 8.0), 1 mM EDTA, 10 mM NaCl and 1 mM DTT by extensive dialysis. After dialysis, the protein concentration was adjusted to 4 mg/ml by ultracentrifugation. Sample purity was analyzed using SDS-PAGE with coomassie staining.

Activity tests of purified T7RNAP were either performed by *in vitro* transcription using linearized plasmids encoding for genes under a T7 promoter, or by cell free expression of GFP as a reporter gene. For *in vitro* transcription, linearized DNA was purified by ethanol/chloroform extraction and ethanol precipitation. *In vitro* transcription reactions were set up using 50 ng DNA and different amounts of T7RNAP in a volume of 50 µl and incubated for 1 h at 37 °C (Table 2.1). Transcribed mRNA was analyzed by separation on a 0.8 % agarose gel.

Table 2.1: Reaction setup for *in vitro* transcription reaction using the T7RNAP.

Reagent	Amount
Plasmid DNA, linear	50 ng
10x Transcription buffer	400 mM Tris-HCl pH 8.0 120 mM MgCl ₂ 50 mM DTT
RNAse inhibitor	0,1 U/µl
NTPs (A, U, C, G)	2 mM

T7RNAP was aliquoted in 10 mM Tris (pH 8.0), 1 mM EDTA, 10 mM NaCl, 1 mM DTT and 50 % Glycerol and stored at -80 °C.

2.1.2.2 Preparation of *E. coli* S30 extract

The *E. coli* S30 extract is another essential component of the cell free expression system since it contains the essential components for the translation process. These

components are ribosomes, aminoacyl-tRNA synthetases and all translation factors necessary for initiation, elongation and product release. Furthermore, it contains important components like acetate kinase and residual *E. coli* lipids or membrane fragments at approximately 100 µg/ml of S30 extract [96].

For extract preparation, the RNase deficient *E. coli* strain A19 was used. Before starting to work with the non antibiotic resistant *E. coli* strain and after amplification, a PCR was performed to confirm the absence of any microbiological contamination. As pre-culture 100 ml sterile LB medium was inoculated with A19 plated and incubated under rigorous shaking at 37 °C overnight. A fermenter was used to sterilize 7 l of 2x (referred to a final volume of 10 l) YPTG medium. At the second day it was filled up to the final volume with sterile filtered glucose and phosphate buffer and heated under stirring at 500 rpm to 37 °C and inoculated with the overnight culture 1:100. Cell growth in the oxygen enriched media was monitored by measuring OD₆₀₀ every 30 min. When cells were in the logarithmic growth phase, the OD₆₀₀ reached values of around 4. At this point cells were rapidly chilled below 12 °C using ice-cold water and harvested by centrifugation at 4,000 g and 4 °C for 15 min in pre-cooled beakers. Cells were resuspended in a total volume of 300 ml of 4 °C cold S30A buffer, supplemented with 10 mM 2-mercaptoethanol and pelleted again at 8,000 g and 4 °C for 10 min. This step was repeated twice with an extended final centrifugation step of 30 min. The resulting pellet was weighed (50 – 70 g wet weight from 10 l culture) and resuspended in 110 % (v/w) of S30B buffer with freshly added PMSF and DTT, pre-cooled to 4 °C. Cells were disrupted at a pressure of 20,000 psi using a French press device and centrifuged at 30,000 g and 4 °C for 30 min. The non-turbid upper 2/3 part of the supernatant was transferred to a new centrifugation tube in order to repeat the centrifugation step. Again, the non-turbid upper 2/3 part of supernatant was rescued for the following modified run-off step to remove endogenous mRNA. The supernatant was adjusted to a final concentration of 400 mM NaCl and incubated in a water bath at 42 °C for 45 min. The resulting turbid solution was dialyzed using a 12-14 kDa MWCO tubing against 5 l of cold S30C buffer overnight at 4 °C. The dialysis buffer was exchanged after at least 2 h of dialysis. The dialyzed extract was centrifuged at 30,000 g and 4 °C for 30 min. The upper and non-turbid 2/3 part of the supernatant was aliquoted, shock frozen and stored at -80 °C until further use.

2.1.2.3 Analytical and preparative scale cell-free expression

For cell free reactions first the feeding mix was set up, followed by the reaction mix. The reaction mix contains all essential components, whereas the feeding mix serves as continuous supply for fresh materials. Table 2.2 provides an overview describing the

components of cell free reactions and their function. Table 2.3 provides a scheme for setting up reaction mix and feeding mix.

Table 2.2: Components of cell-free reaction mixture

Component	Function
S30 extract containing Ribosomes Aminoacyl-tRNA synthetases Translation factors	Translation tRNA loading with amino acids Initiation, elongation, termination
Plasmid DNA	Template
PEG800	Mimics viscosity of cytoplasm Supposed to support stability of mRNA Enhances macromolecular crowding effects in CF extracts
Mg ²⁺ and K ⁺	Enzyme activity: pyruvate kinase
Acetate/glutamate	Major anions in <i>E. coli</i> cytoplasm, affect protein/nucleic acid interactions
DTT	Stabilizes T7RNAP
NTPs	Substrates for T7RNAP for translation
RNase inhibitor	Protection of transcribed mRNA from degradation
Complete protease inhibitor	Proteolysis inhibition
Amino acids	Increased degradation of arginin, cystein, tryptophan, methionin and glutamate by residual metabolism in S30 extracts [94]
Folinic acid	Formation of initiator formyl-methionine
Acetyl phosphate	Secondary energy source, together with acetate kinase
Acetate kinase	Intrinsic compound of S30 extract, effective regeneration of ATP, not guaranteed with pyruvate kinase system alone [94]
Phosphoenol pyruvate/pyruvate kinase	Secondary energy source

Table 2.3: Formulation for cell-free reaction set-up. FM: feeding mix, 1 ml total volume RM: reaction mix 18 ml total volume.

Unit	Conc. Stock	RM	Add to RM [μl]	Final conc.	Mg ²⁺ [mM]	K ⁺ [mM]		FM	Add to RM/FM [μl]	Add to FM [μl]
μg/ml	30	Lipids	0,0	variable						
x	1	S30-extract	350,0	0,35	4,9	21		S30-buffer		5950
mg/ml	1	Plasmid	15,0	0,015						255
U/μl	40	Rnasin	7,5	0,30						128
U/μl	300	T7-RNA Pol.	50,0	15,0						850
mg/ml	40	tRNA <i>E.coli</i>	17,5	0,70						298
mg/ml	10	PK	8,0	0,08						136
%	10	Detergent	0,0	variable				Brij35	0	
mM	16,7	RCWMDE	59,9	1,00				RCWMDE	1077,8	
mM	4,0	amino acids	150,0	0,60			0,6	amino acids	2700,0	2550
mM	1000	AcP	20,0	20,00		22		AcP	360,0	
mM	1000	PEP	20,0	20,00		67		PEP	360,0	
x	75	NTP	13,3	1,0				NTP	240,0	
mM	500	DTT	4,0	2,0				DTT	72,0	
mg/ml	10	Folinic acid	10,0	0,10				Folinic	180,0	
x	50	Complete	20,0	1				Complete	360,0	
x	24	HEPES b.	36,7	1,0		50		HEPES b.	660,0	
mM	1000	Mg(OAc) ₂	8,1	8,1	8,1			Mg(OAc) ₂	145,8	
mM	4000	KOAc	32,5	130,0		130,0		KOAc	585,0	
%	40	PEG8000	50,0	2				PEG8000	900,0	
%	10	NaN ₃	5,0	0,05				NaN ₃	90,0	
		H ₂ O	122,5	variable				H ₂ O	2205,4	1199
			877,5						15795	15801
		MIX I Volume	877,5						7731	15801
		Volume RM	1000	TOTAL	13	290,0		Volume RM+FM	18000	17000
		from RM/FM	429,5		mM Mg ²⁺	mM K ⁺			7731	Volume FM
								for RM	-429,5	
								for FM	7301,2	

2.1.2.4 Liposome preparation

Lipids were purchased solubilized in chloroform and transferred to a glass flask. Most of the chloroform was evaporated under an argon stream, and a thin lipid film formed while rotating constantly the flask. Traces of chloroform were removed by incubating the flask in a vacuum chamber overnight. The lipids were weighed and dissolved at desired concentrations (5 mg/ml – 30 mg/ml) in lipid buffer. Harsh mixing for 30 min formed multilamellar vesicles. Unilamellar liposomes were formed by passing the multilamellar vesicles through an Avanti Polar lipids mini extruder, equipped with a 200 nm Whatman polycarbonate membrane filter and two filter supports on each side. The liposomes were used for L-CF expression directly. Since signal recognition particle (SRP) and the SRP receptor FtsY are present in the S30 extract, a protein insertion into the bilayer might be feasible. FtsY usually facilitates the interaction between SRP and the translocon and is also known to interact with DOPC lipids [122].

2.1.3 Purification

Depending on cell-free expression modes, different purification strategies were applied. In case of P-CF expressed protein the first purification step was the centrifugation at 10,000 g for 20 min to pellet the protein, followed by solubilization and further purification by binding to Ni-NTA beads. Ni-NTA binding was the first purification step for D-CF produced protein. L-CF produced AQP6 was purified with a sucrose gradient ultracentrifugation. Detailed purification protocols are stated in the results section.

2.2 Protein expression with the *Semliki Forest virus* system

Heterologous protein overexpression with the *Semliki Forest virus* expression system can be divided into three major parts. First cloning of the DNA template into the pSFV2gen vector, followed by the second step: *in vitro* transcription and transfection of mammalian cells with the generated RNA to induce virus production. Finally, the infection of cells with the produced virus in order to overexpress the desired protein is carried out.

2.2.1 DNA template design

A requirement for heterologous protein expression using the SFV system is subcloning of the gene of interest into a SFV expression vector like pSFV2gen. The target gene and virus specific genes are under control of a SP6 promoter, ensuring an efficient *in vitro* transcription using the SP6 polymerase.

2.2.2 Transcription and translation

2.2.2.1 *In vitro* transcription

In order to produce high amounts of biological active RNA, *in vitro* transcription was carried out. The pSFV and pHelper vectors contain a SP6 promoter, which allows RNA transcription using SP6 RNA polymerase. For efficient reactions (run-off transcriptions of the SP6 RNA polymerase to an defined end), plasmids were linearized using *SpeI* and *NruI* restrictions enzymes for pHelper and pSFV respectively [123]. Linearization was carried out at RT overnight to ensure complete reactions and analyzed on agarose gels. Linear DNA was purified by agarose gel extraction or phenol/chloroform extraction followed by ethanol precipitation and resuspendend in RNase free water at a concentration of 500 ng/ μ l. For *in vitro* transcription reactions of 500 to 5,000 ng linear DNA were used.

Table: 2.4: Reaction set-up for *in vitro* transcription reactions.

Component	Concentration
Linear plasmid DNA	0.5 μ g
m ⁷ G(5')ppp(5')G-CAP	4 mM
rNTP (GTP)	1 mM
rNTPs (ATP, CTP, UTP)	5 mM
10x SP6 buffer	1 x
SP6-RNA polymerase	1 x
RNase inhibitor	1 x

For setting up the *in vitro* transcription reaction, all components were warmed to room temperature to prevent DNA precipitation caused by spermidin in the SP6 buffer (Table 2.4). RNase free 1.5 ml reaction tubes were used for a total volume of 50 μ l or multiples. The reaction mix was incubated at 37 °C for 30 min to 3 h. Afterwards, 1 μ l of reaction mix was analyzed for size and quality on a 0.8 % agarose gel. In case of successful *in vitro* transcription, RNAs were used for transfection of BHK (baby hamster kidney) cells directly.

2.2.2.2 Transfection of mammalian cells

For transfection with biological active RNA, the mammalian cells have to be in the logarithmic growth phase. Therefore, cells were detached with trypsin/EDTA from tissue culture flasks when reaching approximately 80 % confluency and resuspended in cell culture medium. Cells were pelleted at 500 g for 5 min, resuspended in 20 ml PBS and pelleted again. For electroporation, the cell pellet was resuspended to a final concentration of 1×10^7 cells/ml. For each electroporation, 750 μ l of cell suspensions were mixed with 50 μ l of recombinant produced RNA (pre-mixed expression vector and pHelper at ratios of 1:1, 2:1 or 1:2) and filled into a 0.4 cm electroporation cuvette. Electroporation was carried out using a Bio-Rad Gene Pulser with two pulses at 1.5 kV and 25 μ F capacity for 0.7 ms. Afterwards, cells were diluted with 30 ml cell culture medium and incubated in a 175-cm² tissue culture flask for 12 – 36 h at 37 °C and 5 % CO₂. Electroporation of cells from one 175-cm² tissue culture flask resulted in 10 ml virus stock. For large-scale production, cells were grown in 300-cm² tissue culture flasks. Thus, virus stocks up to 90 ml could be obtained.

2.2.2.3 Harvesting and activation of recombinant virus

The virus produced in BHK cells was harvested after an incubation of 12 – 48 h. The virus is secreted by the cells and therefore in the cell culture medium. The medium was decanted and centrifuged at 1,000 g for 1 min and 4 °C to pellet remaining cells. The supernatant containing the virus was sterile-filtered through a 0.22 μ m syringe filter to remove cell debris and contaminants, aliquoted (1 ml for virus tests, 10 ml for infections) and directly used for infection. Alternatively, it was shock frozen in liquid nitrogen for long-term storage at -80 °C.

Virus particles were produced using the pHelper-2 vector, which provides additional safety. Because of a point mutation in the p62 precursor, the virus is not infectious until cleavage into E2 and E3 membrane proteins occurs. Therefore, the virus has to be treated with α -chymotrypsin at concentrations substantially higher than physiological levels.

Virus stocks were activated by α -chymotrypsin (20 mg/ml stock solution; 1 mg/ml final concentration) at RT for 30 min. Afterwards, α -chymotrypsin was inactivated by aprotinin (10 mg/ml stock solution; 0.5 mg/ml final concentration). The infection of cells with activated virus stock was performed instantly.

2.2.2.4 Titer determination

Before setting up large-scale expression reactions, virus titers of each batch were determined by incubating cells with dilution series of produced virus. To evaluate the expression levels of virus batches, test expressions were performed using HEK293 (human embryo kidney), BHK (baby hamster kidney) or CHO (chinese hamster ovary) cell lines. Expression levels were determined by immunofluorescence with antibodies targeting the C-terminal 6xHis-tag of AQP6. Before test infections cells were plated into 6-well plates and grown to a confluency of 80 %. Different volumes of virus stocks were added to the cells (0 μ l, 50 μ l, 100 μ l, 250 μ l, 500 μ l, 1,000 μ l respectively) and incubated for 12 – 48 h. Expression of AQP6 was analyzed by SDS-PAGE and immunoblotting. Therefore, after removing the media and washing with PBS 300 μ l lysis buffer was added per well, followed by an incubation of 5 min. Cells were pelleted for 5 min at 1,000 g, resuspended in SDS-sample buffer, incubated for 15 min at RT, and directly applied on SDS gels (15 μ l sample per well).

2.2.2.5 Infection of mammalian cells and protein expression

For protein expression, cells were cultivated in 175-cm² or 300-cm² tissue culture flasks to 80 % confluency at time of infection. Two hours before infection, cell culture medium was replaced with fresh medium and the volume was reduced by 50 %. For expression virus stocks were transferred into the tissue culture flasks. After the incubation time of 2 h, flasks were filled up with cell culture medium to the volume before removing media. Expression was carried out at 33 °C or 37 °C for 12 – 36 h. After expression, cells were harvested by centrifugation at 500 g for 15 min and stored at -80 °C until further use.

2.2.3 Purification

2.2.3.1 Membrane preparation and solubilization

Cells were thawed or used directly after harvesting and diluted with the same volume of breaking buffer. Cells were lysed by a single passage through pre-cooled microfluidizer at a pressure of 1,000 bar. Membranes and cell-debris were pelleted by ultracentrifugation at 150,000 g and 4 °C for 45 min. Peripheral proteins were removed by urea/alkaline stripping according to [124]. Therefore, ca. 0.5 ml crude membranes were homogenized in 10 ml of 4 M urea, 5 mM Tris-HCl, pH 8.2, 5 mM EDTA and 0.03 %

NaN₃. Homogenized and urea stripped membranes were pelleted by ultracentrifugation as before and resuspended and homogenized in 10 ml of 20 mM NaOH. After pelleting again using the same ultracentrifugation settings, membranes were resuspended and homogenized in 5 ml of 20 mM Tris-HCl buffer, pH 7.5, 100 mM NaCl, 10 % glycerol and 0.03 % NaN₃. Aliquots of stripped membranes were shock frozen and stored at -80 °C or used directly for solubilization. Stripped membranes were diluted in solubilization buffer containing detergent at desired concentrations and incubated for different time courses at 4 °C or RT for solubilization. Solubilized protein was separated from unsolubilized material by ultracentrifugation at 200,000 g and 4 °C for 1 h.

2.2.3.2 Ni-NTA purification (IMAC)

Solubilized protein was purified by immobilized metal ion affinity chromatography (IMAC) using a nitrilotriacetic acid (NTA) agarose matrix and immobilized nickel to which the polyhistidine-tag binds with micromolar affinity. The supernatant containing *e.g.* the solubilized protein of interest was diluted with purification buffer and added to Ni-NTA beads, pre-equilibrated with the same buffer without detergent. For binding, Ni-NTA protein mixture was incubated at 4 °C for 4 h or overnight. After incubation, Ni-NTA beads were separated from buffer by filtration through a Bio-Rad mini-column. Washing with 10 – 50 column volumes of buffer containing 5 mM imidazole washed out unbound and unspecific bound protein. AQP6 was eluted by applying 300 µl elution buffer supplemented with 100 - 500 mM imidazole and incubation for 5 min. This step was repeated seven times. The elution buffers contained detergent in a lower concentration (*e.g.* 1.2 % OG or 0.05 % DDM).

Alternatively, solubilized protein was directly purified by FPLC using a 1 ml His-Trap column at a flow rate of 0.5 ml/min. Unbound protein was washed out with 10 ml buffer containing 5 mM imidazole. AQP6 was separated and eluted with a linear gradient from 5 mM to 300 mM imidazole over 20 column volumes. Peak fractions were collected and analyzed for protein content with SDS-PAGE and immunostaining.

For further purification and characterization, elution fractions containing AQP6, were analyzed by size exclusion chromatography. A Superdex 200 10/300 GL column was pre-equilibrated with washing buffer. A maximum of 500 µl of selected elution fractions were injected and loaded onto the gel-filtration column at a flow rate of 0.5 ml/min. Chromatograms were recorded at a wavelength of 280 nm and elution fractions were collected for further analyses and reconstitution experiments.

2.2.3.3 Reconstitution

After size exclusion chromatography, 25 % of the original amount of AQP6 was recovered and used for reconstitution. Therefore, protein was mixed with *e.g. E. coli* polar lipids solubilized in OG and incubated for 30 min at room temperature. The ternary mixture was loaded into a Slide-A-Lyzer (Pierce) dialyzing cassette (MWCO 10,000 Da) and dialyzed 3 days against 5 l washing buffer without detergent at 37 °C. After the first day the buffer was replaced with a fresh one. Proteoliposomes were harvested by ultracentrifugation at 200,000 g and 4 °C for 45 min over sucrose gradient. Proteoliposome containing fractions were recovered, diluted with washing buffer and centrifuged again using the same settings. The supernatant was removed and the proteoliposome pellet was carefully resuspended with washing buffer using a small volume. Proteoliposomes were used directly for activity measurements or adjusted

2.2.4 General cell culture methods

If not stated differently, for cultivation the cells were always kept at a temperature of 37 °C, in an atmosphere of 5 % CO₂ and a relative humidity of 100 %. Together with NaHCO₃ in the media, the CO₂ content of the air functions as buffer system to stabilize the pH. This was necessary because of production of CO₂, ammonia and lactate as natural metabolites. Media and buffers applied to the cells were always warmed to 37 °C in a water bath prior the use.

For cultivation of adherent cells tissue culture flasks with coated surfaces were used to allow cells to attach to the surface. To generate subcultures, the old media was decanted and the cells were washed with PBS. For detaching cells in 175-cm² tissue culture flask, an incubation in 2 ml 0.05 % Trypsin/EDTA solutions for 5 min was sufficient. Inactivation of trypsin was achieved by resuspension in 10 ml cell culture media. 1.5 x 10⁶ cells were seeded in 30 ml fresh medium in a new 175-cm² flask. This subcultivation for preservation was necessary every two to three days, when cells reached a high level of confluence. Because of contact inhibition, growth of the culture arrests at a high degree of confluence.

Viability of a culture was tested with 0.4 % trypan blue solution. An aliquot of a culture was mixed with the 0.1 volumes of staining solution and incubated for 1 min. After incubation, cells were counted using a hemocytometer. Trypan blue stains dead cells only; living cells do not absorb the stain. A healthy cell culture contains ca. 98 % unstained, living cells.

For long term preservation, cells in their exponential growth phase ($0.5 - 1 \times 10^7$ cells/ml) were stepwise frozen in cell culture medium containing 10 % (v/v) DMSO to -80 °C and stored in liquid nitrogen. Cells were heated at 37 °C in a water bath for thawing from the liquid nitrogen storage and cultivated in cell culture medium.

2.3 Protein expression with *Pichia pastoris*

The experimental process of AQP6 overexpression with *P. pastoris* started with cloning of the AQP6 gene into the pPICZ α expression vector. The resulting constructs were linearized by *PmeI* or *SacI* restriction enzymes. *P. pastoris* strains X-33 or GS115 were transformed by electroporation and plated on medium containing Zeocin to select transformants with gene integration. Colonies were selected for small-scale expression, and the highest AQP6 expressing clones were used for large-scale expression in shaker flasks or fermenters.

2.3.1 DNA template design

AQP6 was cloned into pPICZ α expression vector using *EcoRI* and *XhoI* restriction sites. The final construct was sequenced originating from the AOX1 promoter. Plasmid DNA was purified in Midi-Prep scale and linearized with *SacI*.

For transformation, 5 ml *P. pastoris* were grown overnight at 30 °C and used for inoculation of 500 ml medium in a 2 l flask. After growing overnight and reaching an OD₆₀₀ of 1.4, cells were pelleted at 1,500 g for 5 min at 4 °C and resuspended in 500 ml ice-cold, sterile water. Cells were pelleted again as before and resuspended in 250 ml ice-cold, sterile water. Resuspended cells were pelleted again as before and resuspended in 20 ml of ice-cold 1 M sorbitol. As final step, cells were centrifuged using the same settings and resuspended in 1 ml of ice-cold 1 M sorbitol. Cells were stored on ice and used for electroporation on the same day.

80 μ l of *P. pastoris* were mixed with 10 μ g of linearized DNA and incubated on ice for 5 min. Then, cells were transformed by electroporation using a Bio-Rad Gene Pulser (settings in Table 2.5).

Table 2.5: Settings for electroporation of *P. pastoris* cells, using a Bio-Rad electroporation device.

Parameter	Setting
Cuvette	0.4 cm
Voltage	1.5 kV
Capacity	25 μ F
Resistance	200 Ω

Cells recovered from electroporation for 1 h at 30 °C and shaking. After incubation the transformation mix was plated on YPD-plates containing 100 µg/ml, 500 µg/ml or 2,000 µg/ml Zeocin and incubated at 30 °C for 2 days. Colonies were selected and plated again on YPD-plates containing 2,000 µg/ml Zeocin. After incubation for 2 days at 30 °C, glycerol stocks were set up for long term storage of *P. pastoris* clones containing the AQP6 gene.

2.3.2 Transcription and translation

The *P. pastoris* expression clone was plated on YPD medium, containing Zeocin and incubated for 2 days at 30 °C. The pre-culture was inoculated by scratching the yeast from the plate, followed by incubation for 1 day under shaking at 30 °C. The expression culture was inoculated with the pre-culture (1:100). After shaking for an additional day and reaching an OD₆₀₀ of 10 the expression was induced by exchanging the glycerol-containing medium with medium containing 0.5 % methanol as single carbon source. The exchange was performed by centrifugation at 2,000 g for 15 min and resuspending the cells with the methanol-containing medium. Additional methanol was added every 24 h to a final concentration of 0,5 %. The expression was carried out for 4 days, corresponding to a final OD₆₀₀ of 30.

2.3.3 Purification

All purification steps were carried out at 4 °C. Cells were harvested by centrifugation at 2,000 g for 15 min and resuspended in a small volume of breaking buffer. At this point, cells were either shock frozen in liquid nitrogen and stored at -80 °C until further use or directly used for cell disruption. Cells were disrupted with a pre-cooled fluidizer (Microfluidics), during 20 rounds at 1,000 bar. Unbroken cells and cell debris were separated from membranes and soluble parts by a low spin centrifugation step at 5,000 g for 30 min. The supernatant containing membranes and soluble proteins was subject to a centrifugation at 150,000 g for 1 h to pellet the membranes. Crude membranes were purified from peripheral proteins by urea/alkaline stripping as described in [124]. Therefore, crude membranes were diluted with 4 M urea, 5 mM Tris-HCl, pH 7.5, 5 mM EDTA, homogenized and pelleted at 150,000 g for 1 h at 4 °C. The pellet was homogenized in 20 mM NaOH and pelleted again, using the same settings. The alkaline stripped pellet was homogenized in 5 mM Tris-HCl, pH 7.5, 5 mM EDTA, 100 mM NaCl, centrifuged at 150,000 g for 1 h at 4 °C and homogenized in 20 mM Tris, pH 7.5, 300 NaCl and 5 % glycerol. Stripped membranes were aliquoted, shock frozen in liquid nitrogen and stored at -80 °C until further use.

AQP6 containing membranes were solubilized in 6 % OG for 2.5 h at RT under stirring. Unsolubilized material was pelleted by ultracentrifugation at 200,000 g for 90 min and 4 °C. Solubilized protein was diluted with 20 mM Tris-HCl, pH 7.5, 300 mM NaCl, 5 % glycerol to a final OG concentration of 1.2 % and incubated with 0.5 ml pre-equilibrated Ni-NTA beads overnight at 4 °C. The mixture was filled into a Bio-Rad mini-column and washed with 10 ml buffer (20 mM Tris-HCl, pH 7.5, 300 mM NaCl, 5 % glycerol and 1.2 % OG). Protein was eluted with washing buffer containing additional 250 mM imidazole in six fractions of 250 µl each. Protein concentration of elution fractions was determined. Purity was examined by SDS-PAGE and western blot.

2.4 Protein analysis

2.4.1 Determination of protein concentration

Concentrations of purified protein were determined using a NanoDrop 2000 micro-volume UV-Vis spectrophotometer (Thermo Scientific) and 2 μ l of protein sample. Table 2.6 provides the extinction coefficients, and the molecular weight of all used AQP6 constructs. Concentrations were calculated by means of the Lambert-Beer's law with the measured absorption at 280 nm.

Table 2.6: Properties of AQP6 constructs used for expression.

Protein	Expression System	Tags	No. of amino acids	MW (g/mol)	Extinction coefficient ($M^{-1} cm^{-1}$)
rAQP6	Cell free	6xHis	282	29.665	38.055
rAQP6	Cell free	TA, 6xHis	300	31.893	44.015
rAQP6	SFV	6xHis	283	29.755	38.055
rAQP6	<i>P. pastoris</i>	6xHis	282	29.665	38.055

2.4.2 SDS-PAGE

Protein samples were separated according to their molecular weight using sodium dodecyl sulfate polyacrylamide electrophoresis (SDS-PAGE). Samples were diluted with sample buffer containing SDS, applied on a 4 % - 12 % denaturing gel (NuPage, Invitrogen) and separated at 120 V for 90 min.

2.4.3 Western blot analysis

Proteins were transferred onto nitrocellulose membrane at 0.8 mA/cm² for 30 min using a TE70X semi-dry blotter (Hoefer). Free binding sites of the membrane were blocked by incubation with 3 % BSA in TBE for 1 h. Protein was detected by incubation with murine anti-penta-His antibody (Sigma) or anti-AQP6-antibody from rabbit (GE) using a 1:5,000 dilution for 1 h, followed by an incubation with the secondary antibody horseradish peroxidase (HRP)-conjugate and detection by the enhanced chemiluminescence (ECL)-kit (Thermo Scientific). Between all steps, the membrane was washed three times for 10 min with TBS-T.

2.4.4 Size exclusion chromatography

A separation of proteins by size was achieved using size exclusion chromatography (SEC). The separation is based on different retention times of proteins while travelling

through a porous matrix. For larger proteins a smaller volume is accessible, because their diffusion into pores of the matrix is restricted due to their size. For SEC a Superdex 200 30/100 GL column with maximum flow rates of 0.5 ml/min at the ÄKTA purifier (GE) was used. Precipitated material was removed prior loading by centrifugation.

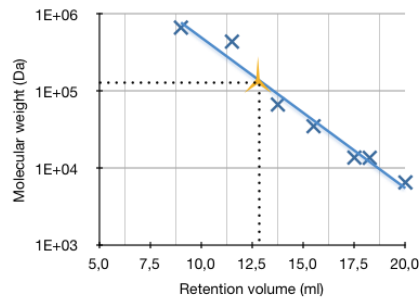


Figure 2.1: Superdex 200 10/300 GL calibration curve (obtained from GE) Size and volume corresponding to the AQP6 tetramer indicated by yellow star.

2.4.5 Single particle negative stain transmission electron microscopy

Single particle specimens were prepared by adsorbing protein solutions (20 µg/ml) for 20 s onto carbon coated copper grids, which were previously rendered hydrophilic by glow discharge in a partial vacuum. After adsorption, the grids were washed three to five times with H₂O and respectively stained for 5 s and 15 s with 2 % uranyl acetate. Images were recorded at nominal defocus values of ca. 0.9 µm on a veleta CCD camera at nominal magnifications of 3,400 – 92,000, which corresponds to pixel sizes of 14.1 – 0.5 nm at the specimen level.

2.5 Protein reconstitution into liposomes

A list of used lipids is stated in Table 2.7. Prior usage for reconstitution experiments, all lipids were dissolved in chloroform and dried under a stream of argon while rotating. Lipids were further dried under vacuum overnight and finally dissolved in reconstitution buffer containing the desired detergent using a sonication bath. The lipid concentration was adjusted to 10 mg/ml. Lipids were further diluted with reconstitution buffer and mixed with purified AQP6 to obtain defined lipid to protein ratios (LPR). The final protein concentration was set to approximately 100 µg/ml and LPRs of 1 to 100 were used. The final lipid concentration was around 2 mg/ml in a final volume of 1 ml to 4 ml. Detergent was removed either by dialysis or absorption onto hydrophobic polystyrene beads (Bio-Beads SM2 (Bio-Rad)). The required amount of Bio-Beads was calculated based on detergent concentrations [125]. After 30 min pre-incubation of the ternary mixture, Bio-Beads were added and incubated overnight under gentle stirring at temperatures between 4 °C and 33 °C. Bio-Beads were exchanged and incubated for additional 2 h at the desired temperature. For detergent removal by dialysis, the ternary mixture was filled into a Slide-A-Lyzer (Pierce) dialyzing cassette (MWCO 10,000 kDa) and dialyzed against a detergent free dialysis buffer of a total volume of 5 l. After dialyzing for 24 h, the buffer was exchanged to a fresh one and dialysis was continued for another 48 h. Control liposomes were prepared in the same way but without adding protein to the reconstitution mixture. After removing the detergent, residual detergent concentrations were far below cmc as verified by Drop-Box measurements [126]. Detergent free liposomes were passed through a 200 nm polycarbonate filter (Whatman), 21 times at 30 °C, using a Mini-extruder (Avanti) in order to obtain a narrow size distribution of unilamellar liposomes.

Table 2.7: Overview of used lipids. All lipids were purchased from Avanti Polar Lipids. Lipids and lipid mixtures contained phosphatidylethanolamine (PE), phosphatidylglycerol (PG), cardiolipin (CA), phosphatidylcholine (PC), phosphatidylethanolamine (PE), phosphatidylinositol (PI), phosphatidylserine (PS) and phosphatidic acid (PA).

Name	Abbreviation	Description
<i>E. coli</i> polar lipid extract	<i>E. coli</i> lipids	67 % (w/w) PE 23.2 % (w/w) PG 9.8 % (w/w) CA
Brain polar lipids extract (porcine)	Brain lipids	12.6 % (w/w) PC 33.1 % (w/w) PE 4.1 % (w/w) PI 18.5 % (w/w) PS 0.8 % (w/w) PA 30.9 % (w/w) unknown
1,2-dimyristoyl-sn-glycero-3-phosphocholine	DMPC	14:0 PC
1,2-dioleoyl-sn-glycero-3-phosphate	DOPA	18:1 PA
1-palmitoyl-2-oleoyl-sn-glycero-3-phosphocholine	POPC	16:0-18:1 PC
1-palmitoyl-2-oleoyl-sn-glycero-3-phosphoethanolamine	POPE	16:0-18:1 PE
Mixture of three lipids, containing POPC as major component	POPC-mix	70 % POPC 15 % DOPA 15 % POPE

2.6 Freeze fracture electron microscopy

2.6.1 Sample preparation

Protein reconstitution was verified by freeze fracture electron microscopy. Proteoliposomes were concentrated by centrifugation at 300,000 g for 45 min at 4 °C. The lipid pellet was carefully resuspended in a small volume of dialysis buffer and 80 % (v/v) glycerol to a final concentration of 30 % (v/v) glycerol as cryoprotectant. Cryoprotected samples were shock frozen in liquid nitrogen and stored at -80 °C or used directly for freeze fracturing. A small droplet was placed onto a copper holder, covered carefully with a second copper holder and quenched in liquid propane. The frozen sample was introduced into a Balzers 300 freeze-etching unit (precooled to -140 °C). The samples were fractured at -125 °C in a high vacuum of 10^{-6} – 10^{-7} mbar by cutting the frozen droplet. The fractured sample was replicated instantly with a 1 – 1.5 nm deposition of platinum from an angle of 45° followed by a 20 nm deposition of carbon at 90°. The replica was rescued and the remaining protein and lipids were dissolved in 2 % SDS. Finally the replica was washed twice with H₂O and fished with a gold TEM grid for observation under the microscope. A detailed description of this complex method can be found in [127].

2.6.2 Sample analysis

Samples were observed with a Philips CM-10 transmission electron microscope (see 2.4.5) Diameters of the proteoliposomes were verified and average numbers of protein particles per proteoliposome were determined by counting the total number of channels per proteoliposome, which is four times the number of particles per proteoliposome, because of tetramer formation. Dividing this result by the average liposome surface area, while assuming that the proteoliposomes form rigid spheres results in the single channel density.

2.7 Water conductance measurements of proteoliposomes

Water permeability of AQP6 was measured with a Bio-Logic SFM 300 stopped-flow light scattering system according to the method described previously [48, 80, 128]. Proteoliposomes in sample buffer were rapidly mixed with an equal volume (50 μ l) of a hypertonic solution containing sample buffer plus 400 mM sucrose. This theoretically results in an outward-directed osmotic gradient of 200 mOsm causing a water efflux and shrinkage of proteoliposomes. Measurements were carried out at 10 °C. Time course of shrinking was monitored with 90° scattered monochromatic light at 436 nm for 2 s. The volume shrinkage induced by the outwardly directed osmotic gradient led to an increase of the scattered light signal. The time course between 0.012 s and start of saturation of the curve was fitted with a single-exponential function. The water permeability factor P_f of the proteoliposomes samples was calculated using the equation:

$$P_f = \frac{k}{(S/V_0) \times V_w \times \Delta_{osm}}$$

Where S/V_0 is initial surface to volume ratio of the vesicles, V_w the partial molar volume of water (18 cm³/mol) and Δ_{osm} the osmotic driving force. The volume of the vesicles was determined by measuring the diameters of vesicles in the freeze fracture electron micrographs, assuming that the largest vesicles were fractured in the equatorial plane.

3 Results & Discussion

Figure 3.1 illustrates the structure of this chapter and the order of results presented.

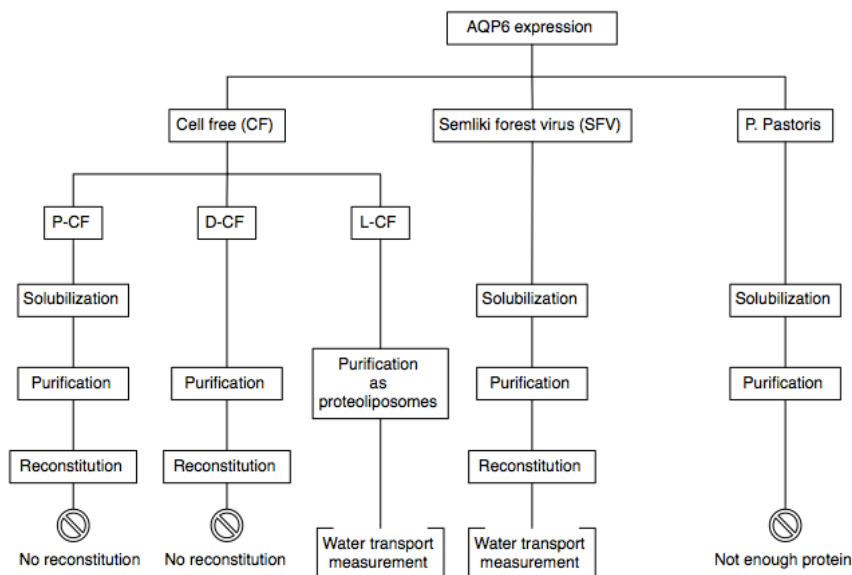


Figure 3.1: Overview of obtained results from the application of different expression systems.

3.1 Cell-free expression of AQP6

In order to develop and optimize cell-free expression of AQP6, reaction components were prepared. Basic components for cell-free reactions are template DNA, T7 RNA polymerase for transcription, S30 extract containing the translation machinery, an energy regeneration system, amino acids and tRNAs. A complete overview of all components is stated in Chapter 2.1.2.3 and below. Expression reactions were carried out in the absence of detergent, as precipitate (P-CF), in the presence of detergent (D-CF), or in the presence of liposomes (L-CF).

3.1.1 Template design

In order to execute the cell-free expressions, the coding sequence of AQP6 from rat (rAQP6) was subcloned into the expression vector pET21a(+) using *Bam*HI and *Eco*RI restrictions sites. Molecular cloning resulted in a construct coding for a N-terminal T7 sequence (the initial 11 amino acids of the T7 gene 10 protein), followed by the rAQP6 sequence and a C-terminal hexa-histidine tag (T7-rAQP6-6xHis), which was confirmed

by restriction analyses and DNA sequencing (see appendix B for sequencing results). The C-terminal 6xHis tag was chosen to ensure efficient purification using immobilized metal ion affinity chromatography (IMAC). N-terminal T7-tags were reported to enhance cell-free expression by optimization of translation initiation [102].

3.1.2 Transcription and translation

3.1.2.1 Basic protocol

To establish complete and efficient expression of the AQP6 construct, a test expression was performed using the P-CF mode. In order to analyze the sample, the pellet resulting from the expression reaction was resolubilized in SDS sample buffer. A SDS gel separation of the pellet and supernatant followed by immunodetection with a penta-histidine antibody revealed signals for the 6xHis-tag in the pellet fraction only. Western blots of the pellet fraction resulted in four visible bands of different strength (Figure 3.2). The most prominent band was at a height according to a molecular weight of 30 kDa, followed by a second strong band at approximately 50 kDa. A weaker signal could be detected at approx. 75 kDa; a very weak signal is visible at a height corresponding to approximately 120 kDa. These bands correspond to the AQP6 mono-, di-, tri- and tetramer. This pattern was observed for heterologously expressed and purified AQPs, like AQP2 (insect cells) or AQP8 (yeast) before [39, 129]. By detection of the C-terminal His-tag full-length synthesis can be assumed.

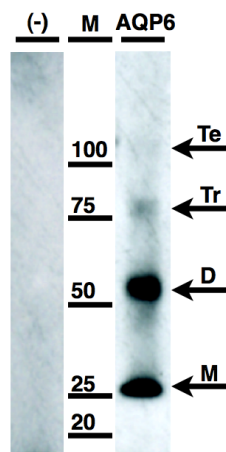


Figure 3.2: Immunodetection of cell-free (P-CF) produced AQP6 in analytical scale without prior purification, to confirm basic expression of used constructs. Arrows indicate AQP6 monomer (M), dimer (D), trimer (Tr) and a very weak signal for the tetramer (Te). Negative control (-), cell-free reaction setup lacking AQP6 DNA template.

Immunodetection of the histidine tagged proteins revealed that the basic protocol for the expression of AQP6 was working. The next step was to optimize concentrations of the reaction components to achieve higher expression yields.

3.1.2.2 Buffer conditions

The components of the cell-free expression system are optimized for a pH around 8.0 [96]. Regarding that this value is close to the pI of AQP6 cell-free reactions at different pH values were performed. At a pH of 6.5 or 9, nearly no expression of AQP6 could be detected. Therefore, expression was performed at pH 8.0 which was changed during subsequent purification.

3.1.2.3 Optimizing parameters for expression

One of the most critical parameters for high-level protein expression is the concentration of Mg^{2+} and K^+ ions [95]. The batch and target dependent optimum is usually in the range between 13 - 25 mM Mg^{2+} and 230 - 300 mM K^+ . Particularly the optimization of Mg^{2+} concentration is important to reach highest yields in cell-free expression systems [96].

For every batch of S30 extract, a P-CF analytical scale screening for optimal Mg^{2+} and K^+ concentrations was performed in the range from 10 – 25 mM in case of Mg^{2+} and from 230 – 300 mM in case of K^+ and analyzed by western blotting to estimate the expression level. For distinctive concentrations of either Mg^{2+} or K^+ , bands of different intensities were observed. The optima, determined after SDS-PAGE and immunostaining, were around 13 mM Mg^{2+} and 290 mM K^+ (Figure 3.3). As expected, different concentrations of Mg^{2+} and K^+ have a remarkable influence in efficiency of the cell-free reaction producing AQP6.

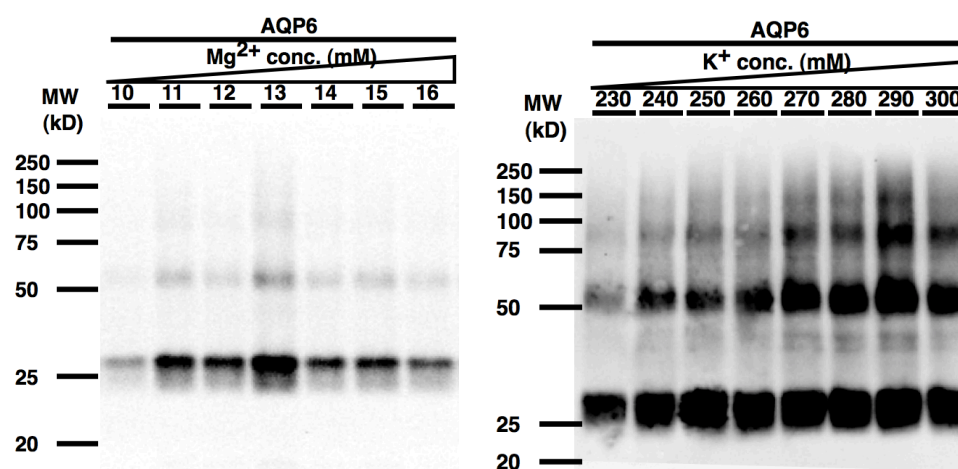


Figure 3.3: Immunodetection of AQP6 P-CF expression reactions as screening for optimal Mg^{2+} and K^+ concentrations.

An overview of all components of the used cell-free reaction and a pipetting scheme for setting up the reaction mix (RM) and feeding mix (FM) is stated in Table 2.3, Chapter 2.1.2.3. Optima for all components were determined and kept constant for all subsequent reactions. In case of reactions in the D-CF or L-CF mode detergent or preformed liposomes, respectively, were added to the reaction at defined amounts. For preparative scale reactions a total reaction mix volume of 1 – 3 ml was adjusted. Cell-free expression reactions in the P-CF mode, using the optimized protocol, resulted in expression rates between 300-800 µg of IMAC purified AQP6 per ml reaction mix. Compared to other cell-free expressed membrane proteins, the observed yield of AQP6 was very low [96].

A final comparison with AQP4 confirmed that low expression yield were inherently due to the nature of AQP6. Additional test expressions in comparison to AQP4 that was shown to express more efficiently [80], resulted in a comparable poor expression of AQP6, too. The immunodetection using penta-His antibodies showed, in addition to a lower overall expression of AQP6 compared to AQP4, a comparable pattern of monomer and multimer bands (Figure 3.4).

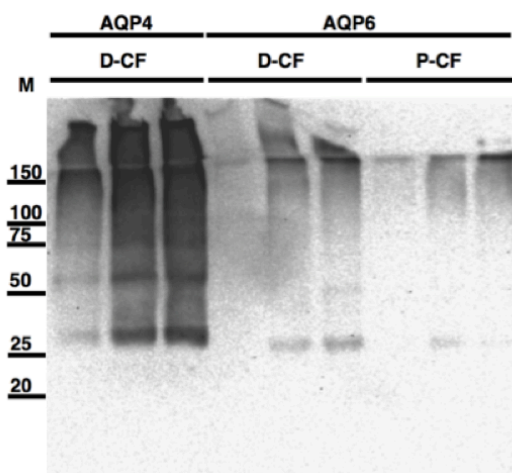


Figure 3.4: Verification of AQP6 expression in comparison to AQP4 by immunodetection of His-tagged AQPs. Same amounts of reaction mixture of three independent D-CF reactions were loaded. AQP6 P-CF reaction: pellet was resuspended in corresponding volume of water.

Besides of the satisfactory expression yields, the general appearance of AQP6 as analyzed by SDS-PAGE was comparable to other AQPs. This means that bands corresponding to mono-, di-, tri- and tetramers could be visualized by immunodetection. Remarkably, the ratio of multimers to monomers was reverse for

AQP4 expressed and treated in the same way. Furthermore in case of unpurified AQP4 a greater portion of potential higher oligomers was visible as black bands on the top of the gel after immunodetection, whereas in case of AQP6 the intensity of staining in this area was less. Since the lower expression rates of AQP6 could not be explained with toxic effects, translation efficiencies were optimized by N-terminal tag variations.

3.1.2.4 Altering N-terminal tags to optimize transcription and translation

The low expression rate of AQP6 compared to AQP4 and other membrane proteins led to the decision to redesign the DNA template. It is known that the template design can have a high impact on expression efficiency [130].

In order to reach higher expression levels several N-terminal tags were tested. N-terminal tags can have a strong influence on the efficiency of cell-free expression. It was shown, that the T7-tag enhances the expression of GPCRs at high levels, in comparison to expression without the T7-tag, where almost no expression could be detected [102]. To enhance the expression of AQP6, N-terminal tags were tested, which are known for their potential of positive effect to expression levels [107].

Table 3.1: DNA sequences of N-terminally altered tags.

#	Tag name	Sequence	% GC	Result expression
1	Shifted His	aaatcatcatcatcatca	28	+
2	R	aaagtcatccttgtaatc	44	o
3	AT	aaatattataaatattat	0	+++
4	G	aaaagtaaaggagaagaa	28	o
5	TEV	agagaacctgtacttcca	44	o
6	iAT	aaataatatttataata	0	+++
7	Shifted AT	aatattatatatttatat	0	+++
8	T7	accatttgctgtccaccgctcatgctagccat	55	o
	Hybridization sequence	ctggaagtgctgtttcagggcccg		

For testing the influence of changes in protein expression due to N-terminal tag variation, an analytical scaled test expression of AQP6 was carried out using a PCR amplified construct as template. As control, a reaction with the existing N-terminal T7-tag was set up in the same way. The resulting protein pellets were resuspended in SDS buffer and analyzed by SDS-PAGE followed by western transfer and immunodetection. On the western blot, signals of different intensities, due to different expression levels

were visible. The expression levels with AT-rich N-terminal tags were significantly higher than with the tested GC-rich tags or with the T7-tag used before (Figure 3.5). Due to these results, the AT-tag was chosen to be cloned as N-terminally into the rAQP6-6xHis expression vector. Correct cloning was verified by DNA sequencing. The final sequence of the AT-rAQP6-6xHis construct is stated in Appendix B. This N-terminally optimized construct was used for all following experiments.

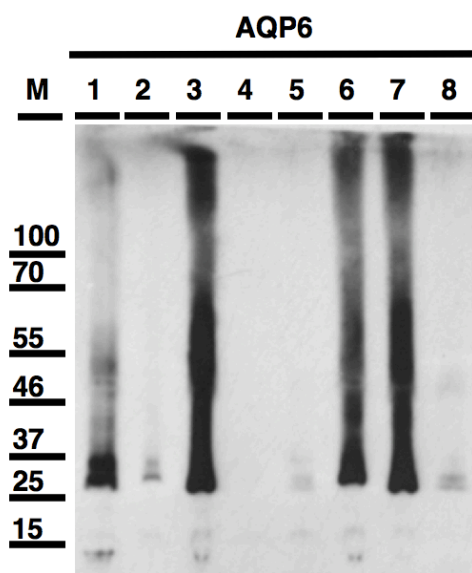


Figure 3.5: Immunodetection of cell-free reactions, expressing AQP6 with altered N-terminal tags. Reaction mix pellet was loaded on the gels, numbers refer to tested tags as stated in Table 3.2.

3.1.2.5 Evaluation of detergents for expression and solubilization

Detergents were investigated for posttranslational solubilization in the P-CF mode and co-translational solubilization in the D-CF mode. The selection of detergents was made on existing data for solubilization rates of membrane proteins [102].

P-CF

For evaluation of detergents in the P-CF mode cell-free expression of AQP6 was carried out in analytical volumes of 55 μ l reaction mix and 850 μ l feeding mix. Precipitated AQP6 was concentrated for further analyses of detergent by an initial centrifugation step at 13,000 g and 4 $^{\circ}$ C for 15 min. In order to remove co-precipitated S30 extract protein, samples were washed with water twice. Finally, the protein pellet was resuspended and homogenized in resuspension buffer containing the detergent.

Most effective solubilization of AQP6 could be reached using the long-chain phosphoglycerol LPPG, the long-chain phosphocholine LMPG or fos-choline 16 at a final

concentration of 1 % each. Fos-choline 12 (DPC) was less effective and led to 80 % of solubilized AQP6 only. DDM was even less effective, 2.5 % DDM solubilized less than 50 % of AQP6 (Figure 3.6).

LMPG and LPPG are the most efficient detergents for the solubilization of precipitated membrane proteins. AQP6 is solubilized completely by them. The same was observed for cell-free produced AQP4 and GPCRs of cell-free origin [80, 94].

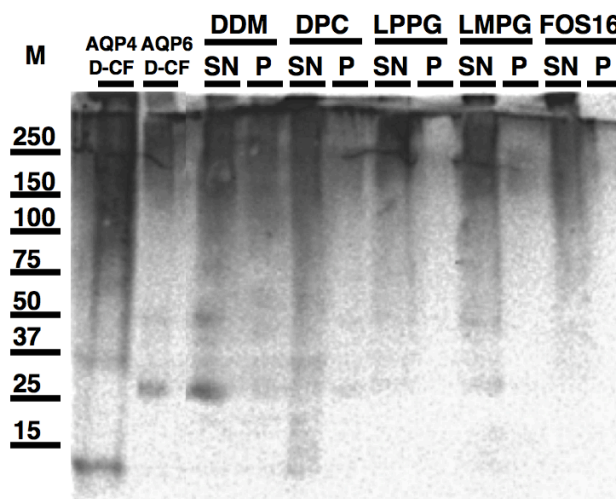


Figure 3.6: P-CF solubilization trials, testing different detergents for solubilization of the pellet after P-CF reaction. Immunodetection using a penta-His antibody after incubation for 4 h in 2.5 % DDM, 1 % DPC, 2 % LPPG, 2 % LMPG, or 1 % FOS-16. Supernatant (SN) and pellet (P) fractions were loaded on the gel after centrifugation. D-CF reaction mix of AQP4 and AQP6 was loaded as reference.

D-CF

In case of the protein quality is not sufficient in P-CF mode, the D-CF mode is an alternative. Here, the protein is expressed in presence of a detergent at a concentration above its cmc. As a result, the membrane protein will undergo co-translational solubilization. In the D-CF mode yields are usually lower than in P-CF mode, due to negative effects of detergents on expression efficiency. However, the lower protein yield usually comes along with a better sample quality in terms of homogeneity and functionality. In order to identify the appropriate detergent for D-CF mode, detergents from different families were tested in analytical scale reactions (Figure 3.7).

The tested detergents were OG, DDM, Digitonin, Brij35, Brij78 and Triton-X 100. The highest yields and solubilization rates were achieved in 0.5 % Brij78 (approximately 85-times cmc). DDM and beta-OG were not capable to solubilize AQP6 completely at concentrations that did not inhibit the cell-free reaction at significant levels. The

inhibitory effects of high detergent concentration were already shown [102]. Here, high concentrations of beta-OG resulted in complete solubilization of only small amounts of expressed AQP6 (Table 3.2). DDM had no inhibitory effects at a concentration of 0.2 % on the expression reactions, but was not able to solubilize AQP6 completely.

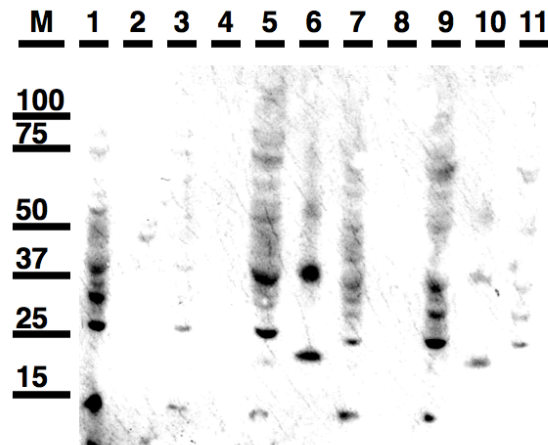


Figure 3.7: D-CF expression and immunostaining of AQP6. 1: Supernatant (SN) 0.5 %Brij78; 2: Pellet (P) 0.5 % Brij78; 3: SN 2 % OG; 4: P 2 % OG; 5: SN 1.2 % OG; 6: P 1.2 % OG; 7: SN 1 % Triton X-100; 8: P Triton X-100; 9: SN 0.2 % DDM; 10: P 0.2 % DDM; 11: SN 0.5 % digitonin.

Table 3.2: Detergents tested for cell-free expression reactions, either for solubilization after P-CF expression or directly added to reaction mixture (D-CF). P-CF: +++: highest solubilization; ++ efficient for solubilization; +: capable for solubilization but major part still in pellet; D-CF: +++: highest expression rates and protein in SN; ++ high expression rates + low expression rates; o no expression detected.

Detergent	Conc. P-CF	Conc. D-CF	Result P-CF	Result D-CF
LPPG	2 %	-	+++	n/a
LMPG	2 %	-	+++	n/a
Fos-16	1 %	-	+	n/a
DPC	1 %	-	++	n/a
DDM	2.5 %	0.2 %	+++	++
Beta-OG	3 %	2 %; 1.2 %	+	o; ++
Triton X-100	2.5 %	1 %	+	++
Brij35	-	0.5 %; 1 %	n/a	+++; ++
Brij78	-	0.5 %; 1 %	n/a	+++; ++
Digitonin	-	0.5 %	n/a	+
SDS	2 %	-	+++	n/a

The best detergent for resolubilization was LMPG (2 %) and for expression in D-CF mode Brij35 (0.5 %). In presence of DDM purified AQP6, expressed in P-CF or D-CF mode, was compared by SDS-PAGE and western blot (Figure 3.8). For both cell-free expression modes the expected pattern was visible. There were no differences between the two expression modes. The signal strength for monomers and oligomers was the same, leading to the assumption that in both modes the tetramer formation (in SDS-containing sample buffer) is the same. In contrast to these results, only a very weak monomer band was visible for AQP6 expressed in presence of lipids (L-CF).

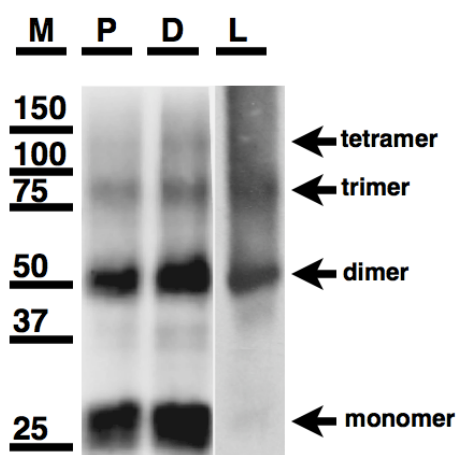


Figure 3.8: Comparison of P-CF (P), D-CF (D) and L-CF (L) produced AQP6, obtained by western blot. Arrows indicate monomer, dimer, trimer and tetramer. P-CF and D-CF expressed AQP6 was not purified from the reaction mix, L-CF was purified by sucrose gradient; the fraction containing liposomes was loaded on the gel.

3.1.3 Purification

A basic purification protocol for P-CF and D-CF produced AQP6 was developed. Taking advantage of the 6xHis tag the main part of purification was an IMAC. In detail, to purify the P-CF AQP6, the reaction mix was centrifuged after solubilization for 20 min at 4 °C and 100,000 g. The supernatant (P-CF) or the D-CF reaction mix was diluted with binding buffer. For binding to the Ni-NTA resin, shaking overnight was necessary. Shorter binding periods led to insufficient binding and large amounts of protein in the flow through and wash fractions. Due to weak binding of AQP6 to the resin, purification by FPLC and a Ni-NTA column was insufficient and resulted in significantly lower yields.

Table 3.3: Purification conditions for highest yields.

Expression Mode	Detergent Expression	Detergent Purification	Buffer pH	Yield mg/ml
D-CF	0.2 % DDM	0.05 % DDM	Tris pH 7.4	0.1
D-CF	0.5 % Brij35	0.05 % DDM	Tris pH 7.4	0.6
D-CF	0.5 % Brij35	1.2 % OG	Tris pH 7.4	0.5
P-CF	2 % LMPG	0.05 % DDM	Tris pH 7.4	0.7
P-CF	2 % LMPG	1.2 % OG	Tris pH 7.4	1.5

The highest AQP6 yield was achieved by protein expression in P-CF mode, solubilization with 1 % LMPG and purification in presence of 1.2 % OG using Ni-NTA beads. Impurities were completely washed out and were not visible in final elution fractions on coomassie stained SDS gels (Figure 3.9, left). A more detailed analysis of the whole purification process by immunoblotting revealed that a portion of AQP6 remains in the pellet fraction after solubilization with 3 % OG for 4 h (Figure 3.9, right). A considerable amount of AQP6 did not bind to the Ni-NTA beads and was washed out with the flow through. The weak binding to the Ni-NTA beads was further demonstrated by washing out AQP6 at an imidazole concentration of 10 mM. After eluting with three column volumes of 100 mM imidazole, a minor part of protein was still bound to the Ni-NTA resin.

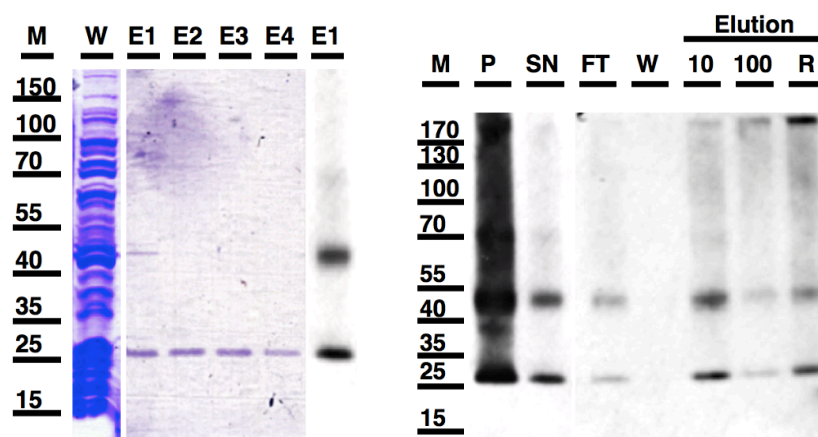


Figure 3.9: Left: SDS gel of AQP6 Ni-NTA purification (P-CF, 1.2% OG). Elution with 100 mM imidazole in 300 μ l fractions (E1-E4). E5: Immunodetection of AQP6 elution fraction E1 with penta-His antibody. **Right: Detailed analyses of AQP6 binding and elution properties.** P: Pellet after solubilization, SN: Supernatant, FT: Flowthrough, W: Wash, 10: Elution with 10 mM imidazole, 100: Elution with 100 mM imidazole, R: Resin, the relative strong signal is due to the higher concentration of Ni-NTA beads.

For structural studies a protein sample of highest quality is required. Objectives of protein quality are homogeneity, monodispersity and functionality. An advantage of the cell-free expression system is the possibility to develop individual expression protocols in terms of basic compounds, buffer and detergent conditions. In order to achieve optimal conditions in relation to protein quantity and quality, the cell-free expressed protein has to be analyzed further after solubilization and purification as for any expression system. Therefore, quality of purified protein was further evaluated by size-exclusion chromatography and negative stain single particle electron microscopy (3.1.4).

Cell free produced AQP6 was subjected to size exclusion chromatography. P-CF AQP6 eluted mainly at the exclusion volume of the used Superdex 200 10/300 GL column, with only minor differences when used different detergents for solubilization and purification (Figure 3.10, summary of all experiments in Table 3.4). Similar elution profiles were recorded for D-CF produced AQP6. However, one condition for D-CF AQP6 could be identified where the AQP6 was eluted mainly at a volume corresponding to the molecular mass of the AQP6 tetramer including the size of the detergent micelle.

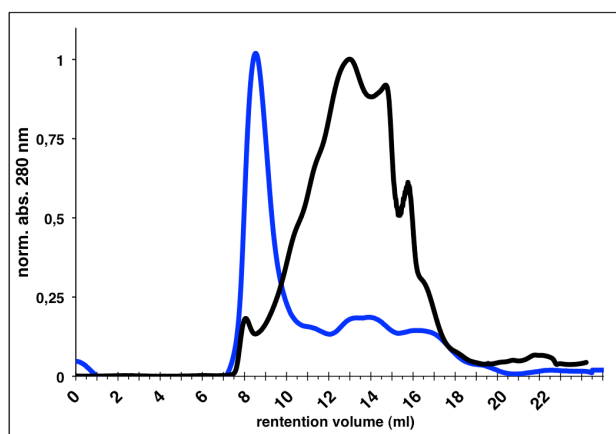


Figure 3.10: Size exclusion chromatograms of P-CF (blue) and D-CF (black) produced AQP6. P-CF AQP6 elutes mainly at exclusion volume of Superdex 200 10/300 column at 8 ml. Elution profile of D-CF AQP6 is shifted to higher volumes. Elution at 12 ml corresponds to mass of AQP6 tetramer and at 15 ml to AQP6 monomer.

Table 3.4: Summary of size exclusion experiments with cell-free produced AQP6. In all, except one D-CF experiment, AQP6 eluted as aggregate.

Expression Mode	Detergent Expression	Detergent Purification	Result
D-CF	0.2 % DDM	0.05 % DDM	Broad peak 12 ml
D-CF	0.2 % DDM	1.2 % OG	Aggregates
D-CF	0.5 % Brij35	0.05 % DDM	Aggregates
D-CF	0.5 % Brij35	1,2 % OG	Aggregates
P-CF	2 % LMPG	0.05 % DDM	Aggregates
P-CF	2 % LMPG	1.2 % OG	Aggregates
P-CF	0.2 % DDM	0.05 % DDM	Aggregates
P-CF	0.5 % DDM	0.05 % DDM	Aggregates
P-CF	2 % OG	1.2 % OG	Aggregates
P-CF	4 % OG	1.2 % OG	Aggregates

3.1.4 Single particle analysis

AQP6 expressed in P-CF and D-CF mode and purified was subjected to negative stain single particle TEM.

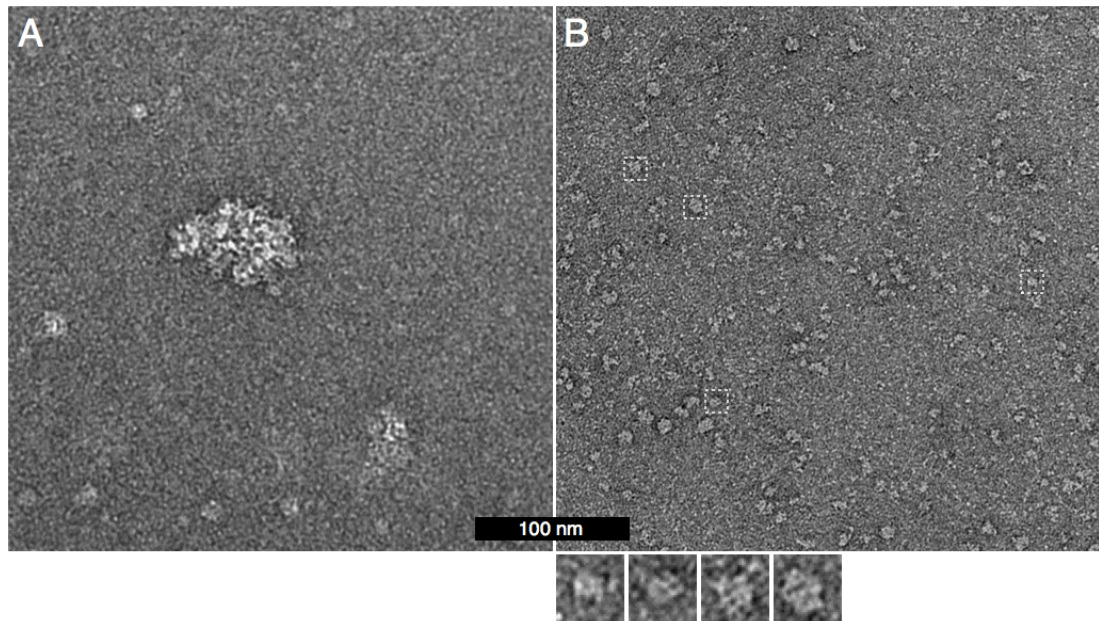


Figure 3.11: Electron micrograph of negatively stained AQP6. **A:** P-CF expressed, solubilized in 2 % LMPG and IMAC purified in presence of 0.05 % DDM, large aggregates are visible. **B:** D-CF expressed in presence of 1 % Brij35 and IMAC purified in presence of 0.05 % DDM, particles of a diameter of 8 nm, as expected for AQP6 are visible besides larger particles. Edge lengths of boxes represent 15 nm.

Analysis of negatively stained single particles confirmed the results of size exclusion chromatography. Aggregates were visible on the electron micrographs for P-CF AQP6. The promising D-CF condition revealed a sample of inhomogeneous quality, but particles corresponding to AQP tetramers in shape and size were visible (Figure 3.11) [131].

3.1.5 Reconstitution into liposomes

The reconstitution into liposomes was the starting point for functional assays of AQP6. Proper folding of cell-free expressed AQP6 should be demonstrated by complete reconstitution into lipid bilayers, followed by further functional tests like water conductance experiments.

A broad range of different AQP6 preparations, purifications of P-CF or D-CF expressed protein, were initially tested with different lipids of natural or artificial source. *E. coli* polar lipids were chosen, because reconstitution of cell free produced AQP4 was demonstrated with *E. coli* polar lipid liposomes [80]. Since AQP6 expression was detected in synaptic vesicles in brain [65], brain polar lipids were used for reconstitution as well.

Solubilized purified protein was either reconstituted into preformed liposomes destabilized by Triton X-100 titration or in the presence of detergent solubilized lipids. After removing the detergent from the ternary mixture by adding Bio-Beads or by dialyses, proteoliposomes were purified either by ultracentrifugation over a continuous sucrose gradient, or a 2-step sucrose gradient. Proteoliposomes were harvested by a second ultracentrifugation and analyzed by SDS-PAGE followed by immunostaining.

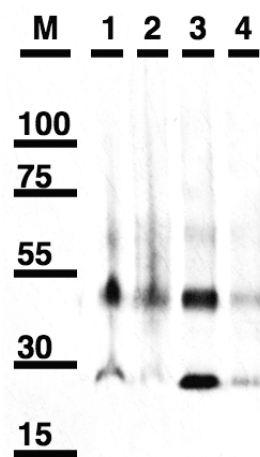


Figure 3.12: Western blot of potential D-CF AQP6 proteoliposomes, purification from precipitated protein by sucrose gradient centrifugation. Lane 1: Brain lipids (LPR 10) precipitate; 2: *E. coli* lipids (LPR 10) precipitate; 3: brain lipids (LPR 10) liposomes; 4: *E. coli* lipids (LPR 10) liposomes.

AQP6 could be detected by immunoblotting in lipid-containing fractions (Figure 3.12). Reconstitution in brain polar lipids showed a stronger signal than the *E. coli* polar lipid condition. Furthermore, AQP6 was partly precipitated and detected in the pellets by immunoblotting. All tested conditions are summarized in Table 3.5.

Further analyses of lipid fractions (*i.e.* proteoliposomes) by freeze-fracture electron microscopy should demonstrate accurate reconstitution of AQP6. Electron micrographs of replicas of freeze fractured liposomes showed empty liposomes for all conditions tested (Figure 3.13). This led to the conclusion that reconstitution reactions were not

successful. However, it turned out that liposomes, which showed signals for AQP6 by immunostaining did not show any protein insertion. This means that a positive western blot signal for the lipid fraction is only necessary but not sufficient in order to proof protein reconstitution. For this reason, all potential proteoliposomes were subsequently analyzed by freeze fracture electron microscopy, with the result that reconstituted protein was not visible as cluster in the membrane of liposomes, but as aggregates (Figure 3.13, A right). Due to this result no further experiments were performed with AQP6 expressed either in P-CF mode or D-CF mode.

Table 3.5: Summary of reconstitution condition tested. AQP6 was detected by immunostaining in the lipid fraction. To verify insertion liposomes underwent a freeze fracture analysis.

Lipid	LPR (w/w)	Condition	Result Western Blot	Result Freeze fracture
Brain polar lipids	10	P-CF, OG	AQP6 in lipid fraction	No insertion
<i>E. coli</i> polar	1; 10; 100	D-CF, DDM; OG	AQP6 in lipid fraction	No insertion
<i>E. coli</i> polar	1; 10; 100	P-CF, OG	AQP6 in lipid fraction	No insertion
POPC-mix	1; 10; 100	P-CF, OG	AQP6 in lipid fraction	No insertion
POPC-mix	1; 10; 100	D-CF, DDM; OG	AQP6 in lipid fraction	No insertion
DOPC	1; 10; 100	D-CF, DDM	AQP6 in lipid fraction	No insertion

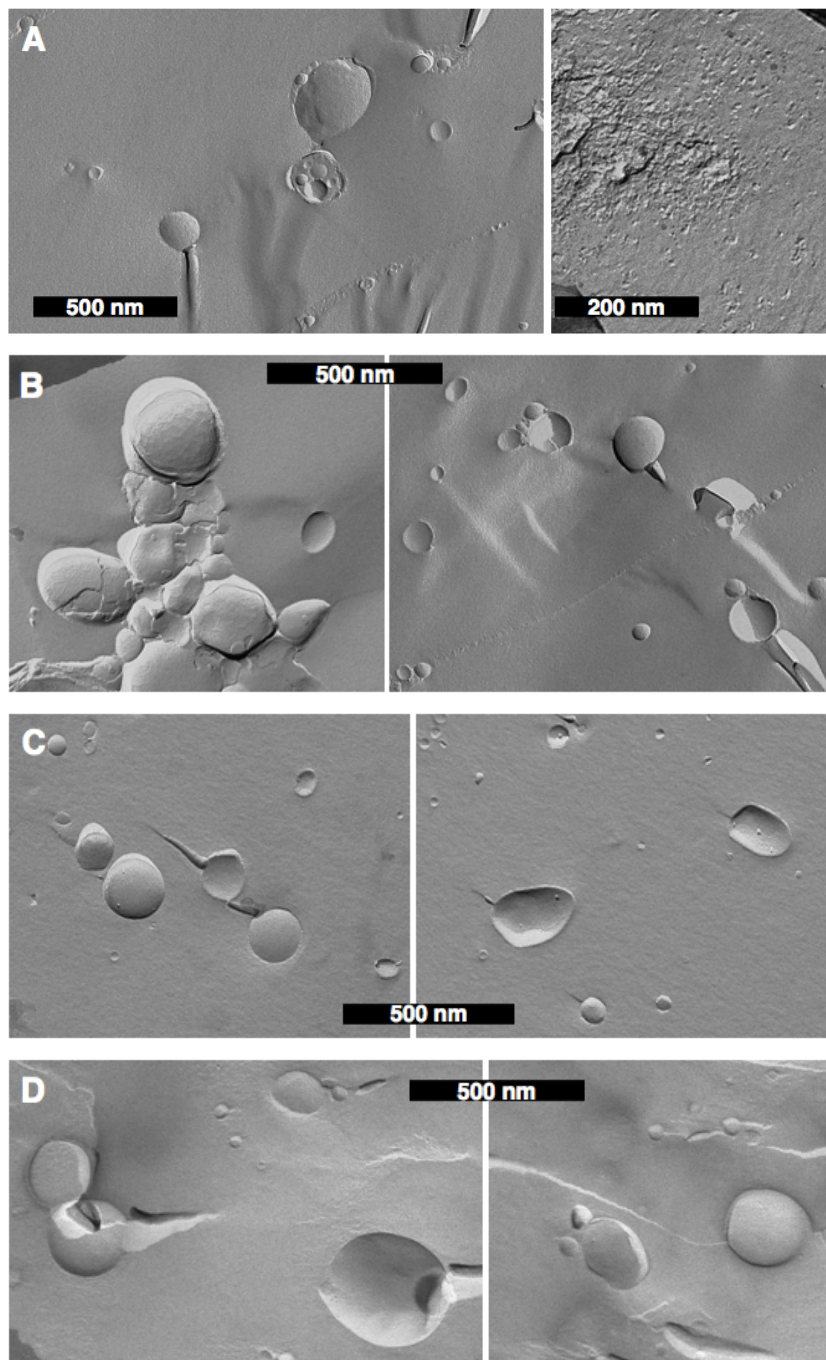


Figure 3.13: Freeze fracture of liposomes from cell-free AQP6 reconstitution reactions using different lipids at LPR of 1. **A:** P-CF brain lipids, no reconstitution of AQP6 in liposomes visible (left), but aggregated protein (right). **B:** P-CF reconstitution with *E. coli* polar lipids results in empty liposomes, as well as **C:** P-CF with DOPC liposomes. **D:** D-CF reconstitution with POPC-mix lipids results in empty liposomes.

3.1.5 Co-translational reconstitution

Cell-free expression in presence of liposomes offers another promising approach to gain protein reconstitution. For co-translational reconstitution of AQP6 a protocol was established. Cell-free expression was carried out as described before, but liposomes, in some cases destabilized by detergent, were directly added to the reaction mix.

Cell-free expression in presence of liposomes was performed with different concentrations of DOPC or *E. coli* polar lipids, respectively. These lipids were chosen because *E. coli* polar lipids are commonly used for reconstitution and liposome formation [80]. DOPC was successfully used before for functional L-CF expression of AQPZ [81] and bacteriorhodopsin [132]. In order to obtain homogeneous liposomes, it was necessary to pass the lipid mixtures through 800 nm and 200 nm filters 21 times, successively using an Avanti mini extruder before adding to the reaction mix.

Table 3.6: Results of expression experiments in presence of lipids. Liposomes were performed either with *E. coli* polar lipids or DOPC and added to the reaction mix. Protein was detected by western blotting and freeze fracture electron microscopy.

Lipid	Concentration (mg/ml)	Detergent	Result
<i>E. coli</i> polar	1.5	-	Insertion ++
DOPC	2.8	-	Insertion +
DOPC	3.8	-	Insertion ++
DOPC	3	-	Insertion +
DOPC	3	CHAPS	Insertion ++

Cell-free expression reactions were set up as described in Chapter 2.1.2.3, but preformed liposomes were added instead of the same volume of water, in order to obtain end concentrations of lipids between 1.5 to 3.8 mg/ml (Table 3.6). Expression reactions were carried out at 33 °C overnight. Liposomes were harvested by sucrose gradient (10 % - 60 % (w/w)) ultracentrifugation and analyzed using SDS-PAGE and western blotting.

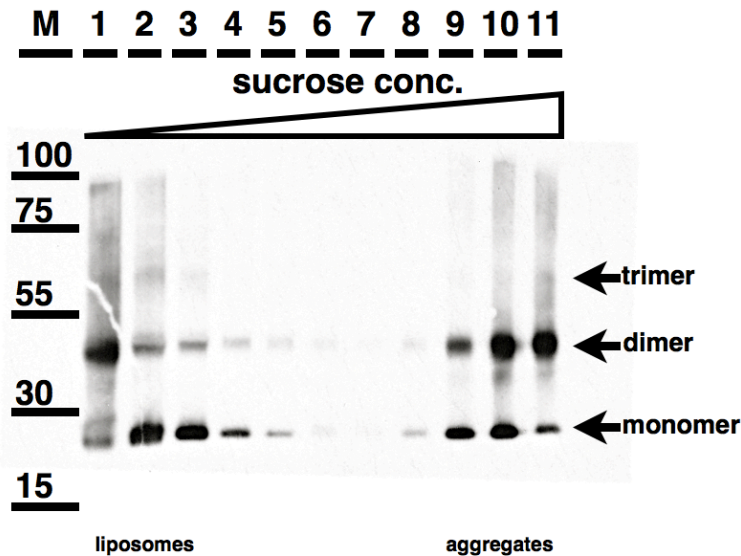


Figure 3.14: Sucrose gradient ultracentrifugation of AQP6 produced by L-CF.

The western blot, using a penta-His antibody for detection (Figure 3.14), showed an AQP typical signal pattern with different oligomeric states, mainly in the upper and bottom fractions taken from the sucrose gradient ultracentrifugation. In the bottom fraction precipitated AQP6 is accumulated, since the density of precipitated protein is higher than the density of 60 % sucrose. Liposomes with a lower density stay at the upper part of the sucrose gradient and were visible by eye due to their milky color. Liposome associated or incorporated AQP6 could be detected by immunostaining.

The separation by a continuous sucrose gradient was improved by a single step sucrose gradient (40 % (w/w) sucrose). The ability to separate (proteo-) liposomes and precipitated protein was comparable to the continuous sucrose gradient, but had the advantage of using smaller volumes and obtaining higher concentrated (proteo-) liposomes.

The separation of AQP6 carrying proteoliposomes and precipitated protein was achievable. However, from these results the insertion of AQP6 into the liposome membrane could not be proven. The problem could be that the nascent protein sticks to the bilayer, but does not insert. Therefore, freeze fracture electron microscopy was applied.

Electron micrographs from freeze fracture replicas showed liposomes of different sizes and small clusters attached to the membrane (Figure 3.15 A, B, arrows). The clusters could be explained with a replica of protein sticking out of the membrane. The size of

the clusters corresponded to the expected size of AQP6 tetramers: approximately 8 nm and an additional 2 nm platinum layer.

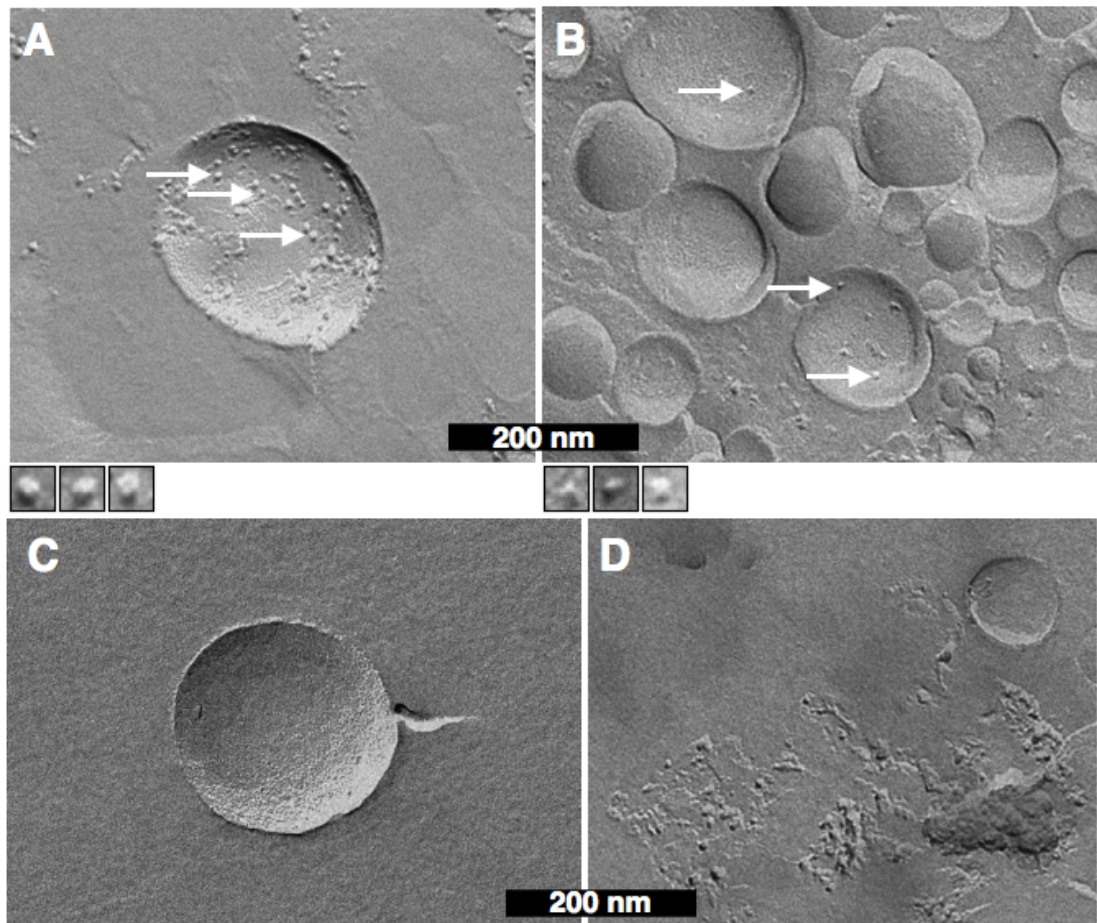


Figure 3.15: Freeze fracture electron microscopy of purified liposomes from L-CF expression. **A, B:** Liposomes resulting from L-CF expression in presence of *E. coli* polar lipid (A) and DOPC (B) liposomes. Clusters at size of AQP6 tetramers were visible in liposomes (arrows). Magnifications of clusters are depicted in little boxes with edge lengths corresponding to 15 nm. **C, D:** L-CF expressed protein, OG solubilized, purified and reconstituted. In this preparation no reconstitution but protein aggregates were visible.

The freeze fracture replicas showed liposomes of different diameters. *E. coli* polar lipids liposomes have a diameter of approximately 200 nm, while DOPC liposome diameters range from diameters of 20 nm to more than 200 nm. The replicas demonstrated that the proteliposomes contained small particles, which is reconstituted AQP6. The presence of liposomes, produced by 1.5 mg/ml *E. coli* polar lipids or 3 mg/ml DOPC, during translation led to insertion of AQP6 (Figure 3.15 (A) and (B)). The sucrose gradient purification demonstrated that reconstituted AQP6 in the liposome fraction was separated not completely from aggregated protein. The same result was obtained for purification by a 40 % sucrose 2-step gradient centrifugation. Freeze fracture analysis showed protein reconstitution from this purification method, too.

Solubilization of L-CF produced AQP6 and reconstitution

Additional experiments should prove whether AQP6, cell-free expressed in presence of liposomes, could be solubilized and reconstituted into liposomes again. This would be in accordance to the theory, that certain membrane proteins need specific lipids for folding [133], and once the protein is in a stable fold, it could be transferred to a different lipid environment using mild detergents.

Cell-free expression was carried in presence of preformed liposomes at a final concentration of 3 mg/ml DOPC. Liposomes were harvested by ultracentrifugation over a single step sucrose gradient as described before (see above). Concentrated liposomes were resuspended and solubilized in a total volume of 500 μ l with solubilization buffer containing 2.5 % beta-OG for 1 h at 4 °C. Unsolubilized material was separated by ultra centrifugation. The supernatant was diluted to 1.5 % beta-OG and incubated with Ni-NTA beads overnight at 4 °C in order to bind His-tagged AQP6. AQP6 was purified and reconstituted with DOPC lipids as described before. Electron microscopy of freeze fracture replicas revealed empty liposomes and precipitated protein (Figure 3.15, C,D).

Purification of proteoliposomes

Since the sucrose gradient ultracentrifugation is the only purification step of the L-CF reaction mixture, additional methods for purifying proteoliposomes, like Ni-NTA purification and filtration were tested. For Ni-NTA purification, proteoliposomes were incubated with Ni-NTA beads overnight and eluted as described before for AQP6. Although, it turned out that proteoliposomes containing AQP6 did not bind to the Ni-NTA beads. The elution fractions did not contain protein, AQP6 was washed out during the washing step. This could have several reasons. AQP6 concentration might be too low, it might have a wrong orientation with the His-tag inside the liposome, or the binding might be too weak to retain the proteoliposomes. Because of these results the purification of proteoliposomes was carried out by a 250 kDa Amicon ultra concentrator (Millipore) after sucrose gradient ultra centrifugation. Smaller proteins and in the L-CF could be removed from the reaction mixture.

The cell-free expression in presence of liposomes demonstrated that the co-translational reconstitution of AQP6 was feasible. The importance of a machinery for membrane insertion of cell-free produced protein remains obscure. The SRP receptor FtsY is present in the cell free extract. FtsY interacts with DOPC lipids and usually facilitates the interaction between SRP and the translocon [122]. In case of the

membrane channel MscL it was shown, that during cell-free expression co-translational insertion is independent of YidC, a component of the insertion pathway [134].

In order to enhance the functional co-translational reconstitution, detergent destabilized liposomes were added to the cell-free reaction. Treatment of liposomes with detergent, before adding to the cell-free reaction mix is supposed to relax the tightly packed liposome structure without degeneration of the liposomes. As a result of destabilizing the liposomes, the energy barrier for a spontaneous incorporation of MPs into a lipid environment might be decreased [132, 135]. Lipids were supplied at final concentrations from 1.5 to 4.5 mg/ml. The zwitterionic detergent CHAPS has a high cmc (0.5 %) and a low aggregation number (10), which favors a removal by dialysis. For this reason it is dialyzed out during the cell-free reaction, leaving detergent free proteoliposomes. To destabilize the liposomes prior to their addition to the RM, final concentrations of 0.5 – 1.5 % CHAPS were mixed with the preformed liposomes and incubated for 30 min at RT before use. The destabilization of liposomes using low concentration of CHAPS led to higher AQP6 concentrations in liposome fraction.

3.1.6 Water conductance of cell-free expressed AQP6

In order to test the water channel activity of cell-free expressed AQP6, expression of AQP6 in the L-CF mode was carried out. Supplementing the reaction mixture with 3 mg/ml preformed DOPC liposomes ensured a co-translational insertion of protein (3.1.5) and was demonstrated before with the expression of *E.coli* AQPZ [81].

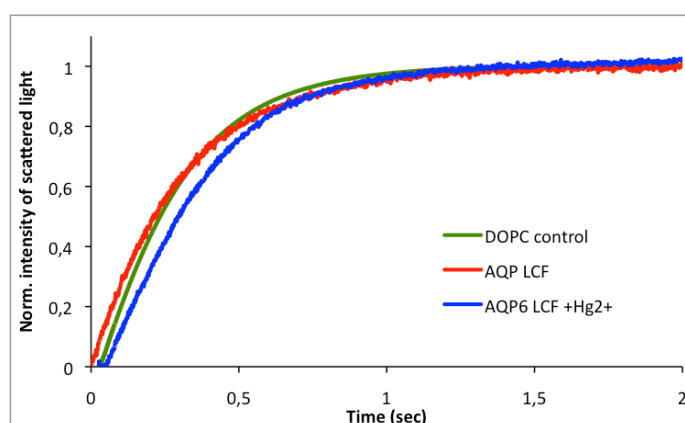


Figure 3.16: Stopped-flow analysis of AQP6 expressed in L-CF mode in presence of DOPC liposomes. Traces displayed similar increases in scattered light when AQP6 was reconstituted into liposomes, when liposomes were incubated with Hg^{2+} before measurement and when control liposomes were empty. Five traces of individual runs per experiment were normalized and averaged.

For determining the rate constants, traces from five experiments were averaged and normalized (Figure 3.16). Averaged traces were fitted to single exponential equations ($y = y_0 - Ae^{-kx}$), with k being the rate constant of the first order kinetic reaction. Calculated water permeability factors are stated in Table 3.7. Shrinkage rates of proteoliposomes without contact to Hg^{2+} , as well as pre-exposed to Hg^{2+} , and of empty control liposomes were close to the same value (3.5 s^{-1} , 2.9 s^{-1} and 3.1 s^{-1}). Hg^{2+} is a known water transport inhibitor for most AQPs, except for AQP6 it was reported to be an activator [34, 136]. Even though, proteoliposomes treated with Hg^{2+} exhibited not a faster shrinkage.

Table 3.7: AQP6 water transport rates obtained by single exponential fitting the measured light scattering traces.

Condition	$k\text{ (s}^{-1}\text{)}$	$P_f\text{ (}\mu\text{m/s)}$
AQP6 L-CF DOPC	3.5	28.5 ± 1.6
AQP6 L-CF DOPC + Hg^{2+}	2.7	21.8 ± 2.9
DOPC lipids, empty liposomes	3.1	23.0 ± 1.1

The water permeability factors (P_f) were calculated as described in Chapter 2.7. The volume of liposomes was determined by measuring their diameters in freeze fracture micrographs. The average diameter of DOPC liposomes was $174 \pm 10\text{ nm}$. Water permeability factors of $28.5\text{ }\mu\text{m/s}$ for AQP6 liposomes without Hg^{2+} treatment and $21.8\text{ }\mu\text{m/s}$ for AQP6 liposomes exposed to Hg^{2+} were calculated. Empty DOPC liposomes showed a water permeability of $23.0\text{ }\mu\text{m/s}$. Compared to cell-free expressed mouse AQP4 M23 determined water permeability factors for AQP6 were lower. Water permeability for AQP4 M23 reconstituted into *E. coli* polar lipids liposomes ranged from ca. $50\text{ }\mu\text{m/s}$ (P-CF expression) to ca. $130\text{ }\mu\text{m/s}$ (D-CF expression) at $10\text{ }^\circ\text{C}$ and LPR 40, where control liposomes showed an average water permeability of $25.5\text{ }\mu\text{m/s}$ [80]. An explanation for similar water permeabilities of AQP6 in the absence or presence of Hg^{2+} , could be that Hg^{2+} does not act as a water channel activator, as reported before [34]. Nevertheless, all determined transport rates exhibit very low values compared to empty liposomes. The determined values for water permeability should reviewed carefully, because they are influenced by numerous factors. This has to be taken into account, when different samples are compared. The most likely reason for measuring a very low water conductance is that AQP6 was not reconstituted in its active conformation. Especially for the cell-free expressed AQP6 it is imaginable that

the folding of the protein might be incomplete or incorrect. The *E. coli* based cell-free system lacks a eukaryotic chaperone machinery. The efficiency of protein folding in cell-free systems is still a subject of discussion [137, 138]. It was not possible to investigate whether low water transport activity of AQP6 is due to non-functional protein or to a very low inherent water transport activity.

3.2 *Semliki* Forest virus expression of AQP6

3.2.1 Template design

At DNA level, the *Semliki* Forest virus expression system is composed of two vectors, the expression vector and the helper vector. For expression of AQP6, a construct with a C-terminal 6xHis tag was cloned into the pSFV2 expression vector, using *RsrII* and *XhoI* restriction sites. Restriction sites were generated by PCR using appropriate primer. Correct cloning was confirmed by DNA sequencing. See appendix B for full sequence.

Table 3.8: Primers used for *RsrII* and *XhoI* restriction site generation.

Primer <i>RsrII</i> AQP6 forward	Primer <i>XhoI</i> AQP6 reverse
5`cgggtccgatggctagcatgactggtggaca	5`ctcgagttaatggtgatggtgatggtgcacgc

3.2.2 Transcription

3.2.2.1 *In vitro* transcription

In order to overexpress AQP6 in mammalian cells, the genetic information of AQP6 and viral proteins has to be transcribed into RNA. Therefore an *in vitro* transcription reaction of the expression vector and helper vector was performed using SP6 RNA polymerase.

Template DNA quality and quantity

In order to obtain highest yields in the *in vitro* transcription reaction, linearized DNA was used as template. Linearization by digestion with *NruI* or *SpeI* at restriction sites closely behind the coding regions prevented very long transcripts by securing efficient termination. Completeness of digestions was checked on a 0.8 % agarose gel. For complete digestion incubation overnight at 37 °C was necessary. DNA was either purified from an agarose gel by a GenElut DNA-binding column (Sigma-Aldrich) or by phenol/chloroform extraction. Between these methods no difference in purity and in *in vitro* transcription yields was visible. Due to higher DNA recovery rates, DNA purification by GenElute columns was carried out routinely. The total amount of DNA used as template for RNA production was 0.5 µg DNA in a total volume of 60 µl. It turned out that higher DNA concentrations did not lead to higher RNA amounts. It was possible to scale up the reaction by four times without losing efficiency.

MEGAscript Kit (Ambion) compared to SP6 polymerase (Roche Applied Science)

The MegaScript (Ambion) *in vitro* transcription kit was compared to separately purchased SP6 polymerase and nucleotides and RNase free water (Roche Applied Science). There was no visible difference in terms of RNA yield and quality. For these reasons, the lower-priced products (Roche Applied Science), which were not sold as an *in vitro* transcription kit, were used.

GTP/Cap analogue ratio

For translation in eukaryotes mRNA 5'-end modification by a cap structure (m⁷G(5')ppp(5')G) is essential. The m⁷G-cap protects the mRNA for degradation and is important for translation initiation [139]. In order to produce capped mRNA in the *in vitro* transcription reaction, GTP concentration was decreased ten times and replaced by m⁷G(5')ppp(5')G [140]. This led to very low yields of RNA and could be increased with a greater part of GTP. The optimal GTP/Cap analogue ratio was determined to be 1:4. Higher concentration of the m⁷G-cap did not lead to significant higher yields but to more degradation as observed on a 0.8 %-agarose gel.

Reaction time

The optimal reaction time and temperature was found to be 60 min at 37 °C. Shorter incubation times resulted in lower yields because of incomplete reactions. Incubation longer than 90 min resulted in degraded RNA.

Table 3.9: Components of optimized *in vitro* transcription reaction.

Component	Final concentration	Volume (μl)
ATP	1 mM	0.6
CTP	1 mM	0.6
UTP	1 mM	0.6
GTP	0.25 mM	0.75
Cap analogue	1 mM	0.6
10 x SP6 Buffer	1x	6
Linear template DNA	0.5 μg	10
RNase Inhibitor	1 U/μl	0.5
Enzyme mix – SP6	500 U/ml	2

The mRNA coding for AQP6, produced by *in vitro* transcription was directly used for virus production, *i.e.* for electroporation.

3.2.2.2 Virus production

Virus production was carried out as described before [141-143]. To produce recombinant virus for protein expression, SFV-AQP6 RNA has to be packed into SFV virus particles. Therefore, RNA of pHelper and pSFV-AQP6 were mixed and introduced into BHK cells by electroporation. For virus production 1 x 10⁷ BHK cells were used, grown to a confluency of 90 %, which corresponds to the logarithmic growth phase.

In the BHK cells, RNA is amplified and the RNA carrying the packing signal (SFV-AQP6) is packed into virus particles. To optimize the system for highest virus titers, the RNA-virus ratio, electroporation variables and reaction time were modified (Table 3.10). Virus was tested either by titer determination or directly by western-blot analysis after infection and heterologous protein production.

Table 3.10: Setting for electroporation of BHK cells.

Parameter	Setting
Voltage	360 V
Capacity	75 μ F
Resistance	∞
Cuvette	4 mm

Transfected BHK cells were incubated for 12 h to 48 h in order to produce virus particles. Virus titers reached a maximum after 40 h incubation. The virus was harvested carefully, because to a weak attachment of BHK cells. Longer incubation times led to an increased number of dead cells. The virus titer strongly correlated with pH changes of cell culture media, directly visible as color shift from red to yellow of pH indicator (phenol red) in the media.

3.2.2 Translation

Heterologous protein overexpression was carried out mainly in BHK cells, but HEK and CHO5 cells were tested, as they were used for mammalian membrane protein expression in the SFV expression system before [52, 143]. For overexpression cells have to be infected by SFV, containing the genetic information of the desired protein. After infection the strong viral promoter induces translation. Virus infection and translation were carried out at 33 °C or 37 °C for 24 h to 60 h.

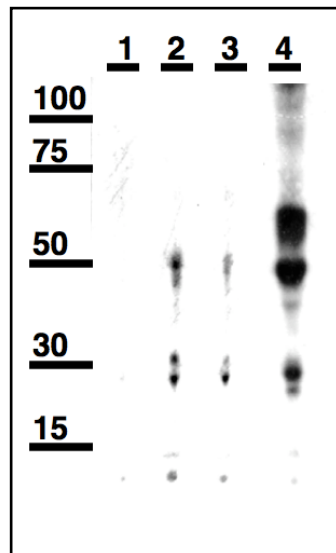


Figure 3.17: Immunodetection of His-tagged AQP6 in whole cells. 1: negative control, BHK cells infected with virus packed with empty pSFV2; 2: CHO5 cells, 3: HEK cells, 4: BHK cells infected with virus coding for AQP6.

Cells were disrupted and analyzed by SDS-PAGE and subsequent immunodetection. The western blot exhibited bands of different intensity for CHO5, HEK and BHK cells (Figure 3.17, Table 3.11). Since the negative control did not show any signal in the immunodetection, it was assumed that the band just below 30 kDa and above 50 kDa were AQP6 monomer and dimer. Additional signals at ca. 45 kDa and higher molecular weights were observed for BHK cells, which could be explained with membrane patches sticking to protein or incomplete solubilization, having in mind that whole cells were analyzed on the gel. The double band at ca. 30 kDa could be explained with different glycosylation states of AQP6, since AQP6 has one potential glycosylation site. Best expression results were observed using BHK cells for protein production. Expression levels in HEK or CHO5 cells were considerably lower. Incubation times longer than 48 h did not lead to higher expression rates; therefore incubation was stopped after 48 h.

Table 3.11: Expression levels of AQP6 in different cell lines. Determined by immunodetection with penta-histidine antibody.

Cell line	Expression level	Expression temp. (°C)
BHK	+++	37
CHO5	o	37
HEK 293	o	37

For AQP6 production, the following protocol was established: BHK cells were grown in three T300 flasks to 90 % confluency. This amount of cells resulted in two T75 flasks virus stock (60 ml) after transfection. Virus was harvested after 48 h, aliquoted, and

shock frozen in liquid nitrogen and stored at -80 °C for months or used directly. Before infection of cells, virus stocks were treated with 1 mg α -chymotrypsin per 10 ml and incubated at RT for 30 min in order to activate the virus. Reaction was terminated by inactivation of α -chymotrypsin with 0.5 mg aprotinin per 10 ml. Derived from virus titer determination one T300 tissue culture flasks (300 cm²) containing cells, 80 %-confluent cells were infected with approx. 10 ml virus stock. Protein expression took two days at 33 °C in 75 ml fresh DHI-5 (see A.4.2) medium.

Overall the AQP6 yield after purification was increased by an incubation temperature of 33 °C instead of 37 °C during infection and translation. Furthermore, the pH of the containing media was stable at an expression temperature of 33 °C.

3.2.3 Solubilization

BHK cell membranes were harvested by ultracentrifugation and stripped by urea/alkali treatment. Final membrane preparations were subjected to solubilization experiments by resuspending in 1 ml volume and dilution with buffer containing detergent at desired concentration (Table 3.12). Solubilization was carried out at RT for 2 h followed by an ultracentrifugation at 100,000 g. Solubilization overnight at 4 °C showed no remarkable differences. Supernatants and insoluble pellets were analyzed by immunostaining in order to detect His-tagged AQP6 (Figure 3.18).

Table 3.12: Solubilization of AQP6 from BHK membranes with different detergents.

Detergent	Concentration	Solubilization rate
Beta-OG	4 %	++
DDM	1 %	+++
DM	3 %	o

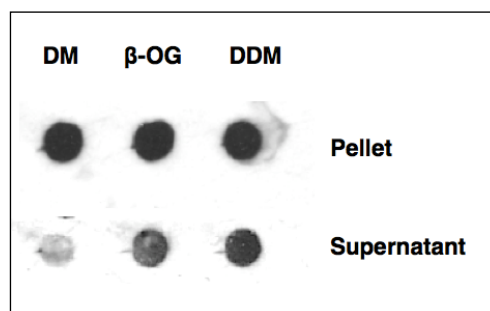


Figure 3.18: Solubilization trials of BHK membranes by dot blot - immunodetection with penta-His antibody.

Best solubilization was obtained in 1 % DDM and by 4 % OG. With 3 % DM the amount of AQP6 in the soluble fraction was very low. Because of their ability to solubilize AQP6, DDM and OG were used for solubilization in preparative scale.

3.2.4 Purification

IMAC (Ni-NTA)

Since a 6xHis tag is engineered at the AQP6 C-terminus, the key purification step is an affinity chromatography using a Ni-NTA column or Ni-NTA beads in a batch procedure. The supernatant was loaded on a 5 ml His-Trap column (GE) at a flow rate of 0.3 ml/min in presence of 5 mM imidazole to eliminate unspecific binding. Unbound protein was washed out with 15 mM imidazole at a flow rate of 1 ml/min, followed by an imidazole gradient from 15 mM to 500 mM over 10 column volumes. SDS-PAGE and western blotting of concentrated flow through, wash and elution fractions revealed that the major part of AQP6 was present in the flow through fraction. Another part of AQP6 was eluted during washing, the remaining AQP6, which was eluted between 50 mM and 500 mM imidazole, provided a comparatively weak signal in the western blot (Figure 3.19).

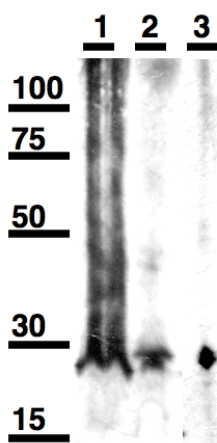


Figure 3.19: Ni-NTA purification, immunodetection with penta-His antibody. AQP6 elutes with flow through, 5 mM imidazole (1) and at 15 mM imidazole (2), only small amount were detected at higher imidazole concentration, 50 - 500 mM imidazole. (3).

In order to improve the binding of AQP6 to the Ni-NTA, a batch protocol was applied. The solubilization supernatant was incubated with pre-equilibrated Ni-NTA beads (250 μ l slurry) under shaking at 4 °C overnight in the presence of 5 mM imidazole in a

total volume 10 ml. The beads were washed with 10 ml washing buffer containing 15 mM imidazole and eluted with elution buffer supplemented with 250 mM imidazole in 150 μ l fractions. Using this protocol protein yield was increased. Although, AQP6 was still detected in the wash fraction. For analysis by SDS-PAGE, only flow through and wash fraction were concentrated (Figure 3.20).

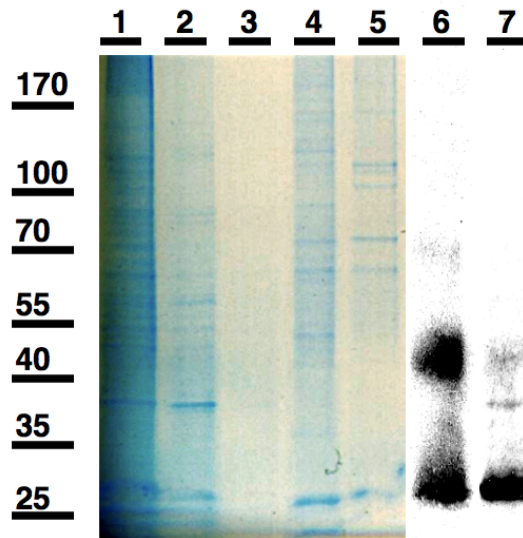


Figure 3.20: Ni-NTA purification of AQP6 using a batch procedure. 1: Flow through; 2-3: Wash fractions; 4-5: elution; 6-7: Immunostaining of 4 and 5.

The reason for the weak binding of AQP6 to the Ni-NTA might be the design of the affinity tag. It is engineered to the protein without any linker. It is possible that the histidine residues at the C-terminus are partly covered with the detergent micelle. This could lead to the elution at low imidazole concentrations compared to other hexahistidine tagged proteins. To circumvent this weak binding, binding time was increased by batch binding overnight. Besides this, due to the smaller bead volume, an elution at higher protein concentrations became possible, avoiding a concentration of protein with spin filters. Despite the batch binding, the protein eluted still at relatively low imidazole concentration (100 mM) and an extensive washing procedure was only possible at low imidazole concentrations. This led to impurities in the elution fractions and the need of an additional purification step, *e.g.* size exclusion chromatography.

Size exclusions chromatography

Ni-NTA purified AQP6 was further purified and analyzed by size exclusion chromatography. Initial purification conditions resulted in elution of the main fraction at the void volume (8 ml) of the Superdex 200 10/300 GL column (Figure 3.21, green curve). By variation of the detergent concentration, decreasing of the solubilization time and addition of glycerol to the buffer, a shift of the elution chromatogram to larger volumes (*i.e.* smaller particles) was obtained. A solubilization time of 1 h at room temperature in presence of 6 % OG resulted in a chromatogram with two additional peaks (blue curve). The peak at 12.5 ml retention volume corresponds to the tetramer mass, including the detergent micelle, the peak at 15.5 ml corresponds to the AQP6 monomer mass. By the addition of 5 % (v/v) glycerol to the solubilization and purification buffers, the rate of aggregates was decreased and the monomer peak became the maximum of the gel-filtration profile (black curve).

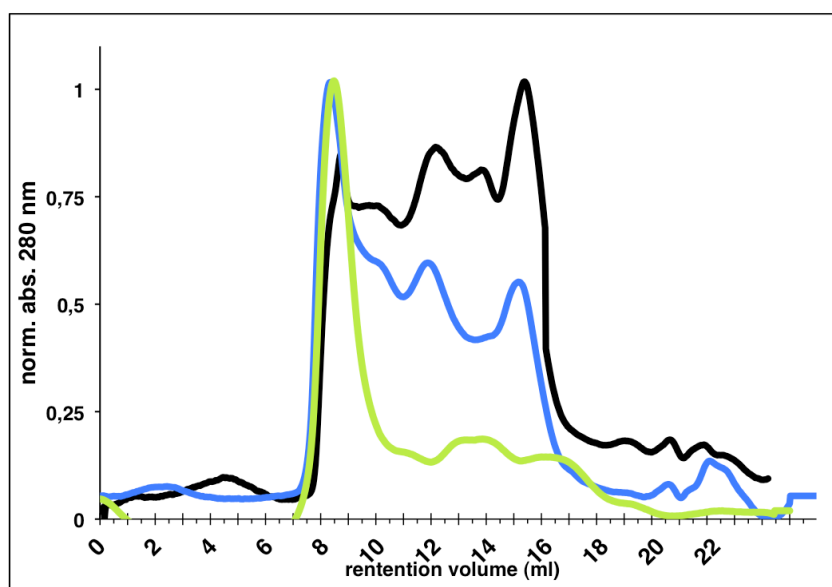


Figure 3.21: Size exclusion chromatography of AQP6 expressed in BHK cell, obtained by separating by a Superdex 200 10/300 GL column and detected absorbance at 280 nm. Initial solubilization and purification resulted in aggregated protein samples eluted at the void volume of the column (green curve). An improved solubilization protocol led to a shift of chromatograms to larger volumes was obtained (blue and black curve), even though aggregation could not be avoided completely.

The elution fractions at a retention volume of 12 ml were used for further reconstitution experiments. SDS-PAGE and coomassie staining revealed protein bands at approx. 28 kDa, 50 kDa and 120 kDa, corresponding to the AQP6 monomer, dimer and tetramer (Figure 3.22).

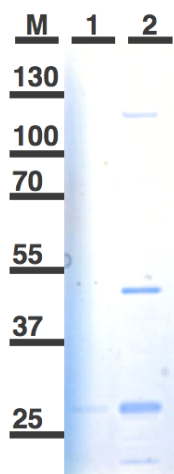


Figure 3.22: SDS-gel of concentrated tetramer fractions from gel filtration, collected at 12 ml (black curve in Figure 3.21). 1: 15 μ l of elution fraction, 2: concentrated elution fraction.

Table 3.13: Summary of purification results in different detergents and buffer conditions.

Detergent	Buffer	pH	Gel filtration	Comment
OG	NaP _i	8.0	Aggregates	-
DM	NaP _i	8.0	Aggregates	No solubilization
OG	NaP _i	8.5	Aggregates	-
OG	Tris-HCl	7.5	Aggregates, but additional tetramer and monomer peak	Best condition
DDM	Tris-HCl	7.5	Aggregates	-
OG	Tris-HCl	6.5	Aggregates	-

Compared to AQP3 expressed with the SFV expression system, yields of AQP6 were in the same range (100 μ g/100 ml), but about 10 to 100 times lower than expression levels for GPCRs like V2R (ca. 1 mg/l), Ste2p or P2X₂ (between 0.1 and 1 mg/ml) [52].

3.2.5 Single particle analysis

Purified AQP6 was subjected to negative stain single particle TEM. Micrographs were prepared from gel-filtrated protein sample (Figure 3.23), either from elution at a retention volume corresponding to aggregates (8 ml) or to AQP6 tetramer (12 ml).

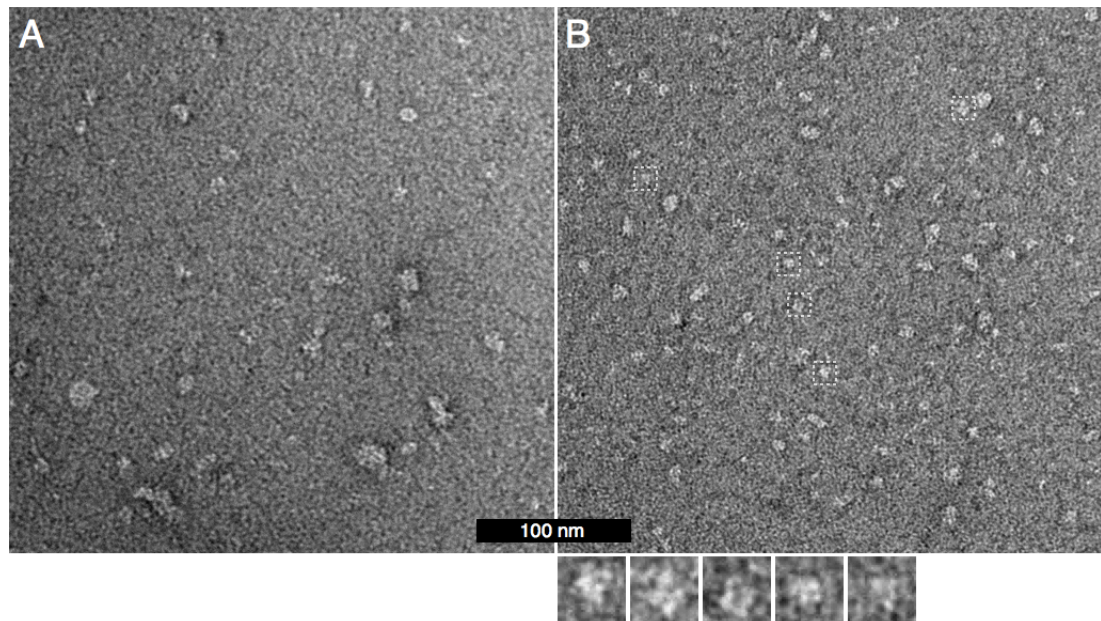


Figure 3.23: Negative stain single particle electron micrograph of AQP6 purified in presence of 1.2 % OG. Aggregate fraction (A) and fraction corresponding to tetramer mass (B). **A:** Large particles are visible. **B:** Particles of expected size (ca. 8 nm diameter) and shape are present besides particles of different sizes. Edge length of small boxes corresponds to 15 nm.

The micrograph of the elution in the range of the void volume showed particles larger in size than AQP6, which were most likely aggregated proteins (Figure 3.23 A). The elution at volumes corresponding to the size of the AQP6 tetramer contained particles, which were most likely AQP6 tetramers. The exhibited a shape and size that were previously reported for AQPs [131].

3.2.6 Reconstitution into liposomes

Purified AQP6 was reconstituted into *E. coli* polar lipids, DMPC or mixture of 70 % POPC, 15 % DOPA, 15 % POPE liposomes. Detergent was removed by dialysis at 33 °C for 3 days. SDS-PAGE followed by immunodetection after liposome recovery over a sucrose gradient showed bands at molecular weights expected for AQP6: monomer band at approx. 28 kDa and dimer at 50 kDa. Compared to cell-free produced AQP6 containing liposomes, the bands for AQP6 purified from BHK cells are at the same heights, suggesting that AQP6 was reconstituted into liposomes or associated to liposomes (Figure 3.24).

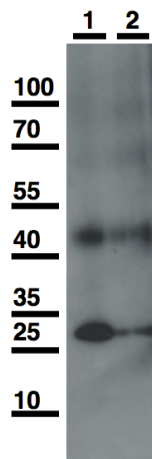


Figure 3.24: Immunodetection (SDS-PAGE, western blot of liposomes) using a penta-His antibody. Signals for AQP6 at expected molecular weights are comparable for cell-free (L-CF) produced AQP6 (1) and AQP6 expressed in BHK cells (2).

Proteoliposomes were freeze-fractured and platinum replicas were analyzed for AQP6 reconstitution using the transmission the electron microscope (Figure 3.25).

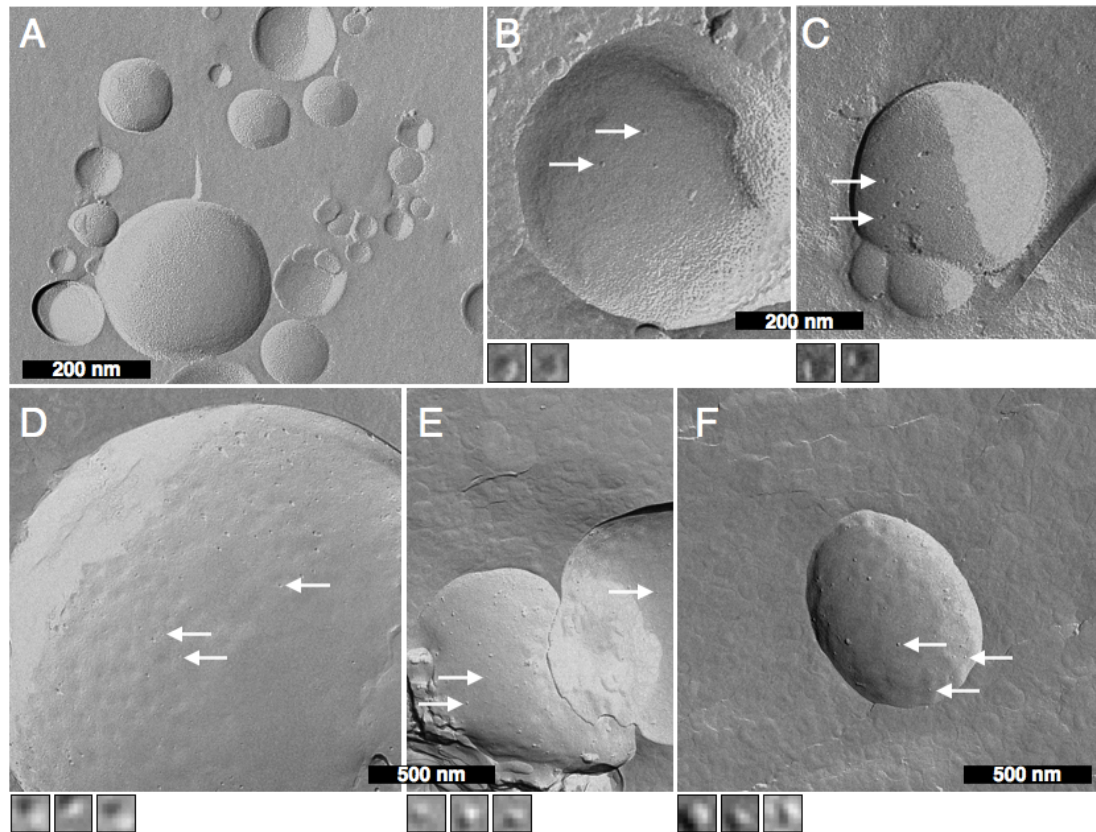


Figure 3.25: Electron micrographs of freeze fractured proteoliposomes, resulting from AQP6 reconstitution. A-C: Mixture of POPC, POPE, and DOPA lipids, LPR 100 (A), 10 (B) and 1 (C). D-F: *E. coli* polar lipids LPR 10 (D, E) and 1 (F) (compare Table 3.14). Small boxes with edge length of 15 nm show magnifications of clusters from the liposome membrane, indicated with arrows.

On the electron micrographs, protein incorporation was visible as small particles sticking out the membrane (Figure 3.25, arrows). Highest protein incorporation rates were reached using *E. coli* polar lipids, reconstitution with the POPC-containing lipid mixture resulted in less protein incorporation and smaller liposomes. Observed liposomes from POPC lipids were unilamellar, whereas the *E. coli* polar lipids formed multilamellar liposomes. Extrusion through a 500 nm pore (21 cycles) decreased the size distribution of vesicles and eliminated multilamellar vesicles (Figure 3.25: F, compare to D and E without extrusion). Determination of the amount of particles revealed that only a small amount of AQP6 was reconstituted, *e.g.* for a LPR of 1 fully packed liposomes were expected. Calculated from LPRs and molecular weight of AQP6, the surface of liposomes should be covered completely with protein at an LPR of 40 or lower. Most likely, only a small amount of AQP6 underwent the reconstitution, whereas the major part precipitated during reconstitution. This result was supported by immunodetection of AQP6 in liposome fractions and in the precipitate after sucrose gradient purification of the proteoliposomes. In general, the number of particles

followed the LPR *i.e.* lower LPRs resulted in more visible particles. The total number of particles was higher in *E. coli* polar lipid liposomes. In control liposomes, a negative control without adding AQP6, no particles were visible. A similar result was obtained for DMPC liposomes.

Table 3.14: Overview of reconstitution results, analyzed by freeze fracture electron microscopy.

Lipid	LPR (w/w)	Result	Figure 3.26
<i>E. coli</i> polar	1	Insertion	D, E
<i>E. coli</i> polar	10	Insertion	F
<i>E. coli</i> polar	100	Very few particles	n.a.
DMPC	10	No insertion	n.a.
DMPC	100	No insertion	n.a.
POPC-mix	1	Few particles	C
POPC-mix	10	Few particles	B
POPC-mix	100	Very few particles	A

For a more detailed analysis, the obtained micrographs were used to quantify reconstituted AQP6 by counting particles in the liposomes. It was assumed, that a single particle corresponds to an AQP6 tetramer, *i.e.* four protein monomers (Figure 3.26).

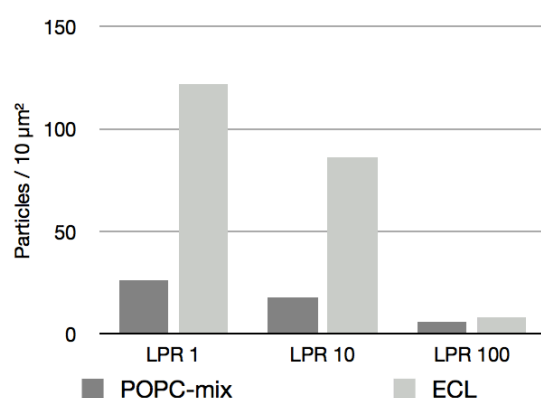


Figure 3.26: Determination of amounts of protein particles in proteoliposomes. Counting of particles revealed an increasing number of particles in proteoliposomes with lower LPRs for POPC lipid mix and *E. coli* polar lipids (ECL) tested.

In *E. coli* polar lipid liposomes more than 100 single channels per 10 μm² were counted at a LPR of 1. At a LPR of 100 nearly no channels were present in the liposomes. The same was observed for the synthetic lipid mixture (POPC-mix) at a LPR of 100, with increasing protein in relation to lipid, incorporation rate in POPC-mix liposomes was

only little increased. In general, even at an LPR of 10 in *E. coli* lipids liposomes fully covered liposomes were expected. This means, that AQP6 was not reconstituted completely. The SEC chromatograms demonstrated that AQP6 aggregated to great extend. This lead to the assumption, that the major part of purified AQP6 was not reconstituted, but aggregated during detergent removal. As a result proteoliposomes were sparsely populated with protein.

3.2.7 Water conductance of heterogously expressed AQP6

In order to test the water channel activity of AQP6, the protein was purified and reconstituted into proteoliposomes at LPR 10. For reconstitution *E. coli* polar lipids were chosen, because of better reconstitution rates for AQP6 compared to other lipids as tested with cell-free expressed AQP6 (3.2.6). An additional reason for choosing these lipids was, that *E. coli* polar lipids were commonly used for reconstitution of AQPs and other membrane proteins to carry out activity assays [144-146].

Water channel activity was measured by exposing proteoliposomes to an osmotic shock and monitoring the increase in 90° light scattering caused by vesicle shrinkage at 10 °C. To determine the rates, five traces of individual experiments were normalized and averaged (Figure 3.27). Averaged traces were fitted to single exponential equations ($y = y_0 - Ae^{-kx}$), with k being the rate constant of the first order kinetic reaction. Calculated rates and water permeabilities are stated in Table 3.15. Differences in liposomes shrinkage between proteoliposomes and empty control liposomes werw detected. Hg²⁺ is a known water transport inhibitor for most AQPs, except for AQP6, where it was reported to be an activator [34, 136]. Proteoliposomes treated with Hg²⁺ showed a little slower shrinkage, suggesting that Hg²⁺ had no activation effect on water permeability of AQP6 in this experiment.

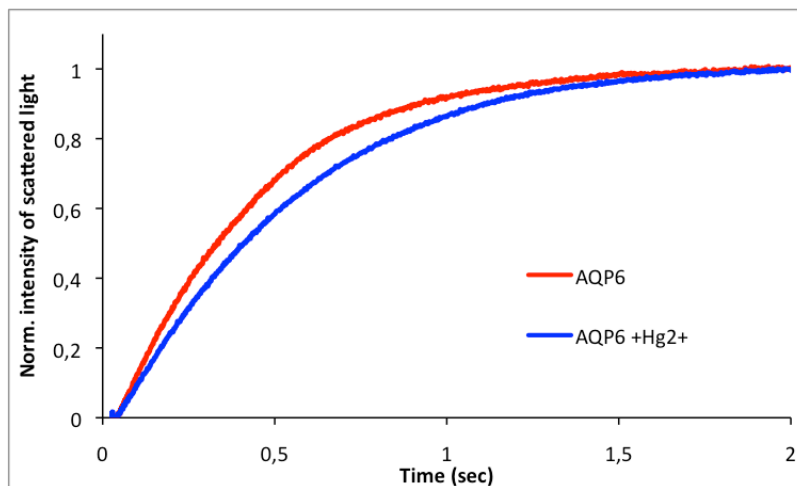


Figure 3.27: Stopped-flow analysis of reconstituted AQP6. Traces display an increase in scattered light when AQP6 was reconstituted into liposomes (LPR10). The presence of Hg^{2+} resulted in a minor difference in the rate, the shrinkage was little slower. Five traces of individual runs per experiment were normalized, averaged and fitted into single exponentials.

Table 3.15: AQP6 water transport rates obtained by single exponential fitting the measured and averaged light scattering traces and calculated water permeability factors (P_f). Literature values were obtained for empty control liposomes.

Condition	Temp °C	Radius (μm)	k	P_f ($\mu\text{m/s}$)
AQP6 <i>E. coli</i> lipids	10	115.5	2.1	22.0 ± 7.1
AQP6 <i>E. coli</i> lipids + Hg^{2+}	10	115.5	1.5	15.4 ± 4.3
Control <i>E. coli</i> lipids [80]	10	56.5	10.7	55.9 ± 3.7
Control <i>E. coli</i> lipids [147]	5	65	2.4	5.1 ± 0.8
Control <i>E. coli</i> lipids [147]	20	65	13.5	57 ± 0.8

The permeability factors (P_f) were calculated as described in Chapter 2.7. From analysis of freeze fracture micrographs the average diameter of liposomes was determined (223 ± 65 nm). This resulted in P_f values of $21.9 \mu\text{m/s}$ for untreated liposomes and $15.4 \mu\text{m/s}$ for liposomes treated with Hg^{2+} (Table 3.15). The osmotic water permeability factors calculated were lower than reported for other AQPs. For example, for AQPZ at LPR10 a water permeability factor of $330 \mu\text{m/s}$ was determined, while the water permeability of control vesicles was $51 \mu\text{m/s}$ [147]. In case of AQP2 permeabilities of $129 \mu\text{m/s}$ (LPR60) and $72 \mu\text{m/s}$ (LPR90) were obtained [145]. For *E. coli* lipids vesicles a P_f value of $55.9 \mu\text{m/s}$ at a temperature of 10°C was reported [80]. Comparing these results to the water permeability of AQP6 one could conclude that AQP6 is a relatively poor water channel or did not conduct water at all. In addition an activation of the channel could

not reached with Hg^{2+} as reported before [34]. Another reason for the low water conductance of AQP6 could be caused at levels of purification and reconstitution. It was not possible to reach a purification of AQP6 free from aggregates. It is possible, that AQP6 was not obtained in a 100 % active confirmation. The liposomes contained few particles at a LPR of 10, suggesting that the major part of protein was not reconstituted during detergent removal but aggregated. As result only a small amount of AQP6 contributes to the water efflux during the osmotic shock, leading to lower water permeability factor for the whole liposomes.

3.3 *Pichia pastoris* expression of AQP6

3.3.1 Template design

The *Pichia pastoris* expression vector pPICZ α was the base for heterologous overexpression of AQP6. AQP6-6xHis was cloned into pPICZ α using *EcoRI* and *XhoI* restriction sites, generated by PCR. The following table shows the primers used for AQP6 subcloning.

Table 3.16: Nucleotide sequences of primer used for AQP6 pPICZ α subcloning.

Primer <i>EcoRI</i> AQP6 forward	Primer <i>XhoI</i> AQP6 reverse
5'gaactgccgaattcaaaaatggagcctgggctgtg	5'ggcccaacctgctcgagttaatggtgatggtgatg

Subcloning resulted in the *P. pastoris* expression construct. The final construct was sequenced using the AOXI site of pPICZ α as origin. See appendix B for full sequence.

The vector DNA was linearized by *SacI* and transformed into *Pichia pastoris* X-33 or GS115 cells by electroporation.

3.3.2 Transcription and translation

Testexpression

The AQP6 gene was integrated into the *P. pastoris* genome by homologous recombination. Recombinant yeast cells were selected using Zeocin as selection marker. Therefore, transformed yeast was spread out on YPD plates containing Zeocin with concentrations ranging from 100 – 2000 $\mu\text{g/ml}$. As multiple insertions usually lead to higher protein expression rates and higher Zeocin resistance, mutant colonies were picked from plates with the highest Zeocin concentration (2000 $\mu\text{g/ml}$) and plated again on YPD plates with the same or higher concentration of Zeocin. The AQP6 expression was carried out by growing cells under shaking at 30 °C in 10 ml BMGY and exchanging the media to BMMY after 24 h. By switching the carbon source from glycerol to methanol, gene expression under the control of the AOX1 alcohol oxidase promoter was induced. Every 24 h methanol was added to a final concentration of 0.5 % to compensate for consumption. The expression rates of AQP6 for different clones were verified after 24h and 120 h by western blot analysis.

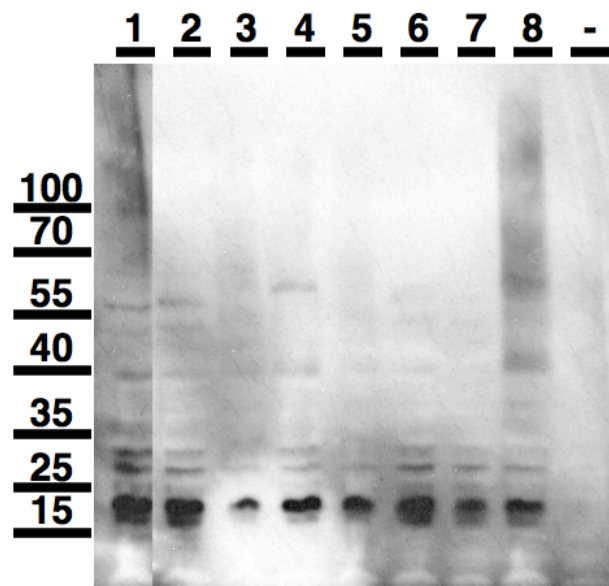


Figure 3.28: Evaluation of test expression of AQP6 from different clones by western blot. Lanes 1-8 represent different *P. pastoris* clones showing AQP6 expression at different levels.

Figure 3.28 shows a western blot analysis of different clones grown for 24 h in BMGY and additional 24 h in BMMY, thus 24 h after induction with methanol. Recombinant produced protein was detected with a penta-His antibody. Bands at different intensities were visible, due to different expression levels. Expression levels in different clones might alter because of variation in the number of recombination events [148]. At approx. 30 kDa a double band is visible, which might be explained with different glycosylation products of AQP6. These double bands are reported as glycosylation pattern of AQPs, like AQP9 [44]. Bands at higher molecular weights might be explained with oligomers of AQP6 that are stable in SDS. Bands at approx. 40 kDa were not observed before for AQP6. The most intensive band at approx. 20 kDa is most likely a degradation product of AQP6. Since *P. pastoris* is confronted with high amounts of heterologous protein, degradation might be initiated.

The negative control did not show a signal on the western blot. Highest expression rates were reached 120 h after first induction with methanol. Clones with highest AQP6 expression levels were chosen for large-scale expression and purification attempts.

Large-scale production

Large-scale protein expression was carried out in 5 l baffled flasks, filled with 1 l BMGY or BMMY, respectively. For setting up the pre-culture, the *P. Pastoris* clone was plated on YPD, incubated at 30 °C for 36 h and scratched to inoculate BMGY. After 24 h, the expression culture was inoculated and grown until reaching an OD₆₀₀ of 10. Cells were

pelleted at 2,000 g for 10 min to exchange the media to BMMY. After induction, expression was carried out for 4 -5 days until reaching an OD₆₀₀ of 30. Every 24 h methanol was added to 0.5 %.

3.3.3 Solubilization

After induction for several days, cells were harvested and broken using a microfluidizer. Unbroken cells and cell debris were removed by centrifugation at 5,000 g for 30 min. Supernatants were collected and underwent an ultracentrifugation at 100,000 g and 4 °C for 1 h. Pelleted membranes were homogenized, aliquoted and stored at -80 °C. The first step of purification was an urea / alkaline stripping of the harvested *P. pastoris* membranes. Therefore, membranes were homogenized and pelleted in presence of 4 M urea and 20 mM NaOH, respectively. As final step, NaOH was removed by homogenization of the membranes in Tris-HCl. The urea/alkaline stripping was monitored by western blotting of the single steps (Figure 3.29).

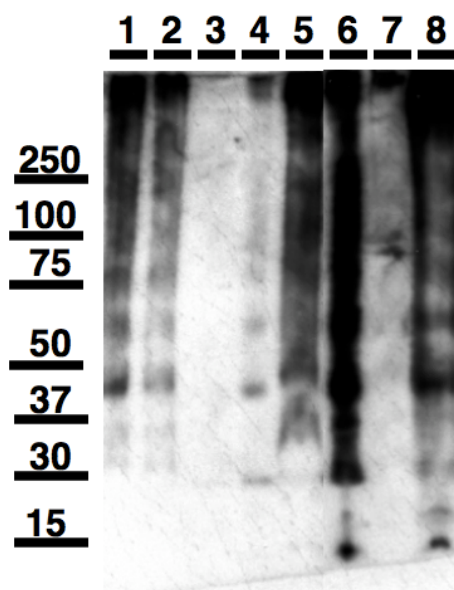


Figure: 3.29: Urea/alkaline stripping of membranes. 1: pellet low spin, 2: pellet crude membranes, 3: supernatant urea, 4: pellet urea, 5: supernatant NaOH, 6: pellet NaOH, 7: supernatant Tris, 8: pellet of stripped membranes in Tris buffer.

In order to identify suitable detergents and solubilization conditions, several detergents were tested. In detail, 2 % CHAPS, 6 % OG, 5 % DM and 2 % DDM were tested. After incubation with washed membranes, solubilization mixture was centrifuged at 100,000 g for 1 h, supernatants and pellets were subject of a SDS-PAGE and western blotting (Figure 3.30). For all detergents a high amount of unsolubilized protein was detected. In case of OG and DM, protein was detected in supernatants.

When tested for crude membranes (not stripped), similar solubilization conditions did not lead to mentionable amounts of protein in the supernatant. Incubation times longer than 4 h did not enhance the yield of solubilized material.

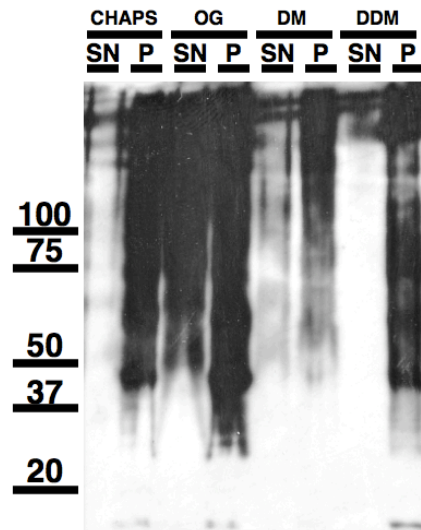


Figure 3.30: Solubilization of *P. pastoris* membranes. 2 % CHAPS, 2 % DDM, 5 % DM, 6 % OG final concentration were used for solubilization, after ultracentrifugation, supernatants (SN) and pellets (P) were loaded on the gel.

P. pastoris membranes less easy to solubilize compared to membranes of bacterial or mammalian cells. The solubilization experiments showed that for efficient solubilization higher amounts of detergent and longer incubation times are necessary. Best results were observed when using OG for solubilization, a relatively harsh detergent [149]. For further experiments and solubilization in preparative scale, OG was used in a final concentration of 6 % and a total volume of 10 ml per liter expression culture. Best results, *i.e.* highest protein concentration in the supernatant, were observed after incubation for 4 h at room temperature and ultracentrifugation for 1 h at 150,000 g.

3.3.4 Purification

For preparative purification of AQP6, stripped and solubilized membranes were prepared. Solubilized material was subjected to Ni-NTA agarose binding overnight in 20 mM Tris, pH 7.5, 150 mM NaCl and 5 mM imidazole. The detergent concentration was adjusted to 1.2 % OG. Protein was washed with 10 volumes buffer containing 10 mM imidazole and eluted with buffer containing 250 mM imidazole. All elution fractions were analyzed by SDS-PAGE and western blotting (Figure 3.31).

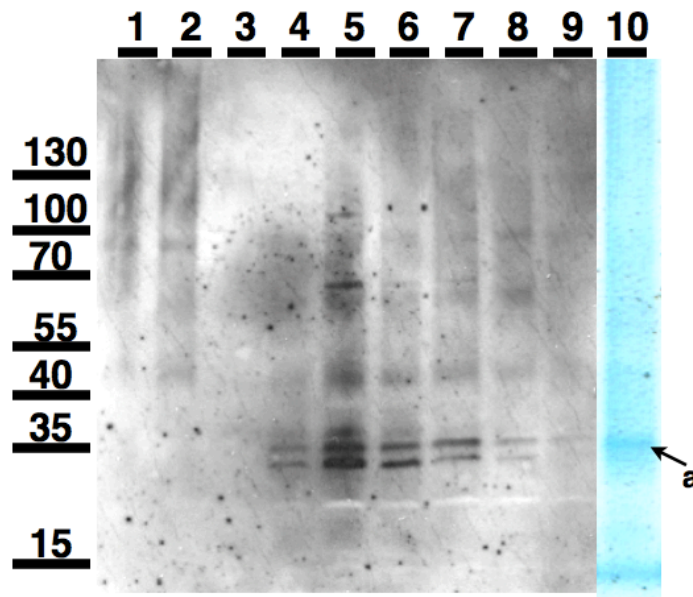


Figure 3.31: Ni-NTA purification of AQP6, western blot, 1: flow through; 2,3 : wash; 4-9 elution; 10: elution (5) coomassie stain

The overall protein yield was very low. 200 μ g purified protein per liter expression culture were obtained. After immunodetection, a double band at a molecular weight of around 30 kDa was visible in the elution fractions, concluding that this is AQP6 in its glycosylated and non-glycosylated form or in differently glycosylated forms. Another explanation for the double band might be N-terminally degraded AQP6. Bands at higher molecular weights indicate the presence of AQP6 oligomers. In general the immunoblot of purified AQP6 matches the immunoblot of the test expression, with the difference that the bands at around 20 kDa are not present after purification. These might be degradation products of AQP6. Existence of AQP6 in purified fractions was confirmed by mass-spectroscopic analysis (band 'a', Figure 3.31, compare Figure 3.32).

In order to obtain a higher yield of purified AQP6, the expression was scaled up using a 20 l fermenter. Cells were harvested and membranes were stripped and solubilized as before, protein purification by affinity binding was carried out as before.

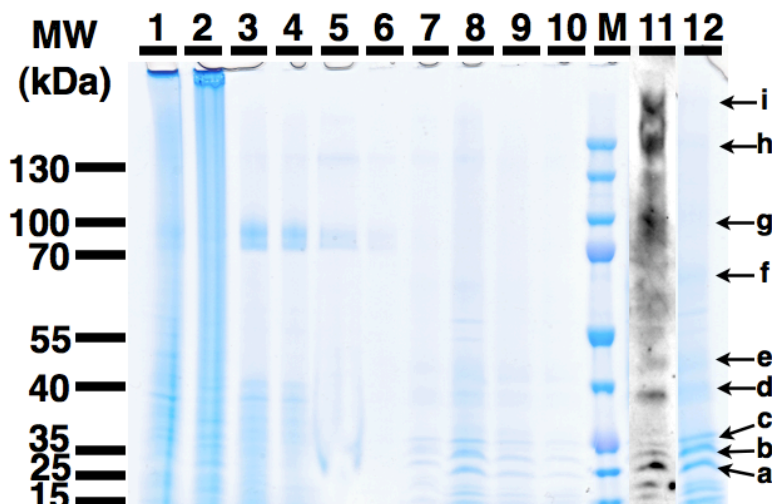


Figure 3.33: Purification of AQP6 from *P. pastoris* fermenter culture. 1: Solubilization pellet; 2: Solubilization supernatant; 3: Flowthrough; 4-6: Wash fractions; 7-10: Elution; 12: Elutions 8-9 concentrated; 11: Immunodetection of 12. Band a – i were further analyzed by mass spectroscopy in order to identify AQP6 fragments. AQP6 peptides were detected in bands a,b, d, f, g, h and i.

In order to proof heterologous expression of AQP6 in *P. pastoris* a mass spectroscopic analysis was carried out. Therefore, single bands of the elution fraction were cut from the SDS-gel and trypsin digested. Peptides of AQP6 were identified by database search of the recorded m/z values (Table 3.17). Trypsin digestion of AQP6 results in a small number of large and hydrophobic peptides, thus it is not surprising, that only three different peptides were detected. These peptides are not located in the transmembrane regions of the protein, but in loop E and the C-terminal end. The presence of C-terminally located peptides is the proof for full-length expression of AQP6 in *P. pastoris*.

Table 3.17: Identified peptides of AQP6 after trypsin digestions by mass spectroscopic analysis.

Peptide	Position of amino acids	Region
SFGPAVIVGK	197 - 206	Extracellular loop E
LAILVGTTK	243 - 251	C-terminal cytoplasmic
LAILVGTTKVEK	243 - 254	C-terminal cytoplasmic
VVDLEPQK	255 - 262	C-terminal cytoplasmic
VVDLEPQKK	255 - 263	C-terminal cytoplasmic

By using a fermenter, the total yield of purified AQP6 was improved, due to the greater amount of starting material, but it was low overall. Due to the weak binding of AQP6 (from shaking and fermentation culture) to Ni-NTA the imidazole concentration during washing steps had to be kept low. This led to notable impurities by histidine rich

P. pastoris proteins, because unspecific binding was not sufficiently inhibited. Mass spectroscopic analyses of purified AQP6 fractions revealed a major impurity by *P. pastoris* transketolase, a single band at approximately 74 kDa on the SDS gel. A further purification by size exclusion chromatography turned out to be difficult because of the similar molecular weight of the transketolase homodimer (149 kDa) and AQP6 homotetramer (120 kDa). For this reason a second purification step, using SEC was not capable.

3.3.5 Single particle analysis

Purified protein was negatively stained and TEM images were taken. Protein particles were visible with the shape and size of an AQP on the micrographs (Figure 3.34). Subsequent mass spectroscopic analyses identified the purified protein as *P. pastoris* transketolase. Transketolase homodimers are similar in shape and size to AQP homotetramers [150]. In order to reduce impurities *i.e.* transketolase and other endogenous proteins, it was washed with hundredfold the Ni-NTA bead volume during purification. As a result the transketolase was no longer visible on SDS gel (compare Figure 3.33 lane 6 and 7) but simultaneously the yield of AQP6 decreased.

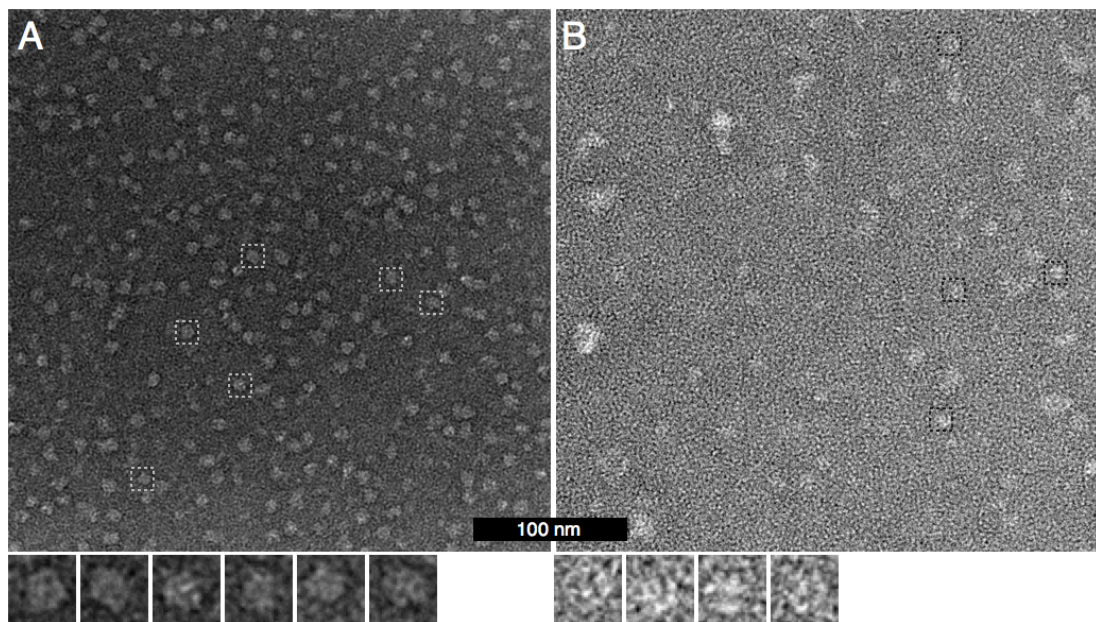


Figure 3.34: Electron micrograph of negatively stained protein sample. A: Particles are in shape and in size comparable to AQP6, but mass spectroscopic analysis identified *P. pastoris* transketolase besides AQP6. **B:** Purified AQP6 N60G, intensive washing removed transketolase, although there are still impurities by larger proteins besides proteins in shape and size of AQP6. Edge length of boxes corresponds to 15 nm.

Surprisingly, the activation of transketolase expression in *P. pastoris* has not been noted during heterologous overexpression of other AQPs (*e.g.* SoPIP and AQP8 [43, 79]). This led to the assumption that an AQP6 activity is responsible for the obtained transketolase upregulation, although a possible biochemical mechanism is unknown. To support the assumption of an upregulation of transketolase by AQP6 activity, a non-functional mutant of AQP6 (AQP6 N60G) was overexpressed in *P. pastoris*. But it turned out that transketolase was expressed as well in high amounts in *P. pastoris* expressing AQP6 N60G, indicating that the anion channel activity of AQP6 is not responsible for transketolase over expression. Besides this, it was reported that during the methanol induction phase the transcription of transketolase is upregulated [151]. Nevertheless, reasons for the high expression rates observed remain obscure.

4 Conclusion

AQP6 has unusual and interesting features: The location of AQP6 is restricted to intracellular vesicles and the physiological role of AQP6 is most likely not to facilitate water or glycerol transport. However, it is thought to act in acid base homeostasis [53]. AQP6 is a pH gated anion channel and Hg²⁺, a known water channel inhibitor, enhances its water permeability [34]. Since purified AQP6 was not available for functional and structural studies, the first and main task was to establish expression and purification protocols.

Expression

In principle the overexpression of AQP6 was possible in all three systems (cell-free, SFV-BHK cells and *P. pastoris*), although, the expression and purification yields remained low. In the cell-free systems reasonable initial expression yields could be improved after adding a N-terminal sequence tag to the open reading frame of the AQP6 gene. After this change of the expression construct the expression yields were in the range achieved for other membrane proteins [94], but lower than for mouse AQP4 [80], which was used as a positive control for expression, purification and reconstitution experiments.

Purification

An additional problem arose during the purification of AQP6 in all systems, resulting from the low binding affinity of AQP6 to the Ni-NTA matrix. Because the interaction was not strong, AQP6 eluted at low imidazole concentrations. Initially, AQP6 was cloned with a hexa-histidine tag without any linker to the ORF, resulting in a short C-terminal tail. As a result of this, the histidine tail might be partially covered by the detergent micelle hindering interactions with the Ni-NTA matrix. Due to the weak interaction washing out nonspecifically bound protein was only possible with relatively low imidazole concentrations resulting in AQP6 protein fractions containing impurities. The weak binding was a problem of special importance during purification of AQP6 expressed in *P. pastoris*. The yeast proteom is known to be histidine-rich [152, 153]. For this reason, major impurities after purification of AQP6 from *P. pastoris* were observed and immunodetection by penta-histidine antibodies showed unspecific signals. Another problem during purification of AQP6 from *P. pastoris* membranes was the co-purification of α -transketolase, an enzyme involved in methanol metabolism

[151]. Due to the washing with low imidazole concentrations, transketolase was co-purified, resulting in protein concentrations of up to 3.2 mg/ml. It was difficult to distinguish between AQP6 and transketolase by SDS-PAGE and single particle negative stain TEM, because transketolase has approximately twice the molecular weight of AQP6 and forms homodimers. These homodimers are similar to AQP6 in shape and size [150]. For this reason a second purification step, using size exclusion chromatography was initially not feasible. Unfortunately, only mass spectroscopic analyses allowed AQP6 and transketolase to be identified.

Transketolase upregulation was not reported before for the expression of AQPs in *P. pastoris* leading to the assumption that the activity of AQP6 is responsible for promoting transketolase expression. Because the heterologous overexpression of the non-functional AQP6 N60G mutant also induced transketolase upregulation in *P. pastoris*, it is not the anion channel activity of AQP6 that could be the reason for this cellular response.

Reconstitution

The reconstitution experiments demonstrated that immunodetection of liposome fractions after ultracentrifugation is not a proof for correct reconstitution. In the case of cell-free expressed AQP6 in absence or in presence of detergent, AQP6 was detected in the fractions of liposomes, but electron micrographs of freeze fractured liposomes showed no protein reconstitution. However, precipitated protein associated to the liposomes was visible. Freeze fracture electron microscopy in combination with immunodetection is the method of choice for demonstrating protein reconstitution.

Water conductance

Water transport measurements by stopped-flow light scattering demonstrated, that AQP6 expressed in cell-free systems or in BHK cells and reconstituted into liposomes did not show enhanced water transport rates compared to empty control liposomes. Compared to other AQPs the water permeability of AQP6 was low. In addition measurements in presence of Hg^{2+} , which was reported to be an activator of water permeability of AQP6 [34], did not result in a higher water permeability. There are several possible reasons: The most likely one is that only a small amount of AQP6 was reconstituted in its active conformation. Especially for the cell-free expressed AQP6 it is possible that the folding of the protein might be incomplete. The *E. coli* based cell-free systems lacks a eukaryotic chaperone machinery. The folding efficiency in cell-free systems is still a subject of discussions. There are no high-resolution structures of cell-

free expressed eukaryotic membrane proteins available. Functional studies are often performed as binding assays with radioactive ligands. From a signal detected in such experiments it is difficult to estimate the amount of protein in a physiological conformation, because potential binding pockets are folded partially promoting ligand binding to some extent. Ligand binding is not a solid proof for correct folding of the entire protein.

The application of detergents for solubilization of cell-free produced protein and for extracting protein from cell membranes implies always submitting the protein to a non-physiological condition. Destabilization of the protein structure and detergent induced denaturation are possible. The type of detergent, its concentration, and incubation time are therefore critical. Finally it could not be conclusively answered whether water transport activity of AQP6 is low or whether the protein was reconstituted in a non-functional conformation.

Appendix A - Materials

A.1 Bacterial Strains

Strain	Genotype	Reference
<i>E. coli</i> BL21 (DE3)	<i>hsdS</i> , <i>gal</i> (λ cl, <i>ts857</i> , <i>cmd1</i> , <i>hsdR17</i> , <i>recA1</i> , <i>endA1</i> , <i>gyrA96</i> , <i>thi-1</i> , <i>relA1</i>)	[154]
<i>E. coli</i> DH5 α	(F ⁻ , <i>endA1</i> , <i>hsdR17</i> ($r_k^- m_k^-$), <i>supE44</i> , <i>thi-1</i> , <i>recA1</i> , <i>gyrA</i> (Nal ^r), <i>relA1</i> , Δ (<i>lacZYA-argF</i>)U169, Φ 80 <i>lacZ</i> Δ M15)	[155]
<i>E. coli</i> K-12 strain A19	(<i>rna19 gdh A2 his95 relA1 spoT1 metB1</i>)	<i>E. coli</i> Genetic stock center, New Haven, CT

A.2 Oligonucleotides

All oligonucleotides were ordered from Microsynth, Switzerland.

Sequence	Application
5'cggctccgatggctagcatgactggtggaca	AQP6 pSFV subcloning, <i>RsrII</i> forward
5'ctcgagttaatggtgatggtgatggtgcacgc	AQP6 pSFV subcloning, <i>XhoI</i> reverse
5'tatgatgaaatattataaatattatctgcaagtgctgtttcagggcccg	AT-tag cloning, forward
5'aattccggggccctgaaacagcacttccagataatattataatatttcatca	AT-tag cloning, reverse
5'gaactgccgaattcaaaaatggagcctgggctgtg	AQP6 pICZ α subcloning <i>EcoRI</i> forward
5'ggcccaacctgctcgagttaatggtgatggtgatg	AQP6 pICZ α subcloning <i>XhoI</i> reverse
5'gttgcaggttgccatcacggttcggcctggccac	AQP6 N60G point mutation forward
5'gtggccagggccgaacgtgatggcaacctgcaac	AQP6 N60G point mutation reverse
5'taatacgactcactatagg	T7 promotor forward (sequencing)
5'tgctagttattgctcagcgg	T7 terminator reverse (sequencing)
5'atttaggtgacactatag	SP6 promotor forward (sequencing)
5'gactggttccaattgacaagc	AOX1 forward (sequencing)

A.3 Vectors

pAR1219, Amp ^R	T7 RNA polymerase expression vector
pET21a(+), Amp ^R , T7 regulatory elements	Cell-free expression vector, Novagen, MERCK chemicals KG (Germany)
pHelper-2, Amp ^R	<i>Semliki</i> Forest virus expression system
pSFV, Amp ^R	<i>Semliki</i> Forest virus expression system
pPICZ α , Zeo ^R	<i>P. pastoris</i> expression system

A.4 Chemicals, reagents and buffers

All chemical were purchased from Sigma-Aldrich, Switzerland when not otherwise stated.

A.4.1 Chemicals and reagent solutions

1,4-dithiothreitol

2-mercaptoethanol

Acetyl phosphate lithium potassium salt

Adenosine 5'-triphosphate disodium salt trihydrate (Roche Diagnostics)

Antifoam Y-30 emulsion

Bactotryptone (Becton Dickinson)

Biotin

Complete protease inhibitor (Roche Diagnostics)

Cytidine 5'-triphosphate disodium salt hydrate

Detergents see separatsection

DNA polymerase iProof (Bio-Rad)

Ethanol, 99 %

Folinic acid calcium salt

Glucose

Glucose monohydrate

Glycerol

Guanosine 5'-triphosphate disodium salt hydrate

HEPES

Imidazole

Isopropyl β -D-1-thiogalactopyranoside (IPTG)

K₂HPO₄

KCl

KH₂PO₄

KOH

m⁷G(5')ppp(5')G (New England Biolabs)

Magnesium acetate tetrahydrate

Methanol

NaCl

NaN₃

Natural amino acids

Ni-NTA Agarose (Qiagen)

Peptone (Becton Dickinson)

Phenol/chloroform/isoamylalcohol 25%/24%/1%(v/v/v)

Phenylmethylsulfonyl fluoride (PMSF)

Phosphoenol pyruvic acid (PEP) monopotassium .salt

Polyethylene glycol (PEG) 8000

Potassium acetate

Pyruvate kinase (Roche Diagnostics)

Restriction enzymes (New England Biolabs)

RNAguard ribonuclease inhibitor (Fermentas)

T4 DNA ligase (New England Biolabs)

Tris-(hydroxymethyl)-aminomethane

tRNA *E. coli* (Roche Diagnostics)

Uridine 5'-triphosphate trisodium salt dihydrate

Yeast extract (Becton Dickinson)

A.4.2 Buffers & media

Buffer for biochemical applications

TBE	89 mM Tris pH 8.0, 89 mM Boric acid, 2 mM EDTA
Blocking buffer	3 % (w/v) BSA in TBS
Gelfiltration buffer	20 mM Tris-HCl, pH 7.5, 300 mM NaCl, 5 % glycerol, 1,2 % OG or 0.05 % DDM
SDS-PAGE running buffer	40 mM MOPS-NaOH, pH 7.0, 10 mM NaAc, 1 mM EDTA
SDS-PAGE sample buffer (5x)	225 mM Tris-HCl, pH 6.8, 50 % glycerol, 5 % SDS, 0.05 % bromophenol blue, 225 mM DTT
Semi-dry transfer buffer	25 mM Tris-HCl, pH 8.3, 150 mM glycine, 10 % methanol
SP6 Buffer (10x)	400 mM HEPES, pH 7.4, 60 mM magnesium acetate, 20 mM
TBS	10 mM Tris-HCl, pH 7.5, 150 mM NaCl
TBS-T	20 mM Tris HCl, pH 7.5, 500 mM NaCl, 0.05 % (v/v) Tween 20, 0.2 % (v/v) Triton X-100

Cell-free expression

Dialysis buffer T7RNAP	10 mM K ₂ HPO ₄ , pH 8.0, 10 mM NaCl, 0.5 mM EDTA, 1 mM DTT
LB (Luria-Bertani) medium	1 % bactotryptone, 5 % yeast extract, 1 % NaCl. Sterilized by autoclaving
Q sepharose buffer A for T7RNAP	30 mM Tris, pH 8.0, 50 mM NaCl, 1 mM EDTA, 10 mM 2-mercaptoethanol, 5 % glycerol
Q sepharose buffer B for T7RNAP	30 mM Tris, pH 8.0, 1 M NaCl, 1 mM EDTA, 10 mM 2-mercaptoethanol, 5 % glycerol
Resuspension buffer for T7RNAP	30 mM Tris-HCl, pH 8.0, 50 mM NaCl, 10 mM EDTA, 10 mM 2-mercaptoethanol, 5 % glycerol, protease inhibitor
S30 A buffer	10 mM Tris-acetate, pH 8.2, 14 mM Mg(OAc) ₂ , 60 mM KCl, 6 mM 2-mercaptoethanol
S30 B buffer	10 mM Tris-acetate, pH 8.2, 14 mM Mg(OAc) ₂ , 60 mM KCl, 1 mM DTT and 0.1 mM PMSF
S30 C buffer	10 mM Tris-acetate, pH 8.2, 14 mM Mg(OAc) ₂ , 60

	mM KOAc, 0.5 mM DTT
YTPG medium (2x)	10 l: 22 mM KH ₂ PO ₄ , 40 mM K ₂ HPO ₄ (autoclaved separately), 100 mM glucose (filtered sterile), 160 g bacto-tryptone, 100 g yeast extract, 50 g NaCl

Cell culture

Cell culture media were ordered at Sigma-Aldrich, Switzerland, ordering numbers are stated in brackets.

	Iscove's Modified Dulbecco's Medium (I3390) 500 ml
	Dulbecco's Modified Eagle's Medium (D5030) 250 ml
	Nutrient Mixture F-12 Ham (N8641) 250 ml
DHI-5	Fetal Bovine Serum (F0804) 50 ml
	Non-essential Amino Acid Solution (M7145) 5 ml
	L-glutamine (G7513) 5 ml
	RPMI 1640 Vitamins Solution (R7256) 5 ml
PBS	Dulbecco's Phosphate Buffered Saline (T8154)
Trypan blue (0.4 %)	(T8154)
Trypsin-EDTA solution	(T3924) 0.5 g porcine trypsin and 0.2 g EDTA, 4Na per liter of Hanks' Balanced Salt Solution with phenol red

P. pastoris expression system

Low salt LB medium	1 % tryptone, 0.5 % yeast extract, 0.5 % NaCl
BMGY (Buffered glycerol complex medium)	1 % yeast extract, 2 % peptone, 100 mM potassium phosphate, pH 6.0, 1.34 % YNB, 4x 10 ⁻⁵ % biotin, 1 % glycerol
BMMY (Buffered methanol complex medium)	1 % yeast extract, 2 % peptone, 100 mM potassium phosphate, pH 6.0, 1.34 % YNB, 4x 10 ⁻⁵ % biotin, 0.5 % methanol
Low salt LB agar plates	Low salt LB medium, 15 g/l agar

YNB (10x)	34 g YNB (yeast nitrogen base), 100 g ammonium sulfate
YPD medium	1 % yeast extract, 2 % peptone, 2 % glucose

A.4.3 Antibodies

Anti-mouse IgG HRP conjugate from goat	(Sigma)
Anti-penta His IgG from mouse	(Sigma)
Anti-rabbit IgG HRP conjugate from goat	(GE Lifescience)
Anti-ratAQP6 IgG from rabbit	(Alomone Labs)

A.4.4 Detergents

All detergents were purchased from Anatrace/Affymetrix.

1-myristoyl-2-hydroxy-sn-glycero-3-(phospho-rac-(1-glycerol)) (LMPG)
(Avanti Polar lipids)

1-palmitoyl-2-hydroxy-sn-glycero-3-(phospho-rac-(1-glycerol)) (LPPG)
(Avanti Polar lipids)

Digitonin

n-Decyl- β -D-Maltopyranoside (DM)

n-dodecyl- β -D-maltoside (DDM)

n-dodecylphosphocholine (DPC/FOS-12)

n-hexadecylphosphocholine (FOS-16)

n-Octyl- β -D-Glucopyranoside (OG)

Polyethylene glycol (23) monododecyl ether (Brij-35) (Sigma)

Polyoxyethylene octyl phenyl ether (Triton X-100) (Sigma)

Polyoxyethylene-(20)-cetylother (Brij-58) (Sigma)

Polyoxyethylene-(20)-stearylother (Brij-78) (Sigma)

A.4.5 Lipids

<i>E. coli</i> polar lipid extract	<i>E. coli</i> lipids
Brain polar lipids extract (porcine)	Brain lipids
1,2-dimyristoyl-sn-glycero-3-phosphocholine	DMPC
1,2-dioleoyl-sn-glycero-3-phosphate	DOPA

1-palmitoyl-2-oleoyl-sn-glycero-3-phosphocholine	POPC
1-palmitoyl-2-oleoyl-sn-glycero-3-phosphoethanolamine	POPE

A.4.6 Equipment

ÄKTA purifier (GE Healthcare)

Cell culture incubator (Heraeus)

Inverted light microscope (Zeiss)

Laminar flow clean bench (Thermo Scientific)

SDS-polyacrylamide gel electrophoresis system (Invitrogen)

Slide-A-lyzer dialysis cassette 10 kDa MWCO (Pierce)

Temperature-controlled shaking incubator (Infors)

Tissue culture flasks (T25, T75, T175 and T300)(NuncBrandProducts).

Western blotting system, semi-dry (Hoefer)

Appendix B - Sequences

<pre> catgaagaatattataaattattatctgcaactctctgttttccagggcccaattcgaagatg M K Y Y K Y Y L Q V L F Q G P N S K M tctcctgggctgtgtaacagggccttacctgctgggtggcgggccttggaccgcatcagc S P G L C N R A Y L L V G G L W T A I S aaggcgctttttgctgagttcctggccacagggctgtacgttttctttggtgtgggctcc K A L F A E F L A T G L Y V F F G V G S gtcctgccctggcccgtggcgcttccctctgtggttcaggttgccatcacgttcaacctg V L P W P V A L P S V L Q V A I T F N L gccacagccacagctgtgcagatctcctggaagaccagcggggcccacgccaaccccgct A T A T A V Q I S W K T S G A H A N P A gtgaccctggcctacctcgtgggatcccacatctctctgccccgggctgtggcctacata V T L A Y L V G S H I S L P R A V A Y I gctgctcagctggctggggctacagttggggctgctcttctttatggggtaactccagga A A Q L A G A T V G A A L L Y G V T P G ggtgtccgagagacccttggagtcacgtgggtccacaacagcacctcgactggccagggc G V R E T L G V N V V H N S T S T G Q A gtggcctggagctgggttctgacgctgcagttgggttctctgtgtctttgcttccatggac V A V E L V L T L Q L V L C V F A S M D agtggcagaccttgggctccccagctgccatgattgggacctctgtggcactgggcat S R Q T L G S P A A M I G T S V A L G H ctcattgggatctacttccactggctggtccatgaaccagctcgtccttcggccctgcg L I G I Y F T G C S M N P A R S F G P A gtcattggttgggaagtttgcagtcattgggatcttctgggtaggaccgctcacaggggct V I V G K F A V H W I F W V G P L T G A gtcctggcttcgctgatctacaactttatcttggtttctctgacaccaagaccgtagcccag V L A S L I Y N F I L F P D T K T V A Q cgattggccatccttgtgggtaccacaaggtggagaaagtggtagacctggagcccag R L A I L V G T T K V E K V V D L E P Q aagaaagaatcacagacgaactcagaggacacagaagtgagcgtgcaccatcaccatcac K K E S Q T N S E D T E V S V H H H H H cattaactcgaag H - L E </pre>

Table B.1: Nucleotide sequence and translation of AT-AQP6-pET21a construct: red: *NdeI* and *XhoI* restriction sites; green: N-terminal tag sequence; yellow: start and stop codons.

<pre> atggtccatggtctcctgggctgtgtaac M S P G L C N agggccttacctgctgggtggcgggccttggaccgcatcagcaaggcgctttttgctgag R A Y L L V G G L W T A I S K A L F A E ttcctggccacagggctgtacgttttctttggtgtgggctccgctcctgccctggcccgtg F L A T G L Y V F F G V G S V L P W P V gcgcttccctctgtggttcaggttgccatcacgttcaacctggccacagccacagctgtg A L P S V L Q V A I T F N L A T A T A V cagatctcctggaagaccagcggggcccacgccaaccccgctgtgaccctggcctacctc Q I S W K T S G A H A N P A V T L A Y L gtgggatcccacatctctctgccccgggctgtggcctacatagctgctcagctggctggg V G S H I S L P R A V A Y I A A Q L A G gctacagttggggctgctcttctttatggggtaactccaggagggtgtccgagagaccctt A T V G A A L L Y G V T P G G V R E T L ggagtcaacgtgggtccacaacagcacctcgactggccagggcgggtggcctggagctgggt G V N V V H N S T S T G Q A V A V E L V ctgacgctgcagttgggttctctgtgtctttgcttccatggacagtcggcagaccttgggc L T L Q L V L C V F A S M D S R Q T L G tccccagctgccatgattgggacctctgtggcactgggcatctcattgggatctacttc S P A A M I G T S V A L G H L I G I Y F actggctggtccatgaaccagctcgtccttcggccctgcggtcattggttgggaagttt T G C S M N P A R S F G P A V I V G K F </pre>

```

gcagtcattggatcttctgggtaggaccgctcacaggggctgtcctggcttcgctgatc
A V H W I F W V G P L T G A V L A S L I
tacaactttatcttggttctgacaccaagaccgtagccagcgattggccatccttg
Y N F I L F P D T K T V A Q R L A I L V
ggtaccacaaagggtggagaaagtggtagacctggagccccagaaganagaatcacagac
G T T K V E K V V D L E P Q K X E S Q T
Aactcagaggacacagaagtgagcgtgcaccatcaccatcaccatgattaacctggattc
N S E D T E V S V H H H H H H H D - L E F

```

Table B.3: Nucleotide sequence and translation of AQP6-pSFV2 construct: red: *RsrII* and *XhoI* restriction sites; green: yellow: start and stop codons.

```

gaattcaaaaatggagcctgggctgtgtaac
M E P G L C N
agggcttacctgctgggtggcgggctttggaccgcatcagcaaggcgctttttgctgag
R A Y L L V G G L W T A I S K A L F A E
ttcctggccacagggctgtacgttttctttgggtgtgggctccgctcctgccctggcccgt
F L A T G L Y V F F G V G S V L P W P V
gcgcttccctctgtggtgacaggttgccatcacgttcaacctggccacagccacagctgtg
A L P S V L Q V A I T F N L A T A T A V
cagatctcctggaagaccagcggggccacgccaacccccgctgtgaccctggcctacctc
Q I S W K T S G A H A N P A V T L A Y L
gtgggatcccacatctctctgccccgggctgtggcctacatagctgctcagctggctggg
V G S H I S L P R A V A Y I A A Q L A G
gctacagttggggctgctcttctttatggggtaactccaggaggtgtccgagagaccctt
A T V G A A L L Y G V T P G G V R E T L
ggagtcaacgtggtccacaacagcacctcgactggccaggcggtggccgtggagctgggtt
G V N V V H N S T S T G Q A V A V E L V
ctgacgctgcagttgggttctctgtgtctttgcttccatggacagtcggcagaccttgggc
L T L Q L V L C V F A S M D S R Q T L G
tccccagctgcatgattgggacctctgtggcactgggcatctcattgggatctacttc
S P A A M I G T S V A L G H L I G I Y F
actggctgttccatgaaccagctcgtccttcggccctgcggtcattggtgggaagttt
T G C S M N P A R S F G P A V I V G K F
gcagtcattggatcttctgggtaggaccgctcacaggggctgtcctggcttcgctgatc
A V H W I F W V G P L T G A V L A S L I
tacaactttatcttggttctgacaccaagaccgtagccagcgattggccatccttg
Y N F I L F P D T K T V A Q R L A I L V
ggtaccacaaagggtggagaaagtggtagacctggagccccagaaganagaatcacagac
G T T K V E K V V D L E P Q K X E S Q T
aactcagaggacacagaagtgagcgtgcaccatcaccatcaccattaacctggattc
N S E D T E V S V H H H H H H H - L E

```

Table B.2: Nucleotide sequence and translation of AQP6-pPICZ α construct: red: *EcoRI* and *XhoI* restriction sites; green: yellow: start and stop codons.

Abbreviations

2D	Two dimensional
3D	Three dimensional
ADP	Adenosine diphosphate
AOX1	Alcohol oxidase 1
AQP	Aquaporin
AQPZ	Aquaporin Z from <i>Escherichia coli</i>
ATP	Adenosine tri-phosphate
BHK cells	Baby hamster kidney cells
BSA	Bovine serum albumine
CHAPS	3-(3-cholamidopropyl)-demethylammonio)1-propanesulfonate
CHO cells	Chinese hamster ovary cell
cmc	critical micelle concentration
CTP	Cytidine triphosphate
D-CF	Cell-free expression in presence of detergent
DDM	n-dodecyl- β -D-maltopyranoside
DM	n-decyl- β -D-maltopyranoside
DMPC	1,2-dimyristoyl-sn-glycero-3-Phosphocholine
DNA	Deoxyribonucleic acid
DOPA	1,2-dioleoyl-sn-glycero-3-phosphate
DOPC	1,2-dioleoyl-sn-Glycero-3-ohosphocholine
DTT	Dithiothreitol
<i>E. coli</i>	<i>Escherichia coli</i>
EDTA	Ethyl-n-diamin-tetraacetat
EM	Electron microscopy
GlpF	Glycerol facilitator from <i>Escherichia coli</i>
GPCR	G protein coupled receptor
GTP	Guanosine triphosphate
HEK cells	Human embryonic kidney cells
HEPES	2-(4-(2-hydroxyethyl)piperazin-1-yl)ethanesulfonic acid
His	Histidine
HRP	Horseradish peroxidase
IgG	Immunoglobulin G
kDa	Dalton

L-CF	Cell-free expression in presence of lipids
LB	Luria Bertani
LPR	Lipid to protein ratio
MD	Molecular dynamics
MIP	Major intrinsic protein
NDI	Nephrogenic diabetes insipidus
NiNTA	Ni ²⁺ -nitrilotriacetic acid
NPA	Asparagine - proline - alanine
NTPs	Nucleoside triphosphate
OD	Optical density
P-CF	Cell-free expression of membrane proteins without detergent
<i>P. pastoris</i>	<i>Pichia pastoris</i>
PAGE	Polyacrylamide gel electrophoresis
PCR	Polymerase Chain Reaction
PDB	Protein data bank (http://www.rcsb.org/pdb/)
pI	Isoelectric point
P _i	Phosphate group
PMSF	Phenylmethylsulfonylfluoride
POPC	1-palmitoyl-2-oleoyl-sn-glycero-3-phosphocholine
POPG	1-palmitoyl-2-oleoyl-sn-glycero-3-(phospho-rac-(1-glycerol))
RNA	Ribonucleic acid
SDS	Sodium dodecyl sulfate
Sf9 cells	<i>Spodoptera frugiperda</i> cells
T7RNAP	T7 RNA polymerase
TEM	Transmission electron microscope
Tris	Tis(hydroxymethyl)-aminoethane
Triton X-100	polyethylene glycol p-(1,1,3,3-tetramethylbutyl)-phenyl ether
tRNA	Transfer RNA
UTP	Uracil triphosphate
vH ⁺ -ATPase	Vacuolar-type H ⁺ -ATPase
YPD	Yeast peptone dextrose

References

1. Yeagle, P.L., *Modulation of membrane function by cholesterol*. Biochimie, 1991. **73**(10): p. 1303-10.
2. van Meer, G., D.R. Voelker, and G.W. Feigenson, *Membrane lipids: where they are and how they behave*. Nat Rev Mol Cell Biol, 2008. **9**(2): p. 112-24.
3. von Heijne, G. and D. Rees, *Membranes: reading between the lines*. Curr Opin Struct Biol, 2008. **18**(4): p. 403-5.
4. Montelione, G.T. and S. Anderson, *Structural genomics: keystone for a Human Proteome Project*. Nat Struct Biol, 1999. **6**(1): p. 11-2.
5. Chandy, G., et al., *Comparison of the water transporting properties of MIP and AQP1*. J Membr Biol, 1997. **159**(1): p. 29-39.
6. Karan, D.M. and R.I. Macey, *The permeability of the human red cell to deuterium oxide (heavy water)*. J Cell Physiol, 1980. **104**(2): p. 209-14.
7. Denker, B.M., et al., *Identification, purification, and partial characterization of a novel Mr 28,000 integral membrane protein from erythrocytes and renal tubules*. J Biol Chem, 1988. **263**(30): p. 15634-42.
8. Verkman, A.S., *Mechanisms and regulation of water permeability in renal epithelia*. Am J Physiol, 1989. **257**(5 Pt 1): p. C837-50.
9. Preston, G.M., et al., *Appearance of water channels in Xenopus oocytes expressing red cell CHIP28 protein*. Science, 1992. **256**(5055): p. 385-7.
10. Sui, H., et al., *Structural basis of water-specific transport through the AQP1 water channel*. Nature, 2001. **414**(6866): p. 872-8.
11. Verkman, A.S., *Aquaporins in clinical medicine*. Annu Rev Med, 2012. **63**: p. 303-16.
12. Verkman, A.S., *Mammalian aquaporins: diverse physiological roles and potential clinical significance*. Expert Rev Mol Med, 2008. **10**: p. e13.
13. Gonen, T., et al., *Aquaporin-0 membrane junctions reveal the structure of a closed water pore*. Nature, 2004. **429**(6988): p. 193-7.
14. Nielsen, S., et al., *CHIP28 water channels are localized in constitutively water-permeable segments of the nephron*. J Cell Biol, 1993. **120**(2): p. 371-83.
15. Schnermann, J., et al., *Defective proximal tubular fluid reabsorption in transgenic aquaporin-1 null mice*. Proc Natl Acad Sci U S A, 1998. **95**(16): p. 9660-4.
16. Nielsen, S., J. Fror, and M.A. Knepper, *Renal aquaporins: key roles in water balance and water balance disorders*. Curr Opin Nephrol Hypertens, 1998. **7**(5): p. 509-16.
17. Nielsen, S., et al., *Congestive heart failure in rats is associated with increased expression and targeting of aquaporin-2 water channel in collecting duct*. Proc Natl Acad Sci U S A, 1997. **94**(10): p. 5450-5.
18. Ivarsen, P., et al., *Increased urinary excretion of aquaporin 2 in patients with liver cirrhosis*. Gut, 2003. **52**(8): p. 1194-9.
19. Ishibashi, K., et al., *Molecular cloning and expression of a member of the aquaporin family with permeability to glycerol and urea in addition to water expressed at the basolateral membrane of kidney collecting duct cells*. Proc Natl Acad Sci U S A, 1994. **91**(14): p. 6269-73.
20. Hara-Chikuma, M. and A.S. Verkman, *Aquaporin-3 facilitates epidermal cell migration and proliferation during wound healing*. J Mol Med (Berl), 2008. **86**(2): p. 221-31.
21. Hiroaki, Y., et al., *Implications of the aquaporin-4 structure on array formation and cell adhesion*. J Mol Biol, 2006. **355**(4): p. 628-39.

22. Li, L., et al., *Proinflammatory role of aquaporin-4 in autoimmune neuroinflammation*. FASEB J, 2011. **25**(5): p. 1556-66.
23. Steinfeld, S., et al., *Abnormal distribution of aquaporin-5 water channel protein in salivary glands from Sjogren's syndrome patients*. Lab Invest, 2001. **81**(2): p. 143-8.
24. Yasui, M., *pH regulated anion permeability of aquaporin-6*. Handb Exp Pharmacol, 2009(190): p. 299-308.
25. Maeda, N., T. Hibuse, and T. Funahashi, *Role of aquaporin-7 and aquaporin-9 in glycerol metabolism; involvement in obesity*. Handb Exp Pharmacol, 2009(190): p. 233-49.
26. Ferri, D., et al., *Ontogeny, distribution, and possible functional implications of an unusual aquaporin, AQP8, in mouse liver*. Hepatology, 2003. **38**(4): p. 947-57.
27. Carbrey, J.M., et al., *Aquaglyceroporin AQP9: solute permeation and metabolic control of expression in liver*. Proc Natl Acad Sci U S A, 2003. **100**(5): p. 2945-50.
28. Hatakeyama, S., et al., *Cloning of a new aquaporin (AQP10) abundantly expressed in duodenum and jejunum*. Biochem Biophys Res Commun, 2001. **287**(4): p. 814-9.
29. Ishibashi, K., et al., *Cloning and identification of a new member of water channel (AQP10) as an aquaglyceroporin*. Biochim Biophys Acta, 2002. **1576**(3): p. 335-40.
30. Gorelick, D.A., et al., *Aquaporin-11: a channel protein lacking apparent transport function expressed in brain*. BMC Biochem, 2006. **7**: p. 14.
31. Itoh, T., et al., *Identification of a novel aquaporin, AQP12, expressed in pancreatic acinar cells*. Biochem Biophys Res Commun, 2005. **330**(3): p. 832-8.
32. Smith, B.L. and P. Agre, *Erythrocyte Mr 28,000 transmembrane protein exists as a multisubunit oligomer similar to channel proteins*. J Biol Chem, 1991. **266**(10): p. 6407-15.
33. Song, Y. and A.S. Verkman, *Aquaporin-5 dependent fluid secretion in airway submucosal glands*. J Biol Chem, 2001. **276**(44): p. 41288-92.
34. Yasui, M., et al., *Rapid gating and anion permeability of an intracellular aquaporin*. Nature, 1999. **402**(6758): p. 184-7.
35. Fruhbeck, G., *Obesity: aquaporin enters the picture*. Nature, 2005. **438**(7067): p. 436-7.
36. Murata, K., et al., *Structural determinants of water permeation through aquaporin-1*. Nature, 2000. **407**(6804): p. 599-605.
37. Ren, G., et al., *Visualization of a water-selective pore by electron crystallography in vitreous ice*. Proc Natl Acad Sci U S A, 2001. **98**(4): p. 1398-403.
38. de Groot, B.L., A. Engel, and H. Grubmuller, *A refined structure of human aquaporin-1*. FEBS Lett, 2001. **504**(3): p. 206-11.
39. Schenk, A.D., et al., *The 4.5 Å structure of human AQP2*. J Mol Biol, 2005. **350**(2): p. 278-89.
40. Ho, J.D., et al., *Crystal structure of human aquaporin 4 at 1.8 Å and its mechanism of conductance*. Proc Natl Acad Sci U S A, 2009. **106**(18): p. 7437-42.
41. Tani, K., et al., *Mechanism of aquaporin-4's fast and highly selective water conduction and proton exclusion*. J Mol Biol, 2009. **389**(4): p. 694-706.
42. Horsefield, R., et al., *High-resolution x-ray structure of human aquaporin 5*. Proc Natl Acad Sci U S A, 2008. **105**(36): p. 13327-32.
43. Agemark, M., et al., *Reconstitution of water channel function and 2D-crystallization of human aquaporin 8*. Biochim Biophys Acta, 2012. **1818**(3): p. 839-50.
44. Viadiu, H., T. Gonen, and T. Walz, *Projection map of aquaporin-9 at 7 Å resolution*. J Mol Biol, 2007. **367**(1): p. 80-8.
45. Fu, D., et al., *Structure of a glycerol-conducting channel and the basis for its selectivity*. Science, 2000. **290**(5491): p. 481-6.

46. Heymann, J.B. and A. Engel, *Aquaporins: Phylogeny, Structure, and Physiology of Water Channels*. News Physiol Sci, 1999. **14**: p. 187-193.
47. de Groot, B.L. and H. Grubmuller, *Water permeation across biological membranes: mechanism and dynamics of aquaporin-1 and GlpF*. Science, 2001. **294**(5550): p. 2353-7.
48. Zeidel, M.L., et al., *Reconstitution of functional water channels in liposomes containing purified red cell CHIP28 protein*. Biochemistry, 1992. **31**(33): p. 7436-40.
49. Walz, T., Y. Fujiyoshi, and A. Engel, *The AQP structure and functional implications*. Handb Exp Pharmacol, 2009(190): p. 31-56.
50. de Groot, B.L., et al., *The mechanism of proton exclusion in the aquaporin-1 water channel*. J Mol Biol, 2003. **333**(2): p. 279-93.
51. de Groot, B.L. and H. Grubmuller, *The dynamics and energetics of water permeation and proton exclusion in aquaporins*. Curr Opin Struct Biol, 2005. **15**(2): p. 176-83.
52. Eifler, N., et al., *Functional expression of mammalian receptors and membrane channels in different cells*. J Struct Biol, 2007. **159**(2): p. 179-93.
53. Beitz, E., et al., *Determinants of AQP6 trafficking to intracellular sites versus the plasma membrane in transfected mammalian cells*. Biol Cell, 2006. **98**(2): p. 101-9.
54. Chen, Z.H., et al., *Involvement of beta-adrenergic receptor in synaptic vesicle swelling and implication in neurotransmitter release*. J Cell Mol Med, 2011. **15**(3): p. 572-6.
55. Lopez, I.A., et al., *Immunohistochemical localization of aquaporins in the human inner ear*. Cell Tissue Res, 2007. **328**(3): p. 453-60.
56. Iandiev, I., et al., *Immunolocalization of aquaporin-6 in the rat retina*. Neurosci Lett, 2011. **490**(2): p. 130-4.
57. Shin, L., et al., *Involvement of vH(+)-ATPase in synaptic vesicle swelling*. J Neurosci Res, 2010. **88**(1): p. 95-101.
58. Perin, P., et al., *Aquaporin-6 expression in the cochlear sensory epithelium is downregulated by salicylates*. J Biomed Biotechnol, 2010. **2010**: p. 264704.
59. Rabaud, N.E., et al., *Aquaporin 6 binds calmodulin in a calcium-dependent manner*. Biochem Biophys Res Commun, 2009. **383**(1): p. 54-7.
60. Laforenza, U., et al., *Aquaporin-6 is expressed along the rat gastrointestinal tract and upregulated by feeding in the small intestine*. BMC Physiol, 2009. **9**: p. 18.
61. Ichikawa, H., et al., *Electrophysiological properties of AQP6 in mouse parotid acinar cells*. J Med Invest, 2009. **56 Suppl**: p. 347-9.
62. Taguchi, D., et al., *Expression and immunolocalization of aquaporin-6 (Aqp6) in the rat inner ear*. Acta Otolaryngol, 2008. **128**(8): p. 832-40.
63. Matsuki-Fukushima, M., et al., *Presence and localization of aquaporin-6 in rat parotid acinar cells*. Cell Tissue Res, 2008. **332**(1): p. 73-80.
64. Nagase, H., et al., *Molecular cloning and characterization of mouse aquaporin 6*. Biochem Biophys Res Commun, 2007. **352**(1): p. 12-6.
65. Jeremic, A., W.J. Cho, and B.P. Jena, *Involvement of water channels in synaptic vesicle swelling*. Exp Biol Med (Maywood), 2005. **230**(9): p. 674-80.
66. Hagstrom, S., et al., *[Congenital nephrogenic diabetes insipidus. A four-month-old girl with delayed psychomotor development]*. Ugeskr Laeger, 2005. **167**(16): p. 1759-61.
67. Pohl, P., *Combined transport of water and ions through membrane channels*. Biol Chem, 2004. **385**(10): p. 921-6.
68. Schrier, R.W. and M.A. Cadnapaphornchai, *Renal aquaporin water channels: from molecules to human disease*. Prog Biophys Mol Biol, 2003. **81**(2): p. 117-31.
69. Ikeda, M., et al., *Characterization of aquaporin-6 as a nitrate channel in mammalian cells. Requirement of pore-lining residue threonine 63*. J Biol Chem, 2002. **277**(42): p. 39873-9.

70. Hazama, A., et al., *Ion permeation of AQP6 water channel protein. Single channel recordings after Hg²⁺ activation.* J Biol Chem, 2002. **277**(32): p. 29224-30.
71. Ohshiro, K., et al., *Expression and immunolocalization of AQP6 in intercalated cells of the rat kidney collecting duct.* Arch Histol Cytol, 2001. **64**(3): p. 329-38.
72. Promeneur, D., et al., *Regulation of AQP6 mRNA and protein expression in rats in response to altered acid-base or water balance.* Am J Physiol Renal Physiol, 2000. **279**(6): p. F1014-26.
73. Gouet, P., et al., *ESPrpt: analysis of multiple sequence alignments in PostScript.* Bioinformatics, 1999. **15**(4): p. 305-8.
74. Russ, W.P. and D.M. Engelman, *The GxxxG motif: a framework for transmembrane helix-helix association.* J Mol Biol, 2000. **296**(3): p. 911-9.
75. Liu, K., et al., *Conversion of aquaporin 6 from an anion channel to a water-selective channel by a single amino acid substitution.* Proc Natl Acad Sci U S A, 2005. **102**(6): p. 2192-7.
76. Sali, A. and T.L. Blundell, *Comparative protein modelling by satisfaction of spatial restraints.* J Mol Biol, 1993. **234**(3): p. 779-815.
77. Ma, T., et al., *cDNA cloning and gene structure of a novel water channel expressed exclusively in human kidney: evidence for a gene cluster of aquaporins at chromosome locus 12q13.* Genomics, 1996. **35**(3): p. 543-50.
78. Holm, L.M., D.A. Klaerke, and T. Zeuthen, *Aquaporin 6 is permeable to glycerol and urea.* Pflugers Arch, 2004. **448**(2): p. 181-6.
79. Kukulski, W., et al., *The 5A structure of heterologously expressed plant aquaporin SoPIP2;1.* J Mol Biol, 2005. **350**(4): p. 611-6.
80. Kai, L., et al., *Preparative scale production of functional mouse aquaporin 4 using different cell-free expression modes.* PLoS One, 2010. **5**(9): p. e12972.
81. Hovijitra, N.T., et al., *Cell-free synthesis of functional aquaporin Z in synthetic liposomes.* Biotechnol Bioeng, 2009. **104**(1): p. 40-9.
82. Savage, D.F., et al., *Architecture and selectivity in aquaporins: 2.5 a X-ray structure of aquaporin Z.* PLoS Biol, 2003. **1**(3): p. E72.
83. Salom, D., et al., *Heterologous expression of functional G-protein-coupled receptors in Caenorhabditis elegans.* FASEB J, 2012. **26**(2): p. 492-502.
84. Bergeron, M.J., et al., *Frog oocytes to unveil the structure and supramolecular organization of human transport proteins.* PLoS One, 2011. **6**(7): p. e21901.
85. Baneyx, F., *Recombinant protein expression in Escherichia coli.* Curr Opin Biotechnol, 1999. **10**(5): p. 411-21.
86. Hartl, F.U., R. Hlodan, and T. Langer, *Molecular chaperones in protein folding: the art of avoiding sticky situations.* Trends Biochem Sci, 1994. **19**(1): p. 20-5.
87. Winnik and H. Askenasy, *[Some vital indications for lobotomy].* Rev Neurol (Paris), 1950. **83**(5): p. 506-9.
88. Winnik, Z.H. and H. Askenazy, *Our psychosurgical experiences with special reference to the problem of indications (in Hebrew; English summary).* Harefuah, 1950. **39**(2): p. 19-24.
89. Borsook, H., *Protein turnover and incorporation of labeled amino acids into tissue proteins in vivo and in vitro.* Physiol Rev, 1950. **30**(2): p. 206-19.
90. Kim, D.M. and C.Y. Choi, *A semicontinuous prokaryotic coupled transcription/translation system using a dialysis membrane.* Biotechnol Prog, 1996. **12**(5): p. 645-9.
91. Spirin, A.S., et al., *A continuous cell-free translation system capable of producing polypeptides in high yield.* Science, 1988. **242**(4882): p. 1162-4.
92. Kigawa, T., et al., *Cell-free production and stable-isotope labeling of milligram quantities of proteins.* FEBS Lett, 1999. **442**(1): p. 15-9.
93. Klammt, C., et al., *Cell-free expression as an emerging technique for the large scale production of integral membrane protein.* FEBS J, 2006. **273**(18): p. 4141-53.

94. Schwarz, D., et al., *Preparative scale cell-free expression systems: new tools for the large scale preparation of integral membrane proteins for functional and structural studies*. *Methods*, 2007. **41**(4): p. 355-69.
95. Klammt, C., et al., *High level cell-free expression and specific labeling of integral membrane proteins*. *Eur J Biochem*, 2004. **271**(3): p. 568-80.
96. Schwarz, D., et al., *Preparative scale expression of membrane proteins in Escherichia coli-based continuous exchange cell-free systems*. *Nat Protoc*, 2007. **2**(11): p. 2945-57.
97. Shimada, Y., et al., *Functional expression and characterization of a bacterial light-harvesting membrane protein in Escherichia coli and cell-free synthesis systems*. *Biosci Biotechnol Biochem*, 2004. **68**(9): p. 1942-8.
98. Elbaz, Y., et al., *In vitro synthesis of fully functional EmrE, a multidrug transporter, and study of its oligomeric state*. *Proc Natl Acad Sci U S A*, 2004. **101**(6): p. 1519-24.
99. Berrier, C., et al., *Cell-free synthesis of a functional ion channel in the absence of a membrane and in the presence of detergent*. *Biochemistry*, 2004. **43**(39): p. 12585-91.
100. Pornillos, O., et al., *X-ray structure of the EmrE multidrug transporter in complex with a substrate*. *Science*, 2005. **310**(5756): p. 1950-3.
101. Ishihara, G., et al., *Expression of G protein coupled receptors in a cell-free translational system using detergents and thioredoxin-fusion vectors*. *Protein Expr Purif*, 2005. **41**(1): p. 27-37.
102. Klammt, C., et al., *Evaluation of detergents for the soluble expression of alpha-helical and beta-barrel-type integral membrane proteins by a preparative scale individual cell-free expression system*. *FEBS J*, 2005. **272**(23): p. 6024-38.
103. Spirin, A.S., *High-throughput cell-free systems for synthesis of functionally active proteins*. *Trends Biotechnol*, 2004. **22**(10): p. 538-45.
104. Li, Y., E. Wang, and Y. Wang, *A modified procedure for fast purification of T7 RNA polymerase*. *Protein Expr Purif*, 1999. **16**(2): p. 355-8.
105. Ryabova, L.A., et al., *Acetyl phosphate as an energy source for bacterial cell-free translation systems*. *Anal Biochem*, 1995. **226**(1): p. 184-6.
106. Ahn, J.H., et al., *Cell-free synthesis of recombinant proteins from PCR-amplified genes at a comparable productivity to that of plasmid-based reactions*. *Biochem Biophys Res Commun*, 2005. **338**(3): p. 1346-52.
107. Haberstock, S., et al., *A systematic approach to increase the efficiency of membrane protein production in cell-free expression systems*. *Protein Expr Purif*, 2012. **82**(2): p. 308-16.
108. Matthies, D., et al., *Cell-free expression and assembly of ATP synthase*. *J Mol Biol*, 2011. **413**(3): p. 593-603.
109. Strauss, J.H. and E.G. Strauss, *The alphaviruses: gene expression, replication, and evolution*. *Microbiol Rev*, 1994. **58**(3): p. 491-562.
110. Helenius, A., et al., *On the entry of Semliki forest virus into BHK-21 cells*. *J Cell Biol*, 1980. **84**(2): p. 404-20.
111. Lundstrom, K., *Semliki Forest virus vectors for rapid and high-level expression of integral membrane proteins*. *Biochim Biophys Acta*, 2003. **1610**(1): p. 90-6.
112. Berglund, P., et al., *Semliki Forest virus expression system: production of conditionally infectious recombinant particles*. *Biotechnology (N Y)*, 1993. **11**(8): p. 916-20.
113. Lundstrom, K., et al., *Expression of ligand-gated ion channels with the Semliki Forest virus expression system*. *J Recept Signal Transduct Res*, 1997. **17**(1-3): p. 115-26.
114. Michel, A.D., et al., *The binding characteristics of a human bladder recombinant P2X purinoceptor, labelled with [3H]-alpha beta meATP, [35S]-ATP gamma S or [33P]-ATP*. *Br J Pharmacol*, 1996. **117**(6): p. 1254-60.

115. Higgins, D.R. and J.M. Cregg, *Introduction to Pichia pastoris*. Methods Mol Biol, 1998. **103**: p. 1-15.
116. Cregg, J.M., T.S. Vedvick, and W.C. Raschke, *Recent advances in the expression of foreign genes in Pichia pastoris*. Biotechnology (N Y), 1993. **11**(8): p. 905-10.
117. Cereghino, J.L. and J.M. Cregg, *Heterologous protein expression in the methylotrophic yeast Pichia pastoris*. FEMS Microbiol Rev, 2000. **24**(1): p. 45-66.
118. Daly, R. and M.T. Hearn, *Expression of heterologous proteins in Pichia pastoris: a useful experimental tool in protein engineering and production*. J Mol Recognit, 2005. **18**(2): p. 119-38.
119. Rosenberg, M.F., et al., *The human breast cancer resistance protein (BCRP/ABCG2) shows conformational changes with mitoxantrone*. Structure, 2010. **18**(4): p. 482-93.
120. Jamshad, M., et al., *Structural characterization of recombinant human CD81 produced in Pichia pastoris*. Protein Expr Purif, 2008. **57**(2): p. 206-16.
121. Schneider, B., et al., *Membrane protein expression in cell-free systems*. Methods Mol Biol, 2010. **601**: p. 165-86.
122. de Leeuw, E., et al., *Anionic phospholipids are involved in membrane association of FtsY and stimulate its GTPase activity*. EMBO J, 2000. **19**(4): p. 531-41.
123. Ciccarone, V.C., J.A. Jessee, and P. Liljestrom, *The SFV Gene Expression System*. Methods Mol Med, 1998. **13**: p. 237-55.
124. Hasler, L., et al., *Purified lens major intrinsic protein (MIP) forms highly ordered tetragonal two-dimensional arrays by reconstitution*. J Mol Biol, 1998. **279**(4): p. 855-64.
125. Levy, D., et al., *A systematic study of liposome and proteoliposome reconstitution involving Bio-Bead-mediated Triton X-100 removal*. Biochim Biophys Acta, 1990. **1025**(2): p. 179-90.
126. Kaufmann, T.C., A. Engel, and H.W. Remigy, *A novel method for detergent concentration determination*. Biophys J, 2006. **90**(1): p. 310-7.
127. Severs, N.J., *Freeze-fracture electron microscopy*. Nat Protoc, 2007. **2**(3): p. 547-76.
128. Zeidel, M.L., et al., *Ultrastructure, pharmacologic inhibition, and transport selectivity of aquaporin channel-forming integral protein in proteoliposomes*. Biochemistry, 1994. **33**(6): p. 1606-15.
129. Liu, K., et al., *Purification and functional characterization of aquaporin-8*. Biol Cell, 2006. **98**(3): p. 153-61.
130. Junge, F., et al., *Large-scale production of functional membrane proteins*. Cell Mol Life Sci, 2008. **65**(11): p. 1729-55.
131. Braun, T., et al., *The 3.7 Å projection map of the glycerol facilitator GlpF: a variant of the aquaporin tetramer*. EMBO Rep, 2000. **1**(2): p. 183-9.
132. Kalmbach, R., et al., *Functional cell-free synthesis of a seven helix membrane protein: in situ insertion of bacteriorhodopsin into liposomes*. J Mol Biol, 2007. **371**(3): p. 639-48.
133. Opekarova, M. and W. Tanner, *Specific lipid requirements of membrane proteins-a putative bottleneck in heterologous expression*. Biochim Biophys Acta, 2003. **1610**(1): p. 11-22.
134. Berrier, C., et al., *Coupled cell-free synthesis and lipid vesicle insertion of a functional oligomeric channel MscL MscL does not need the insertase YidC for insertion in vitro*. Biochim Biophys Acta, 2011. **1808**(1): p. 41-6.
135. Shimono, K., et al., *Production of functional bacteriorhodopsin by an Escherichia coli cell-free protein synthesis system supplemented with steroid detergent and lipid*. Protein Sci, 2009. **18**(10): p. 2160-71.
136. Chrispeels, M.J. and P. Agre, *Aquaporins: water channel proteins of plant and animal cells*. Trends Biochem Sci, 1994. **19**(10): p. 421-5.
137. Nand, A., et al., *Emerging technology of in situ cell free expression protein microarrays*. Protein Cell, 2012. **3**(2): p. 84-8.

138. Isaksson, L., et al., *Expression screening of membrane proteins with cell-free protein synthesis*. Protein Expr Purif, 2012. **82**(1): p. 218-25.
139. Hornung, V., et al., *5'-Triphosphate RNA is the ligand for RIG-I*. Science, 2006. **314**(5801): p. 994-7.
140. Krieg, P.A. and D.A. Melton, *In vitro RNA synthesis with SP6 RNA polymerase*. Methods Enzymol, 1987. **155**: p. 397-415.
141. Lundstrom, K., et al., *Improved Semliki Forest virus vectors for receptor research and gene therapy*. J Recept Signal Transduct Res, 2001. **21**(1): p. 55-70.
142. Liljestrom, P. and H. Garoff, *A new generation of animal cell expression vectors based on the Semliki Forest virus replicon*. Biotechnology (N Y), 1991. **9**(12): p. 1356-61.
143. Lundstrom, K., et al., *High-level expression of the human neurokinin-1 receptor in mammalian cell lines using the Semliki Forest virus expression system*. Eur J Biochem, 1994. **224**(3): p. 917-21.
144. White, G.F., et al., *Physical properties of liposomes and proteoliposomes prepared from Escherichia coli polar lipids*. Biochim Biophys Acta, 2000. **1468**(1-2): p. 175-86.
145. Werten, P.J., et al., *Large-scale purification of functional recombinant human aquaporin-2*. FEBS Lett, 2001. **504**(3): p. 200-5.
146. Karlsson, M., et al., *Reconstitution of water channel function of an aquaporin overexpressed and purified from Pichia pastoris*. FEBS Lett, 2003. **537**(1-3): p. 68-72.
147. Borgnia, M.J. and P. Agre, *Reconstitution and functional comparison of purified GlpF and AqpZ, the glycerol and water channels from Escherichia coli*. Proc Natl Acad Sci U S A, 2001. **98**(5): p. 2888-93.
148. Clare, J.J., et al., *Production of mouse epidermal growth factor in yeast: high-level secretion using Pichia pastoris strains containing multiple gene copies*. Gene, 1991. **105**(2): p. 205-12.
149. Prive, G.G., *Detergents for the stabilization and crystallization of membrane proteins*. Methods, 2007. **41**(4): p. 388-97.
150. Nikkola, M., Y. Lindqvist, and G. Schneider, *Refined structure of transketolase from Saccharomyces cerevisiae at 2.0 Å resolution*. J Mol Biol, 1994. **238**(3): p. 387-404.
151. Sauer, M., et al., *Differential gene expression in recombinant Pichia pastoris analysed by heterologous DNA microarray hybridisation*. Microb Cell Fact, 2004. **3**(1): p. 17.
152. Peng, J., et al., *A proteomics approach to understanding protein ubiquitination*. Nat Biotechnol, 2003. **21**(8): p. 921-6.
153. Wohlschlegel, J.A., et al., *Global analysis of protein sumoylation in Saccharomyces cerevisiae*. J Biol Chem, 2004. **279**(44): p. 45662-8.
154. Studier, F.W. and B.A. Moffatt, *Use of bacteriophage T7 RNA polymerase to direct selective high-level expression of cloned genes*. J Mol Biol, 1986. **189**(1): p. 113-30.
155. Hanahan, D., *Studies on transformation of Escherichia coli with plasmids*. J Mol Biol, 1983. **166**(4): p. 557-80.

Curriculum vitae

Personal Data

Date of birth: December 18, 1979 in Hattingen, Germany

Scientific education & professional experiences

11/2008 – 06/2012

Center for Cellular Imaging and Nanoanalytics, Biozentrum, University of Basel, Switzerland, Ph.D. student in biochemistry / structural biology, research group of Prof. A. Engel

10/2007 - 09/2008

Max-Planck-Institute of Molecular Physiology Dortmund, Germany, Research department for structural biology, Prof. A. Wittinghofer

10/2006 - 10/2008

Biochemistry Ruhr-University, Bochum, Germany
degree obtained **Master of Science**

10/2003 - 09/2006

Biochemistry Ruhr-University, Bochum, Germany
degree obtained: **Bachelor of Science**

Grants

07/2011

Invited to the 61st **Lindau Nobel Laureates Meeting**
(Physiology/Medicine)

11/2008 - 10/2011

Marie Curie Fellowship for early stage researchers of the *European Commission*

Member of the Initial Training Network Structural Biology of Membrane Proteins

Conferences & Workshops

05/2012

4th annual meeting Structural Biology of Membrane Proteins, Maratea, Italy, Poster presentation

08/2011

TEMIMPS Electron Crystallography Workshop, University of Washington, Seattle, WA, Poster presentation

05/2011

3rd annual meeting Structural Biology of Membrane Proteins, Utrecht University, Oral & poster presentation

08/2010

Workshop on Electron Microscopy of Membrane Proteins
Biozentrum, University Basel, Prof. Henning Stahlberg

06/2010

2nd annual meeting Structural Biology of Membrane Proteins D-BSSE, ETH Zürich, Basel, Oral & poster presentation

03/2010

Protein crystallography course, Prof. Eva Pebay-Peyroula
IBS, Grenoble, France

03/2010

Workshop on Application of Amphipols to Membrane Protein Studies
IBPC, Paris, France

11/2009

Workshop on EM Structure Determination of Challenging Macromolecules, The Scripps Research Institute, La Jolla, CA
Poster presentation

06/2009

1st annual meeting Structural Biology of Membrane Proteins
ITQB, Lisbon, Oral & poster presentation

Publications

Expression and characterization of Aquaporin-6 in different systems. Krüger A, Engel A. in preparation

Kissing G domains of MnmE monitored by X-ray crystallography and pulse electron paramagnetic resonance spectroscopy. Meyer S, Böhme S, Krüger A, Steinhoff HJ, Klare JP, Wittinghofer A. **PLoS Biol.** 2009 Oct;7(10):e1000212. Epub 2009 Oct 6.

Stabilization of G domain conformations in the tRNA-modifying MnmE-GidA complex observed with double electron electron resonance spectroscopy. Böhme S, Meyer S, Krüger A, Steinhoff HJ, Wittinghofer A, Klare JP. **J Biol Chem.** 2010 May 28;285(22):16991-7000. Epub 2010 Mar 30.

Acknowledgements

I would like to thank...

Andreas Engel for giving me the opportunity to work in his labs in Basel and in Cleveland and for his continuous support during my PhD studies.

Henning Stahlberg for embedding me in his group and for his constant support.

Swetlana Martell for supervising me during my first months in Basel.

Patrick Bosshard for introducing me to the lab and for the inspiring discussions.

Thomas Braun for always having time to discuss problems.

Mohamed Chami for educating me in freeze fracturing and his patience.

Ardi Vahedi for my great time in Cleveland.

Fabian Kebbel for critical reading my manuscript.

Mark Hilge for his critical comments and for his helpfulness.

Norbert Uehlein for his support during the stopped flow measurements.

Friederike Junge and Frank Bernhard for introducing me to cell free expression.

And finally, everyone from the Engel and Stahlberg groups for the good atmosphere, the fruitful discussions and a great time in Basel. Many thanks to all of you!

